ABSTRACT

ORTIZ-MEDINA, JUAN FAUSTO. Identification of the Microorganisms and Mechanisms that Drive the Conversion of Nitrogen Gas into Ammonium in Microbial Electrolysis Cells. (Under the direction of Dr. Douglas Call).

Ammonia (NH_3) is one of the most produced chemicals in the world, with over 80% used in agriculture as the main component of fertilizers. The majority of NH_3 is generated from atmospheric nitrogen gas (N_2) through the Haber-Bosch process, requiring around 2% of the world's fossil fuel energy and generating 420 million tons CO_2 annually. Alternatives to produce NH_3 or its protonated form ammonium (NH_4^+) are needed. Microbial electrolysis cells (MECs), a technology that utilizes microorganisms growing in an anode biofilm (bioanode) to transfer electrons and generate products of interest such as hydrogen gas (H_2) at the cathode, may provide an alternative method to generate NH_4^+ by electrically driving the biological fixation of N_2 into NH_4^+ under ambient conditions and high energy efficiency. The overarching objective of this dissertation is to assess the possibility of using MECs to produce NH_4^+.

To accomplish this objective, first I investigated the variability of MEC startup after inoculation with a complex microbial community by characterizing the electrochemical properties and community structure of bioanodes during their initial enrichments. Bioanode replicates were operated at two fixed electrode potentials (representing different electron transfer rates) for one fed-batch cycle. Startup time decreased and maximum current generation increased when the anode was fixed at +0.15 V [vs. standard hydrogen electrode (SHE)] compared to −0.15 V, but the replicates clustered into three distinct activity levels. At −0.15 V, current production strongly followed *Geobacter* species abundance and bioanode resistance, wherein the largest abundance of *Geobacter* was associated with the lowest charge transfer resistance. My findings show that startup

variability occurs at both applied potentials, but the underlying electrochemical and microbial factors driving variability are dependent on the applied potential. Accordingly, *Geobacter* species are critical components of high current-generating bioanode communities.

Secondly, I tested the hypothesis that voltage can increase N_2 fixation and subsequent NH_4^+ production rates in MECs. N_2 fixation rates [based on an acetylene gas (C_2H_2) to ethylene gas (C_2H_4) conversion assay] of a microbial consortium increased significantly when the applied voltage between the anode and cathode increased from 0.7 V to 1.0 V, reaching a maximum of ~40 nmol C_2H_4/(min-mg anode protein) comparable to model aerobic N_2-fixing bacteria. Upon addition of an NH_4^+ uptake inhibitor, NH_4^+ was recovered at rates approaching 5.2×10^{-12} mol NH_4^+/(s-cm^2 anode). Energy demand for NH_4^+ production was as low as 24 MJ/mol NH_4^+ due to the simultaneously produced energy-rich gas in the MECs. *Geobacter* species predominated in the bioanode community, suggesting a key role in current generation and N_2 fixation. These results show that voltage can drive N_2 fixation rates, and MECs may provide a new route for generating NH_4^+.

Lastly, my goal was to better understand the pathways of N_2 fixation in *Geobacter sulfurreducens* and their regulation during anode respiration. To do this, I analyzed gene expression levels (via RNA sequencing) from *G. sulfurreducens* growing on anodes fixed at different potentials (E_{AN}) and varying amounts of NH_4^+. The presence of NH_4^+ expectedly decreased the expression of genes associated with N_2 fixation, as this process is sensitive to NH_4^+. Interestingly, E_{AN} had an unexpected impact on N_2 fixation-related genes. At the low E_{AN} value (−0.15 V vs. SHE), genes associated with the nitrogenase were significantly up-regulated, as well as genes associated with NH_4^+ uptake, transport, and transformation, such as glutamine and glutamate synthetases. The results suggest that cells responded to the highly energy-constrained

conditions at −0.15 V by increasing expression of N_2 fixation pathways and glutamate production. These findings have important implications for understanding N_2 fixation regulatory pathways, allowing us to better identify target genes or operational strategies to enhance NH_4^+ production in MECs.

Identification of the Microorganisms and Mechanisms that Drive the Conversion of Nitrogen Gas into Ammonium in Microbial Electrolysis Cells.

by
Juan Fausto Ortiz-Medina

A dissertation submitted to the Graduate Faculty of
North Carolina State University
in partial fulfillment of the
requirements for the degree of
Doctor of Philosophy

Civil Engineering

Raleigh, North Carolina
2020

APPROVED BY:

_____	_____
Dr. Douglas F. Call Committee Chair	Dr. Francis L. De los Reyes
_____	_____
Dr. Amy M. Grunden	Dr. Michael R. Hyman

BIOGRAPHY

Juan Fausto Ortiz-Medina obtained his Bachelor's Degree in Biotechnology Engineering from the Monterrey Institute of Technology and Higher Education (ITESM) in 2012. He completed his Master's Degree in Environmental Science and Engineering at King Abdullah University of Science and Technology (KAUST) in 2014. During his studies, he performed research that involved microbial electrochemical technologies (METs), and his thesis project involved utilizing these systems to study microorganisms present in Red Sea brine pools. In 2015 he joined Dr. Douglas Call's research group at North Carolina State University to continue working with METs, focusing on microbial communities and understanding the processes that can lead to sustainable production of compounds of interest such as hydrogen gas and ammonium.

ACKNOWLEDGEMENTS

The completion of this dissertation has been the result of many years of efforts and work, in which I received support, feedback and encouragement from many people during this time.

First, I want to thank Dr. Douglas Call, my advisor, for all his advice, support and guidance during all this time as a student. Being the first student of a new research group gave both of us a lot of learning experiences and opportunities to work on, which have translated into forming a very well-established and successful group, and that has greatly contributed in the development of our careers. I wish to thank also all the members of our research group for their encouragement, teamwork and dedication, particularly Qiwen Cheng, Mark Poole, Elvin Hossen and Yazeed Algurainy. They offered me continuous support since they joined the Call Lab and became excellent colleagues, teammates and friends. I also wish to thank Dr. Francis De Los Reyes, Dr. Amy Grunden, and Dr. Mike Hyman, for being part of my Committee and providing me with great advice and closely following up the completion of my projects.

I also want to thank all the friends and colleagues I made at NC State throughout these years, because their support was invaluable during this stage as a PhD student. There are so many people that making a list of names could take several pages, but all the friends I met through the Environmental Engineering department, the Latin American Student Association, and the university staff I collaborated with, contributed greatly to the completion of this dissertation through their friendship and professionalism. And I am truly grateful for it.

Finally, I want to thank my parents, Fausto Ortiz and Ysabel Medina, and my sister Monica Ortiz, that supported me unconditionally even though I am far from home. I am sure they are they are proud of me for reaching this goal. I am blessed to have them as family, and I hope we can celebrate many more achievements to come.

TABLE OF CONTENTS

LIST OF TABLES

LIST OF FIGURES

CHAPTER 1

THE NEED OF SUSTAINABLE ALTERNATIVES OF AMMONIUM PRODUCTION

1.1 A necessity to reduce carbon and energy footprint

The world is currently experiencing global warming. This environmental phenomenon, which translates into an overall increase in Earth's global temperature, has been primarily attributed to anthropogenic activity, which has increased the amount of greenhouse gases (GHG) present in the atmosphere. One of the leading contributors of GHG emissions is the combustion of fossil fuels which mainly produces carbon dioxide (CO_2). In 2018, the energy-related emissions of CO_2 reached an historical maximum at 33.1 Gt CO_2 per year, resulting in an atmospheric concentration of 407.4 ppm CO_2.[1] Following this trend, it is expected that by 2050 the emissions of this gas will increase by 78%.[2] This may result in a long-term increase in global temperature between 1.7 and 2.4 °C.[3] This climate alteration is associated with adverse weather effects such as stronger meteorological phenomena (e.g. hurricanes), rise of sea level and ocean acidification. All these effects can potentially damage current infrastructure,[4] impact the availability of natural resources, decrease the yield of economic activities such as agriculture, fishery and forestry,[5] and overall compromise the wellbeing of humankind in the following decades. Therefore, there is a latent need for sustainable alternatives to conventional processes that rely on fossil fuels.

Among anthropogenic activities, a major source of GHG emissions is agriculture. Crops and livestock are responsible for the emission of CO_2 and other potent GHG, such as methane (CH_4) and nitrous oxide (N_2O).[6] Poor agricultural management practices contribute significantly to the emission of these gases through excess application of fertilizers and poor livestock waste management. This GHG pollution affects other environmental systems, causing phenomena such as eutrophication and acidification of soils and waters.[6] Thus, processes that can lead to a less

impactful agricultural management are increasingly developed and tested as means to directly reduce GHG emissions.

1.2 Ammonia and its importance

Ammonia (NH_3) is one of the most produced chemicals in the world. Its annual global production is between 160-200 million tons, of which 80% is used in agriculture as the main component of several fertilizers.[7] The rest is employed in the manufacture of explosives and chemical commodities such as pharmaceuticals, refrigerants, and cleaning products.[8] Additionally, research on NH_3 as an alternative fuel has increased in recent years due to its capacity to be combusted without releasing CO_2 and because it can be stored at low temperatures and pressures.[9]

Through its use as fertilizer, NH_3 provides the nitrogen that is essential for plant growth. Historically, different sources of fixed nitrogen such as wastes, manure and byproducts from fuels were commonly applied as fertilizers.[10] It was not until Fritz Haber and Carl Bosch developed the catalytic synthesis of NH_3 from nitrogen (N_2) and hydrogen (H_2) gas, better known as the Haber-Bosch process that a thermochemical method of fixed nitrogen production became feasible. This process synthesizes NH_3 through the following reaction:[10]

$$N_2 + 3H_2 \leftrightarrow 2NH_3 \qquad \Delta H_{298K} = -45.7\ kJ/mol$$

While this reaction in thermodynamically favorable under ambient conditions, high temperatures (350 - 550°C) and pressures (150 - 300 atm), along with an iron (Fe) or ruthenium (Ru) catalyst, are employed in order to break the highly stable triple bond in N_2 (N≡N).[11] Despite these conditions and the relatively low conversion yield (around 3%), this process is still used after more than one hundred years of its invention due to its simplicity and immediate industrial scalability. Since the time of its invention, it has become the main driving factor of the exponential

growth of human population by dramatically increasing global agricultural productivity.[12] The process and its energy demand have been optimized numerous times since its industrial adoption, achieving energy requirements as low as 0.48 MJ/mol NH_3 produced[11,13] which allows this process alone to generate at least 130 million tons of NH_3 per year.[13,14]

Although the usefulness of this process is undisputed, many challenges regarding the current need of a more sustainable process remain. The aforementioned high temperatures and pressures are normally maintained through the consumption of non-renewable energy. This results in Haber-Bosch spending around 2% of the world's fossil fuel energy and generating 420 million tons CO_2 annually.[7] In addition to this demand, H_2 is primarily obtained by steam reforming of natural gas,[11] which also is energy intensive and generates CO_2 as a byproduct. Approximately 53% of the H_2 produced globally is used in NH_3 production through the Haber-Bosch process.[15] Therefore, sustainable options to produce H_2 are also important to develop to improve NH_3 production efficiency. Additionally, NH_3 generation through this process is heavily centralized due to the required size of the plants performing this process, giving limited cost-effective opportunities for production in less-demanding scenarios such as developing countries and remote communities.[16]

1.3 Alternatives to the Haber-Bosch process

Due to the intrinsic energy demands of Haber-Bosch to produce NH_3, a suite of alternative processes to generate fixed nitrogen has been developed in recent years. The majority of these methods aim to reduce the dependency on fossil fuels and minimize the energy needed to synthesize NH_3 from N_2 and H_2. The most researched artificial methods are plasma induced, electrochemical and catalytically assisted nitrogen fixation.[11] A brief overview of these

technologies, energetic demands, and their corresponding advantages and disadvantages are described below.

1.3.1 Plasma-induced nitrogen fixation

Plasma is the state of matter described as molecules that are found in the form of ionized gases. As such, it is referred as the fourth state of matter.[13] Plasma is usually obtained through the application of electrical energy, which increases the temperature of the electrons up to at least 10,000 °C due to their small mass. These electrons will collide with the gases of interest to cause excitation, ionization and/or dissociation, creating new species that are more reactive.[13] This process facilitates, therefore, the production of NH_3 by ionizing N_2 and H_2. There are two types of plasma-induced nitrogen fixation: thermal and non-thermal. For thermal fixation, both charged (electrons) and neutral (gases) particles possess similar temperatures to achieve equilibrium.[11] This implies that gases must achieve temperatures even higher than required by the Haber-Bosch process (~700 °C),[11] heavily limiting its applicability as an alternative for nitrogen fixation. On the other hand, non-thermal (non-equilibrium) plasma induced nitrogen fixation only requires collision of high energy electrons with gases at moderate temperatures (25-200 °C) and pressures (0.9-1 atm).[17] This allows the energetic demand to be comparable to Haber-Bosch, achieving in certain cases values as low as 0.29 MJ per mol of N fixed.[11]

Due to the use of electrical current, this technology is considered to be environmentally benign, as the current input can be obtained from renewable energies to minimize its energy and carbon footprints.[18] Additionally, its operational conditions allow for small scale production if decentralized options are desired. On the other hand, there are several limitations for this technology. NH_3 production is still dependent on H_2 as a reactant, therefore the energetic needs

and carbon emissions related to the production of this gas are similar to Haber-Bosch. As such, production of other forms of fixed nitrogen, such as nitric oxide (NO) utilizing air as input, are preferred instead.[14,19] Additionally, the underlying reaction mechanisms are poorly understood,[11,17] which adds a degree of uncertainty in efficiency when more relevant production rates are considered.[18]

1.3.2 Electrochemical nitrogen fixation

Another widely researched alternative for nitrogen fixation is the production of NH_3 through electrochemical cells. These systems consist of electrodes suspended in a conductive electrolyte solution, in which one of them (anode) performs oxidation reactions while the other (cathode) is responsible of reduction processes. Both reactions happen simultaneously due to transfer of electrons throughout the cell. Because formation of this compound from N_2 is a reduction reaction (i.e. NH_3 gains electrons), this reaction can be facilitated electrochemically with a cathode acting as electron donor. Instead of high temperatures and pressures, equilibrium is shifted by applying an external voltage that imparts the required energy to drive the reaction.

In an aqueous based electrochemical cell, the half reaction of N_2 reduction is the following:[16]

$$N_{2\,(g)} + 2H_2O + 6H^+_{(aq)} + 6e^- \rightarrow 2NH_3 * 2H_2O$$

E^o = 0.092 vs. standard hydrogen electrode (SHE)

Thanks to this cathodic reaction, any compound containing hydrogen, or protons already present in the water system, can be used as the source of hydrogen atoms. This offers an advantage compared to other processes as H_2 gas is not directly required, avoiding therefore the energetic and carbon demands associated with its use. For these reasons, electrochemical production of NH_3

has been extensively studied, using a wide array of electrode materials, catalysts, electrolytes and temperatures.[20] The main challenge of electrochemical systems is the competition of NH_3 synthesis with hydrogen evolution reaction (HER), which occurs at similar potentials, with H_2 production overcoming NH_3 at higher applied voltages.[16,20] Despite the large amount of performed research, production rates and faradaic efficiencies (the amount of NH_3 generated per electrons consumed) are still comparatively low, especially at low temperatures.[20] Additionally, a catalyst is needed to accelerate the reaction kinetics. Although Fe- and Ru- based electrodes have been utilized to emulate Haber-Bosch catalysis, it has been reported that other materials, such as platinum (Pt) and silver-palladium (Ag-Pd) have the most promising yields.[20] Therefore, the use of precious metals may impose an additional cost to consider for the production of NH_3 using this method.

1.3.3 Catalyst-assisted nitrogen fixation

One thoroughly researched alternative for NH_3 production is the improvement of catalysts to perform N_2 fixation at more benign temperatures and pressures, thereby lowering the energetic requirements for Haber-Bosch. Some of them are rationally designed to emulate the catalytic properties offered by Fe and Ru-based catalysts used in this process;[21] however, other catalysts are developed based on the catalytic site of nitrogenase, the enzyme responsible for nitrogen fixation in nature. As such, a wide array of catalysts to assist N_2 fixation have been developed over the years. One advantage of developing new catalysts is that their implementation can be additive with other N_2 fixation alternatives and work cooperatively, e.g. exploiting the reductive driving force on electrochemical cells.[22] However, affordability and practicality of materials should always be taken into consideration, especially if these catalysts are expected to represent an improvement over the Haber-Bosch process.

1.4 Biological Nitrogen Fixation (BNF)

In addition to the methods described in the previous section, one of the most well-known alternatives to produce NH_3 from N_2 is biological nitrogen fixation (BNF), a process already occurring in the environment. A suite of microorganisms, termed diazotrophs or nitrogen-fixing microorganisms, perform this process under ambient conditions to obtain nitrogen compounds that are utilized to synthesize biomolecules such as amino acids and nucleic acids. There are two types of diazotrophic microorganisms: symbiotic, which thrive in close association with plant roots (inhabiting special compartments termed nodules), and free-living diazotrophs, which perform N_2 fixation as part of their own metabolism and without the need of a symbiotic partner. Symbiotic N_2 fixation is restricted to bacteria from the group rhizobia and the genus *Frankia*,[23] which grow in close association with plants such as legumes. Comparatively, free-living diazotrophs are widespread across bacterial and archaeal microorganisms, including bacterial phyla such as Alpha-, Beta-, Gamma-, and Delta-proteobacteria, Firmicutes, Cyanobacteria, green-sulfur bacteria,[23] as well as archaeal groups such as methanogens.[24] This allows for these organisms to thrive in a wide array of environments, both terrestrial and marine, which may contain scarce amounts of fixed nitrogen and other nutrients.

To fix N_2, diazotrophs express an enzyme, termed nitrogenase, that catalyzes the conversion of N_2 to NH_3 through the following general reaction:[25]

$$N_2 + 16\,MgATP + 8H^+ + 8\,e^- \leftrightarrow 2NH_3 + H_2 + 16\,MgADP + 16P_i$$

There are three different types of nitrogenases depending on the metals comprising the cofactor associated with the active site of the enzyme: iron-molybdenum (Mo-Fe), vanadium (V) or iron (Fe). The Mo-Fe nitrogenase is the preferentially expressed form due to its higher specific activity, whereas the latter two are normally utilized when molybdenum is scarce.[26] The reaction

requires a considerable amount of metabolic energy, which is provided in the form of adenosine triphosphate (ATP) molecules. Considering the energetic value of ATP, this process theoretically requires around 244 kJ/mol NH_3, an energetic demand potentially lower than Haber-Bosch.[27] However, the process is energetically demanding for the microorganisms as they must divert a fraction of their substrate energy. Therefore, N_2 fixation is only utilized when no other nitrogen sources are available, and it is under strict regulatory controls.[28] Nevertheless, N_2 fixation from free-living diazotrophs is a very common process in the environment, producing around 90 million tons NH_3 $year^{-1}$ globally, which more than half of NH_3 generated through Haber-Bosch (~150 million tons NH_3 $year^{-1}$).[23]

1.5 Ammonium production from BNF

Due to the low energetic requirements and simplicity compared to artificial production options, obtaining ammonium (NH_4^+), the protonated form of ammonia (pK_a = 9.25) from N_2-fixing microorganisms has been considered a promising alternative to Haber-Bosch process. The success of symbiotic diazotrophs that provide nitrogen compounds to legume plants has encouraged research on free-living diazotrophs to emulate stimulation of plant growth.[25] Symbiotic N_2 fixation is directly influenced by the host plant, which promotes the formation of a stable environment (nodule) for diazotrophs to grow, as well as sending molecular signals that stimulate the production of NH_4^+ that the plant readily utilizes. In contrast, free-living diazotrophs utilize this process to generate their own macromolecules, rarely releasing NH_4^+.[29] Surprisingly, attempts to inoculate non-legume crops with external free-living diazotrophs such as *Azospirillum brasilense* (a microorganism commonly found in the rhizosphere) has resulted in increased crop yields, although this outcome has been attributed to production of bacterial growth-promoting

substances, such as auxins, that stimulate root development and uptake of water and nutrients by the plant, rather than direct NH_4^+ assimilation.[30]

Early attempts to obtain NH_4^+ from free-living diazotrophs involved the inhibition of enzymes responsible for NH_4^+ incorporation into the cell, primarily glutamine synthetase. While several inhibitors were tested, L-methionine sulfone and L-methionine sulfoximine (MSX) proved to be the most effective, decreasing its activity by around 70% and, in the case of the latter, binding irreversibly to the enzyme.[31] This led to several studies, published mainly between 1975-1990, that aimed to observe the effects of the inhibitor and increase NH_4^+ production.[32] Among those studies, culturing *Anabaena*, a free-living cyanobacteria, in growth medium with MSX led to the excretion of up to 8 mM NH_4^+.[33] However, due to the overall low NH_4^+ yields and the constant need to provide these compounds, which are as expensive as $234/gram as of 2019,[34] inhibitor addition has been limited to proof-of-concept studies and the selection of inhibitor-resistant strains.[35]

Recently, most contemporary studies focus on obtaining, either by selection or by genetic manipulation, microbial strains with mutations that encourage NH_4^+ excretion. Mutated strains possess deletions of either key NH_4^+ assimilation components (such as the aforementioned glutamine synthetase) or genes that are involved in regulating N_2 fixation. The organisms that are most frequently engineered are free-living diazotrophs with a good understanding of the N_2 fixation pathways, along with the regulation mechanisms involved. Although obtaining a diazotrophic microorganism able to generate NH_4^+ through genetic modification is a promising alternative to produce fixed nitrogen compared to Haber-Bosch, directly applying genetically modified microorganisms in the environment represents a challenge, due to the unpredictability of adaptive mutations, the ability of these organisms to thrive compared with native components, as well as the existing regulations.

1.6 Electrochemical enhancement of BNF

In addition to obtaining a microorganism able to excrete NH_4^+, there is a need to establish an optimal environment where it can fix N_2 effectively and obtain robust, predictable yields with the opportunity for further optimization. As mentioned in the previous sections, nitrogen fixation is a reduction process that involves energetic inputs (either thermal, electrical or organic) to make the reaction favorable and, in the case of BNF, the process must be protected from direct oxygen exposure. With these factors in consideration, a biological electrochemical system (BES) offers a unique, enclosed environment where N_2 fixation can be potentially enhanced, combining the design simplicity of an electrochemical cell with the catalytic activity and affordability of BNF. This system can be operated either as enzymatic fuel cells (EFCs), in which only enzymes are the catalysts, or as microbial electrochemical technologies (METs), where the whole microorganism performs BNF. In the first scenario, electron transfer is possible through enzymes present in the electrolyte solution, along with electrochemically active mediators (e.g., methyl viologen). Oxidative enzymes such as hydrogenases transfer electrons to the anode, moving towards the cathode to reduce N_2 to NH_4^+ via nitrogenases.[36] On the other hand, MET utilizes microorganisms, termed exoelectrogens or electrochemically active bacteria (EAB), that are able to interact with the electrodes either by transferring electrons to the anode or receiving electrons from the cathode. As METs do not normally require a chemical mediator and they are considered self-regenerating catalysts (due to microbial growth), they offer an attractive niche to perform N_2 fixation, and previous studies have confirmed the capability of free-living diazotrophs to thrive in these systems.[37,38]

For this reason, I propose that METs, using free-living diazotrophs as catalysts, can be utilized for generation of NH_4^+. The overall objective of this dissertation is to identify the microbial

components and mechanisms that drive the microbial conversion of N_2 to NH_4^+ in one representative system, microbial electrolysis cells (MEC). The following chapter (Chapter 2) explains in more detail the choice of utilizing METs for this process, identifying the opportunities and challenges of employing these systems. The challenge of unpredictability during microbial enrichment or startup in METs is addressed in Chapter 3, where I characterized the variability in enrichment of anodes from a mixed community during MEC startup through their microbial and electrochemical properties. In Chapter 4, I studied the changes in N_2 fixation and NH_4^+ production in diazotrophic MECs due to external electrochemical stimuli. In Chapter 5, after establishing the proof-of-concept for NH_4^+ generation in MECs, I aimed to understand more deeply how the model exoelectrogen *Geobacter sulfurreducens* fixed N_2 during anode respiration. To do that, I examined changes in the transcriptome and gene expression levels in *G. sulfurreducens* as a function of fixed anode potential and NH_4^+ concentration. The results presented in this dissertation provide insight into the mechanisms of N_2 fixation and characterize the microorganisms involved in this process. My findings lay the foundation for a NH_4^+ production system that may be a viable alternative to the current means of generating this valuable compound.

Chapter 1 References

(1) International Energy Agency. *Global Energy & CO2 Status Report - The Latest Trend in Energy and Emissions in 2018*; 2019.

(2) Organisation for Economic Cooperation and Development. *Climate Change: Meeting the Challenge to 2050*; 2008.

(3) Organisation for Economic Cooperation and Development. *Climate Change: Meeting the Challenge to 2050*; 2008.

(4) Auld, H.; Maclver, D.; Klaassen, J. Adaptation Options for Infrastructure Under Changing Climate Conditions. In *2006 IEEE EIC Climate Change Conference*; IEEE, 2006; pp 1–11. https://doi.org/10.1109/EICCCC.2006.277248.

(5) Adams, R. M.; Rosenzweig, C.; Peart, R. M.; Ritchie, J. T.; McCarl, B. A.; Glyer, J. D.; Curry, R. B.; Jones, J. W.; Boote, K. J.; Allen, L. H. Global Climate Change and US Agriculture. *Nature* **1990**, *345* (6272), 219–224. https://doi.org/10.1038/345219a0.

(6) Brink, C, Kroeze, C, Klimont, Z. Ammonia Abatement and Its Impact on Emissions of Nitrous Oxide and Methane in Europe—Part 1: Method. *Atmos. Environ.* **2001**, *35* (36), 6299–6312. https://doi.org/10.1016/S1352-2310(01)00434-4.

(7) Giddey, S.; Badwal, S. P. S.; Munnings, C.; Dolan, M. Ammonia as a Renewable Energy Transportation Media. *ACS Sustain. Chem. Eng.* **2017**, *5* (11), 10231–10239. https://doi.org/10.1021/acssuschemeng.7b02219.

(8) Giddey, S.; Badwal, S. P. S.; Kulkarni, A. Review of Electrochemical Ammonia Production Technologies and Materials. *Int. J. Hydrogen Energy* **2013**, *38* (34), 14576–14594. https://doi.org/10.1016/j.ijhydene.2013.09.054.

(9) Valera-Medina, A.; Xiao, H.; Owen-Jones, M.; David, W. I. F.; Bowen, P. J. Ammonia for Power. *Prog. Energy Combust. Sci.* **2018**, *69*, 63–102. https://doi.org/10.1016/j.pecs.2018.07.001.

(10) Modak, J. M. Haber Process for Ammonia Synthesis. *Resonance* **2011**, *16* (12), 1159–1167. https://doi.org/10.1007/s12045-011-0130-0.

(11) Cherkasov, N.; Ibhadon, A. O.; Fitzpatrick, P. A Review of the Existing and Alternative Methods for Greener Nitrogen Fixation. *Chem. Eng. Process. Process Intensif.* **2015**, *90*, 24–33. https://doi.org/10.1016/j.cep.2015.02.004.

(12) Erisman, J. W.; Sutton, M. A.; Galloway, J.; Klimont, Z.; Winiwarter, W. How a Century of Ammonia Synthesis Changed the World. *Nat. Geosci.* **2008**, *1* (10), 636–639. https://doi.org/10.1038/ngeo325.

(13) Bogaerts, A.; Neyts, E. C. Plasma Technology: An Emerging Technology for Energy Storage. *ACS Energy Lett.* **2018**, *3* (4), 1013–1027. https://doi.org/10.1021/acsenergylett.8b00184.

(14) Patil, B. S.; Wang, Q.; Hessel, V.; Lang, J. Plasma N_2-Fixation: 1900–2014. *Catal. Today* **2015**, *256*, 49–66. https://doi.org/10.1016/j.cattod.2015.05.005.

(15) Logan, B. E. Ending Our Hydrogen and Ammonia Addiction to Fossil Fuels. *Environ. Sci. Technol. Lett.* **2019**, *6* (5), 257–258. https://doi.org/10.1021/acs.estlett.9b00188.

(16) Deng, J.; Iñiguez, J. A.; Liu, C. Electrocatalytic Nitrogen Reduction at Low Temperature. *Joule* **2018**, *2* (5), 846–856. https://doi.org/10.1016/j.joule.2018.04.014.

(17) Peng, P.; Chen, P.; Schiappacasse, C.; Zhou, N.; Anderson, E.; Chen, D.; Liu, J.; Cheng, Y.; Hatzenbeller, R.; Addy, M.; Zhang, Y.; Liu, Y.; Ruan, R. A Review on the Non-Thermal Plasma-Assisted Ammonia Synthesis Technologies. *J. Clean. Prod.* **2018**, *177*, 597–609. https://doi.org/10.1016/j.jclepro.2017.12.229.

(18) Anastasopoulou, A.; Wang, Q.; Hessel, V.; Lang, J. Energy Considerations for Plasma-Assisted N-Fixation Reactions. *Processes* **2014**, *2* (4), 694–710. https://doi.org/10.3390/pr2040694.

(19) Wang, W.; Patil, B.; Heijkers, S.; Hessel, V.; Bogaerts, A. Nitrogen Fixation by Gliding Arc Plasma: Better Insight by Chemical Kinetics Modelling. *ChemSusChem* **2017**, *10* (10), 2145–2157. https://doi.org/10.1002/cssc.201700095.

(20) Kyriakou, V.; Garagounis, I.; Vasileiou, E.; Vourros, A.; Stoukides, M. Progress in the Electrochemical Synthesis of Ammonia. *Catal. Today* **2017**, *286*, 2–13. https://doi.org/10.1016/j.cattod.2016.06.014.

(21) Guo, C.; Ran, J.; Vasileff, A.; Qiao, S.-Z. Rational Design of Electrocatalysts and Photo(Electro)Catalysts for Nitrogen Reduction to Ammonia (NH_3) under Ambient Conditions. *Energy Environ. Sci.* **2018**, *11* (1), 45–56. https://doi.org/10.1039/C7EE02220D.

(22) Ling, C.; Ouyang, Y.; Li, Q.; Bai, X.; Mao, X.; Du, A.; Wang, J. A General Two-Step Strategy–Based High-Throughput Screening of Single Atom Catalysts for Nitrogen Fixation. *Small Methods* **2019**, *3* (9), 1800376. https://doi.org/10.1002/smtd.201800376.

(23) Smercina, D. N.; Evans, S. E.; Friesen, M. L.; Tiemann, L. K. To Fix or Not To Fix: Controls on Free-Living Nitrogen Fixation in the Rhizosphere. *Appl. Environ. Microbiol.* **2019**, *85* (6). https://doi.org/10.1128/AEM.02546-18.

(24) Dekas, A. E.; Chadwick, G. L.; Bowles, M. W.; Joye, S. B.; Orphan, V. J. Spatial Distribution of Nitrogen Fixation in Methane Seep Sediment and the Role of the ANME Archaea. *Environ. Microbiol.* **2014**, *16* (10), 3012–3029. https://doi.org/10.1111/1462-2920.12247.

(25) Saikia, S. P.; Jain, V. Biological Nitrogen Fixation with Non-Legumes: An Achievable Target or a Dogma? *Curr. Sci.* **2007**, *92* (3), 317–322.

(26) Bellenger, J. P.; Xu, Y.; Zhang, X.; Morel, F. M. M.; Kraepiel, A. M. L. Possible Contribution of Alternative Nitrogenases to Nitrogen Fixation by Asymbiotic N_2-Fixing Bacteria in Soils. *Soil Biol. Biochem.* **2014**, *69*, 413–420. https://doi.org/10.1016/j.soilbio.2013.11.015.

(27) van der Ham, C. J. M.; Koper, M. T. M.; Hetterscheid, D. G. H. Challenges in Reduction of Dinitrogen by Proton and Electron Transfer. *Chem. Soc. Rev.* **2014**, *43* (15), 5183–5191. https://doi.org/10.1039/C4CS00085D.

(28) Merrick, M. J. Regulation of Nitrogen Fixation in Free-Living Diazotrophs. In *Genetics and Regulation of Nitrogen Fixation in Free-Living Bacteria*; Kluwer Academic Publishers: Dordrecht, 2004; pp 197–223. https://doi.org/10.1007/1-4020-2179-8_9.

(29) Van Dommelen, A.; Croonenborghs, A.; Spaepen, S.; Vanderleyden, J. Wheat Growth Promotion through Inoculation with an Ammonium-Excreting Mutant of Azospirillum Brasilense. *Biol. Fertil. Soils* **2009**, *45* (5), 549–553. https://doi.org/10.1007/s00374-009-0357-z.

(30) Okon, Y.; Itzigsohn, R. The Development of Azospirillum as a Commercial Inoculant for Improving Crop Yields. *Biotechnol. Adv.* **1995**, *13* (3), 415–424. https://doi.org/10.1016/0734-9750(95)02004-M.

(31) Ronzio, R. A.; Rowe, W. B.; Meister, A. Mechanism of Inhibition of Glutamine Synthetase by Methionine Sulfoximine. *Biochemistry* **1969**, *8* (3), 1066–1075. https://doi.org/10.1021/bi00831a038.

(32) Colnaghi, R.; Green, A.; He, L.; Rudnick, P.; Kennedy, C. Strategies for Increased Ammonium Production in Free-Living or Plant Associated Nitrogen Fixing Bacteria. *Plant Soil* **1997**, 145–154. https://doi.org/10.1023/A:1004268526162.

(33) Ramos, J. L.; Guerrero, M. G.; Losada, M. Sustained Photoproduction of Ammonia from Dinitrogen and Water by the Nitrogen-Fixing Sustained Photoproduction of Ammonia from Dinitrogen and Water by the Nitrogen-Fixing Cyanobacterium *Anabaena* Sp. Strain ATCC. *Appl. Environ. Microbiol.* **1984**, *48* (1), 114–118.

(34) Millipore-Sigma. L-methionine sulfoximine https://www.sigmaaldrich.com/catalog/product/sigma/m5379?lang=en&region=US.

(35) Thomas, S. P.; Zaritsky, A.; Boussiba, S. Ammonium Excretion by an L-Methionine-DL-Sulfoximine-Resistant Mutant of the Rice Field Cyanobacterium *Anabaena siamensis*. *Appl. Environ. Microbiol.* **1990**, *56* (11), 3499–3504.

(36) Milton, R. D.; Cai, R.; Abdellaoui, S.; Leech, D.; De Lacey, A. L.; Pita, M.; Minteer, S. D. Bioelectrochemical Haber-Bosch Process: An Ammonia-Producing H_2/N_2 Fuel Cell. *Angew. Chemie Int. Ed.* **2017**, *56* (10), 2680–2683. https://doi.org/10.1002/anie.201612500.

(37) Wong, P. Y.; Cheng, K. Y.; Kaksonen, A. H.; Sutton, D. C.; Ginige, M. P. Enrichment of Anodophilic Nitrogen Fixing Bacteria in a Bioelectrochemical System. *Water Res.* **2014**, *64*, 73–81. https://doi.org/10.1016/j.watres.2014.06.046.

(38) Zhou, S.; Han, L.; Wang, Y.; Yang, G.; Zhuang, L.; Hu, P. *Azospirillum Humicireducens* Sp. Nov., a Nitrogen-Fixing Bacterium Isolated from a Microbial Fuel Cell. *Int. J. Syst. Evol. Microbiol.* **2013**, *63* (Pt 7), 2618–2624. https://doi.org/10.1099/ijs.0.046813-0.

CHAPTER 2

MICROBIAL ELECTROCHEMICAL TECHNOLOGIES AS A PLATFORM FOR AMMONIUM PRODUCTION

2.1 Definition of microbial electrochemical technologies

Microbial electrochemical technologies (METs) represent a suite of systems that harness microbial metabolic energy to turn it into valuable products of interest. They consist of electrochemical cells, made up of an anode and cathode, with an electrolyte (e.g., wastewater). Microorganisms are able to be grown in METs and, depending on the configuration, transfer electrons to the anode or receive electrons from the cathode. The microorganisms capable of performing these processes are termed exoelectrogens and exoelectrotrophs, respectively, or simply electrochemically active microorganisms.[1] A basic schematic of these systems is shown in **Figure 2.1**.

The concept of using METs to harvest energy from microorganisms has been known and researched for several years. Although microorganisms were proven to be capable of generating electrical current since 1911,[2] they were not considered as a potential alternative for energy generation until nearly a century later, when it was revealed that some electrochemically active microorganisms were capable of extracellular electron transfer without utilizing artificial chemical mediators.[3] Further association of this technology with environmental engineering processes, such as wastewater treatment that provides organic matter for microbial growth, has helped these technologies to be included as emerging systems that can be incorporated into the food-water-energy nexus.[4]

The first technology conceived under the modern classification of METs is the microbial fuel cell (MFC). In MFCs, microorganisms obtain energy (through the oxidation of organic

substrate) and transfer electrons from their respiration pathways to the anode, which serves as an external, insoluble electron acceptor.[5] These electrons move towards the cathode, where compounds such as oxygen or ferricyanide are utilized as terminal electron acceptors. While moving through the circuit, electrical current is generated. This technology has experienced constant improvement to maximize the current and power outputs.[6] Most research has focused on finding microorganisms with high rates of electron transfer, electrode materials that minimize potential energy losses, and affordable catalysts to increase electron transfer kinetics.[7,8] While efficiency of these systems has increased substantially, a handful of limitations, like the need of using precious metals such as platinum as a cathode catalyst, has prevented a successful upscaling of these technologies to operate in environmentally relevant conditions and generate noticeable amounts of energy as direct current.[9]

Following the operational principle of microbial anode respiration occurring in MFCs, a handful of similar technologies has been developed. One of the most studied is microbial electrolysis cells (MECs). The design is similar to MFCs, with microorganisms growing on the anode and transferring electrons accordingly. However, the electron acceptor is removed, and an external power source is utilized to drive hydrogen gas (H_2) production at the cathode (**Fig. 2.1**).[10] Because of the current generated by the microorganisms, the amount of external energy needed to produce H_2 (~0.2 V theoretically) is lower than that required by electrolysis of water in abiotic electrochemical cells (at least 1.2 V).[11] This positions MECs as a potentially attractive alternative for H_2 production, utilizing microorganisms to degrade organic waste sources and producing this gas in return to offset energetic demands. MECs offer the advantage that energy is stored as the product of interest, H_2, compared to the direct current produced at MFCs that must be utilized on-site. Additionally, H_2 can be used as a feedstock for diverse industries, either as a fuel or as a

chemical precursor. This has helped position MECs as a more promising technology to be applied at larger scales, and a handful of studies have already attempted to operate pilot scale MECs with varying degrees of success.[12,13] One of the shortcomings that MECs experience is that, when they are utilized to treat organic sources, methanogenic microorganisms will consume H_2 and convert it to methane (CH_4).[11] Although CH_4 may be desirable in some situations because of existing infrastructure to utilize it compared to H_2, its production decreases the overall efficiency of the system, and its strength as a greenhouse gas (at least 20 times stronger than CO_2) poses a concern in terms of sustainability.[14] MECs also suffer from scalability issues and cost of materials when a large system is considered, so research is underway to find more affordable materials and replicable conditions.[15]

Another MET that has been developed in recent years is the microbial electrosynthesis cell (MES). Following the principle of MECs to transfer electrons and drive the production of a chemical of interest, microorganisms in MES utilize the electrons generated at the cathode, either directly or by consuming the produced H_2.[16] Through this metabolism, high value products of interest such as butyrate, ethanol and succinate, can be synthesized from CO_2 or simple carbon molecules.[17] This provides a better opportunity for MES for scaling up to relevant production rates, as the products often have lower demands. This also opens the possibility of utilizing genetically engineered microorganisms with novel routes to produce high-value chemicals of interest. However, as in MECs, difficulty in achieving robust and scalable processes is still a challenge to fully implement this technology commercially.

2.2 Microbial metabolism in microbial electrochemical technologies

The common driving force of all METs is microbial metabolism. Microorganisms must obtain energy to fulfill metabolic processes such as growth, maintenance, and reproduction. This energy comes from respiration. During respiration, there is a transfer of electrons from a chemical compound that acts as electron donor to another that serves as electron acceptor (e.g., anode). This generates chemical energy in the form of phosphorylated compounds, such as adenosine triphosphate (ATP) that ultimately provide energy to diverse metabolic pathways in living cells. Depending on the source of electron donors, microorganisms can be either chemolithotrophs (utilize inorganic compounds as electron donors) or chemoorganotrophs (which instead use organic compounds for that function). The theoretical energy gained by cell respiration is dictated by the following equation:[18]

$$\Delta E_r^0 = E_{\text{acceptor}}^0 - E_{\text{donor}}^0$$

Where E^0 represents the oxidation-reduction (redox) potential of either donor or acceptor reactions at standard conditions, and ΔE_r^0 denotes the change due to electron transfer. This change is proportional to the change in free-energy ΔG_r^0 through the Nernst equation:[18]

$$\Delta G_r^0 = -n\text{F}\Delta E_r^0$$

Where *n* represents the number of electrons (e^-) transferred and F is Faraday's constant (96485 C per mole e^-). Therefore a positive value of ΔE_r^0 implies that the reaction is spontaneous, and under most circumstances, will release energy. On the other hand, reactions with a negative value of ΔE_r^0 will require an energy input in order to proceed accordingly.

In METs such as MFCs and MECs, electrochemically active bacteria utilize the anode as electron acceptor. As long as the redox potential of the utilized electron donor is lower (more negative) than the anode potential, bacteria can use the anode as electron acceptor and transfer the

electrons involved in respiration. There are three well-studied methods of electron transfer depending on the type of bacteria and their growth and respiration mechanisms. Bacteria may be able to colonize the surface of the anode, forming a biofilm, and thus transferring the electrons directly through electron transport mechanisms, such as outer-membrane cytochromes (OMCs, **Fig. 2.2A**).[19] Due to the proximity of the cells, this method of electron transfer is highly effective as there are minimal potential losses between the terminal electron transfer and the electrode, although there is a limit on the amount of cells that are able to interact directly with the anode surface. A second method involves the use of electron mediators (known as "electron shuttles") produced by bacteria to transfer electrons (**Fig. 2.2B**).[19] As they do not require direct contact with the electrode, a higher concentration of cells can thrive planktonically in the growth medium. However, availability of mediators is subject to phenomena such as diffusion and turnover rates, which limits the effectiveness of this method for electron transfer. The third method involves the formation of a conductive extracellular matrix along with highly conductive proteins, or "nanowires" (**Fig. 2.2C**).[19] Due to the synthesis of conductive proteins, as well as other secreted chemicals, a matrix is formed to allow exoelectrogenic bacteria to form a biofilm over 100 nm wide. In a mixed microbial community, it is likely that more than one of these mechanisms is occurring at any given time.

2.3 Exoelectrogenic bacteria and their methods of electron transfer

There are a handful of bacteria that possess exoelectrogenic capabilities. Bacteria that are able to respire on electrodes belong to a wide number of phyla, including Firmicutes, Proteobacteria (from the classes Alpha-, Beta-, Gamma-, and Delta- Proteobacteria), and Acidobacteria.[20] Even though they can be obtained from very diverse environmental sources, only

a couple have been extensively studied in terms of mechanisms of electron transfer and metabolism: *Shewanella oneidensis* MR-1, which belongs to the class Gammaproteobacteria, and *Geobacer sulfurreducens* PCA, under the class Deltaproteobacteria. The former is able to respire either by direct contact (i.e., utilizing specialized outer membrane cytochromes such as MtrC and OmcA)[21] or by employing electron shuttles such as riboflavin and flavin mononucleotides (FMN).[22] *G. sulfurreducens* is only capable of direct respiration through its respective OMCs such as OmcE and OmcS,[23,24] although it is also able to form conductive matrices and deliver electrons at long distances through electrically conductive pilin proteins termed "nanowires".[7] These adaptations have allowed *Geobacter* species to produce higher current densities than *Shewanella* spp. (at least 10-fold under the same reactor configurations).[25] Due to their effective extracellular transfer pathways, *Geobacter* enrichments are common in METs inoculated with mixed communities, particularly from soil and wastewater, which are frequent applications for these technologies.[26] This allows *Geobacter* spp. to be one of the primary microorganisms of interest when optimization and development of new MET approaches are desired.

2.4 Utilization of *Geobacter* spp. in diazotrophic microbial electrochemical technologies

One of the most prominent characteristics of *Geobacter* species, besides their high rates of electron transfer, is their ubiquity and adaptability to survive in oligotrophic environments, where they utilize a wide array of electron acceptors such as iron, manganese, and uranium, among others.[27] One of their most intriguing characteristics, however, is their ability to fix nitrogen in these environments. All characterized *Geobacter* spp. possess genes related to biological nitrogen fixation, and some species such as *G. metallireducens* and *G. sulfurreducens* have positively shown nitrogenase activity and expression of N_2 fixation genes under limited fixed nitrogen

conditions.[28,29] The model and representative species of this genus, *G. sulfurreducens*, has several genes and regulons related to this process.[30] Therefore, it would be unsurprising that *Geobacter* spp. can thrive through anode respiration and N_2 fixation conditions in METs. As mentioned in chapter 1, METs offer the possibility of utilizing external electrochemical inputs to stimulate N_2 fixation due to the reductive nature of the process. Utilizing anaerobic METs, such as microbial electrolysis cells (MECs) enriched with *Geobacter*, are thus a novel possibility to develop a responsive system that can be optimized for N_2 conversion into ammonium (NH_4^+). The implications of selecting this technology are researched in the following chapters to understand the performance of diazotrophic *Geobacter* spp. in METs and their role in establishing successful anodic biofilms with optimal N_2 fixation capabilities.

Chapter 2 References

(1) Rojas, C.; Vargas, I. T.; Bruns, M. A.; Regan, J. M. Electrochemically Active Microorganisms from an Acid Mine Drainage-Affected Site Promote Cathode Oxidation in Microbial Fuel Cells. *Bioelectrochemistry* **2017**, *118*, 139–146. https://doi.org/10.1016/j.bioelechem.2017.07.013.

(2) Potter, M. C. Electrical Effects Accompanying the Decomposition of Organic Compounds. *Proc. R. Soc. B Biol. Sci.* **1911**, *84* (571), 260–276. https://doi.org/10.1098/rspb.1911.0073.

(3) Kim, H. J.; Park, H. S.; Hyun, M. S.; Chang, I. S.; Kim, M.; Kim, B. H. A Mediator-Less Microbial Fuel Cell Using a Metal Reducing Bacterium, *Shewanella putrefaciens*. *Enzyme Microb. Technol.* **2002**, *30* (2), 145–152. https://doi.org/10.1016/S0141-0229(01)00478-1.

(4) Mo, W.; Zhang, Q. Energy–Nutrients–Water Nexus: Integrated Resource Recovery in Municipal Wastewater Treatment Plants. *J. Environ. Manage.* **2013**, *127*, 255–267. https://doi.org/10.1016/j.jenvman.2013.05.007.

(5) Logan, B. E.; Hamelers, B.; Rozendal, R.; Schröder, U.; Keller, J.; Freguia, S.; Aelterman, P.; Verstraete, W.; Rabaey, K. Microbial Fuel Cells: Methodology and Technology. *Environ. Sci. Technol.* **2006**, *40* (17), 5181–5192. https://doi.org/10.1021/es0605016.

(6) Logan, B. E.; Wallack, M. J.; Kim, K.-Y.; He, W.; Feng, Y.; Saikaly, P. E. Assessment of Microbial Fuel Cell Configurations and Power Densities. *Environ. Sci. Technol. Lett.* **2015**, *2* (8), 206–214. https://doi.org/10.1021/acs.estlett.5b00180.

(7) Reguera, G.; McCarthy, K. D.; Mehta, T.; Nicoll, J. S.; Tuominen, M. T.; Lovley, D. R. Extracellular Electron Transfer via Microbial Nanowires. *Nature* **2005**, *435* (7045), 1098–1101. https://doi.org/10.1038/nature03661.

(8) Qiao, Y.; Bao, S.-J.; Li, C. M. Electrocatalysis in Microbial Fuel Cells—from Electrode Material to Direct Electrochemistry. *Energy Environ. Sci.* **2010**, *3* (5), 544. https://doi.org/10.1039/b923503e.

(9) Lefebvre, O.; Uzabiaga, A.; Chang, I. S.; Kim, B.-H.; Ng, H. Y. Microbial Fuel Cells for Energy Self-Sufficient Domestic Wastewater Treatment—a Review and Discussion from Energetic Consideration. *Appl. Microbiol. Biotechnol.* **2011**, *89* (2), 259–270. https://doi.org/10.1007/s00253-010-2881-z.

(10) Logan, B. E.; Call, D.; Cheng, S.; Hamelers, H. V. M.; Sleutels, T. H. J. A.; Jeremiasse, A. W.; Rozendal, R. A. Microbial Electrolysis Cells for High Yield Hydrogen Gas Production from Organic Matter. *Environ. Sci. Technol.* **2008**, *42* (23), 8630–8640. https://doi.org/10.1021/es801553z.

(11) Call, D.; Logan, B. E. Hydrogen Production in a Single Chamber Microbial Electrolysis Cell Lacking a Membrane. *Environ. Sci. Technol.* **2008**, *42* (9), 3401–3406. https://doi.org/10.1021/es8001822.

(12) Cusick, R. D.; Bryan, B.; Parker, D. S.; Merrill, M. D.; Mehanna, M.; Kiely, P. D.; Liu, G.; Logan, B. E. Performance of a Pilot-Scale Continuous Flow Microbial Electrolysis Cell Fed Winery Wastewater. *Appl. Microbiol. Biotechnol.* **2011**, *89* (6), 2053–2063. https://doi.org/10.1007/s00253-011-3130-9.

(13) Escapa, A.; San-Martín, M. I.; Mateos, R.; Morán, A. Scaling-up of Membraneless Microbial Electrolysis Cells (MECs) for Domestic Wastewater Treatment: Bottlenecks and Limitations. *Bioresour. Technol.* **2015**, *180*, 72–78. https://doi.org/10.1016/j.biortech.2014.12.096.

(14) Howarth, R. W.; Santoro, R.; Ingraffea, A. Methane and the Greenhouse-Gas Footprint of Natural Gas from Shale Formations. *Clim. Change* **2011**, *106* (4), 679–690. https://doi.org/10.1007/s10584-011-0061-5.

(15) Kundu, A.; Sahu, J. N.; Redzwan, G.; Hashim, M. A. An Overview of Cathode Material and Catalysts Suitable for Generating Hydrogen in Microbial Electrolysis Cell. *Int. J. Hydrogen Energy* **2013**, *38* (4), 1745–1757. https://doi.org/10.1016/j.ijhydene.2012.11.031.

(16) Rabaey, K.; Girguis, P.; Nielsen, L. K. Metabolic and Practical Considerations on Microbial Electrosynthesis. *Curr. Opin. Biotechnol.* **2011**, *22* (3), 371–377. https://doi.org/10.1016/j.copbio.2011.01.010.

(17) Nevin, K. P.; Woodard, T. L.; Franks, A. E.; Summers, Z. M.; Lovley, D. R. Microbial Electrosynthesis: Feeding Microbes Electricity To Convert Carbon Dioxide and Water to Multicarbon Extracellular Organic Compounds. *MBio* **2010**, *1* (2). https://doi.org/10.1128/mBio.00103-10.

(18) Schröder, U. Anodic Electron Transfer Mechanisms in Microbial Fuel Cells and Their Energy Efficiency. *Phys. Chem. Chem. Phys.* **2007**, *9* (21), 2619–2629. https://doi.org/10.1039/B703627M.

(19) Yang, Y.; Xu, M.; Guo, J.; Sun, G. Bacterial Extracellular Electron Transfer in Bioelectrochemical Systems. *Process Biochem.* **2012**, *47* (12), 1707–1714. https://doi.org/10.1016/j.procbio.2012.07.032.

(20) Logan, B. E. Exoelectrogenic Bacteria That Power Microbial Fuel Cells. *Nat. Rev. Microbiol.* **2009**, *7* (5), 375–381. https://doi.org/10.1038/nrmicro2113.

(21) Grobbler, C.; Virdis, B.; Nouwens, A.; Harnisch, F.; Rabaey, K.; Bond, P. L. Effect of the Anode Potential on the Physiology and Proteome of *Shewanella oneidensis* MR-1. *Bioelectrochemistry* **2018**, *119*, 172–179. https://doi.org/10.1016/j.bioelechem.2017.10.001.

(22) Kotloski, N. J.; Gralnick, J. A. Flavin Electron Shuttles Dominate Extracellular Electron Transfer by *Shewanella oneidensis*. *MBio* **2013**, *4* (1). https://doi.org/10.1128/mBio.00553-12.

(23) Nevin, K. P.; Kim, B.-C.; Glaven, R. H.; Johnson, J. P.; Woodard, T. L.; Methé, B. A.; DiDonato, R. J.; Covalla, S. F.; Franks, A. E.; Liu, A.; Lovley, D. R. Anode Biofilm Transcriptomics Reveals Outer Surface Components Essential for High Density Current Production in *Geobacter sulfurreducens* Fuel Cells. *PLoS One* **2009**, *4* (5), e5628. https://doi.org/10.1371/journal.pone.0005628.

(24) Shi, L.; Richardson, D. J.; Wang, Z.; Kerisit, S. N.; Rosso, K. M.; Zachara, J. M.; Fredrickson, J. K. The Roles of Outer Membrane Cytochromes of *Shewanella* and *Geobacter* in Extracellular Electron Transfer. *Environ. Microbiol. Rep.* **2009**, *1* (4), 220–227. https://doi.org/10.1111/j.1758-2229.2009.00035.x.

(25) Nevin, K. P.; Richter, H.; Covalla, S. F.; Johnson, J. P.; Woodard, T. L.; Orloff, A. L.; Jia, H.; Zhang, M.; Lovley, D. R. Power Output and Columbic Efficiencies from Biofilms of *Geobacter sulfurreducens* Comparable to Mixed Community Microbial Fuel Cells. *Environ. Microbiol.* **2008**, *10* (10), 2505–2514. https://doi.org/10.1111/j.1462-2920.2008.01675.x.

(26) Yamamoto, S.; Suzuki, K.; Araki, Y.; Mochihara, H.; Hosokawa, T.; Kubota, H.; Chiba, Y.; Rubaba, O.; Tashiro, Y.; Futamata, H. Dynamics of Different Bacterial Communities Are Capable of Generating Sustainable Electricity from Microbial Fuel Cells with Organic Waste. *Microbes Environ.* **2014**, *29* (2), 145–153. https://doi.org/10.1264/jsme2.ME13140.

(27) Reguera, G.; Kashefi, K. The Electrifying Physiology of *Geobacter* Bacteria, 30 Years On; 2019; pp 1–96. https://doi.org/10.1016/bs.ampbs.2019.02.007.

(28) Bazylinski, D. A.; Dean, A. J.; Schuler, D.; Phillips, E. J. P.; Lovley, D. R. N_2-Dependent Growth and Nitrogenase Activity in the Metal-Metabolizing Bacteria, *Geobacter* and *Magnetospirillum* Species. *Environ. Microbiol.* **2000**, *2* (3), 266–273. https://doi.org/10.1046/j.1462-2920.2000.00096.x.

(29) Holmes, D. E.; Chaudhuri, S. K.; Nevin, K. P.; Mehta, T.; Methé, B. A.; Liu, A.; Ward, J. E.; Woodard, T. L.; Webster, J.; Lovley, D. R. Microarray and Genetic Analysis of Electron Transfer to Electrodes in *Geobacter sulfurreducens*. *Environ. Microbiol.* **2006**, *8* (10), 1805–1815. https://doi.org/10.1111/j.1462-2920.2006.01065.x.

(30) Methe, B. A. Genome of Geobacter Sulfurreducens: Metal Reduction in Subsurface Environments. *Science*. **2003**, *302* (5652), 1967–1969. https://doi.org/10.1126/science.1088727.

Figures

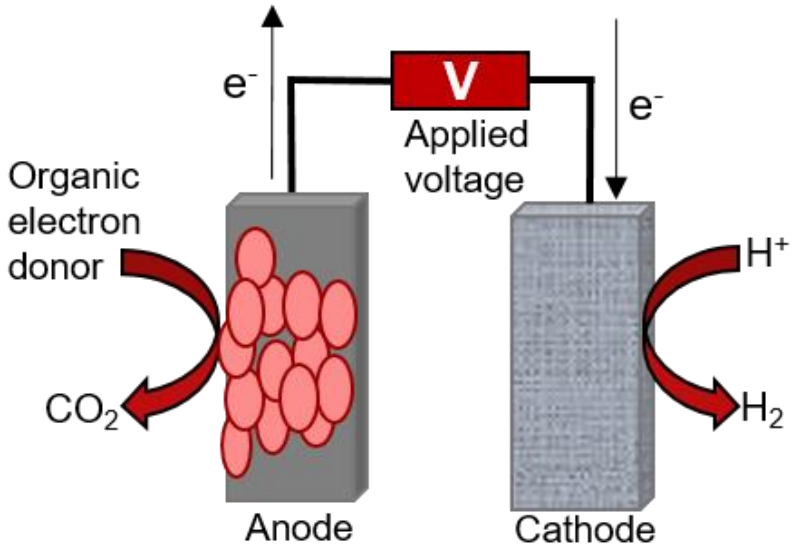

Figure 2.1. Schematic representation of a microbial electrolysis cell (MEC), a typical design of a microbial electrochemical technology (MET). Exoelectrogenic bacteria (depicted as pink ovals) are able to respire on the anode, transferring electrons gained from oxidation of an organic electron to that electrode. If the reaction is favorable, those electrons should be able to reach the cathode where a reduction process completes the circuit. In the case of MECs, an external electric input, such as applied voltage (E_{AP}), is added to drive cathodic production of hydrogen gas (H_2).

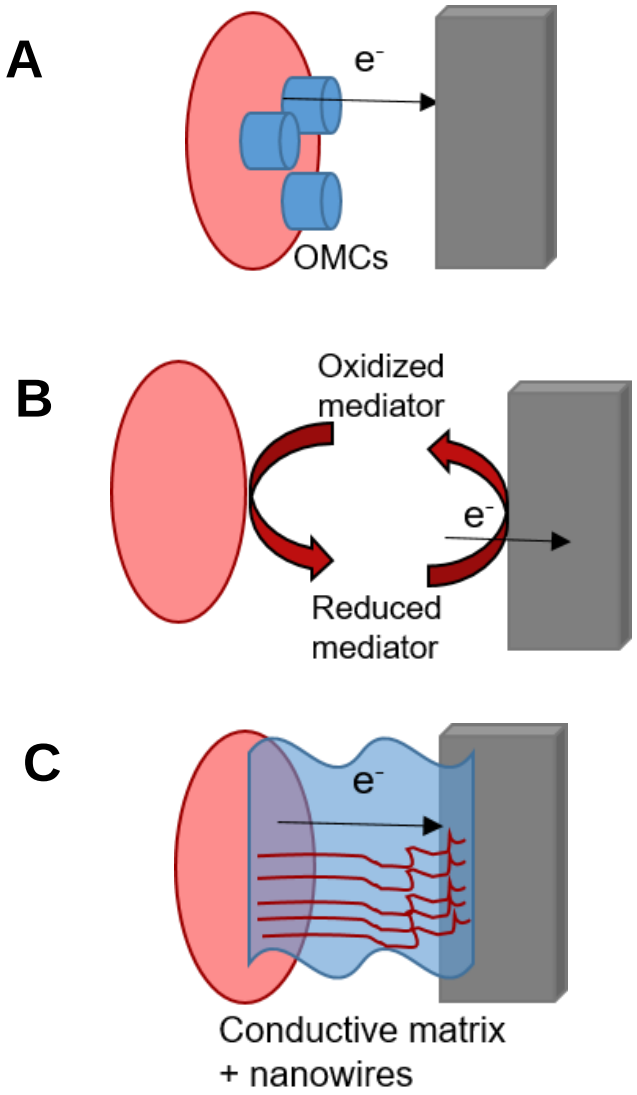

Figure 2.2. Mechanisms of extracellular electron transfer performed by exoelectrogenic bacteria (pink oval). A) outer membrane cytochromes (OMC), which are expressed on bacterial cell surface and transfer electrons directly. B) Mediators or electron shuttles, that carry the electrons throughout the growth medium to the anode. C) Formation of a conductive matrix and connection with nanowires, both transporting electrons if the cells are at a considerable distance from the electrode.

CHAPTER 3

ELECTROCHEMICAL AND MICROBIOLOGICAL CHARACTERIZATION OF BIOANODE COMMUNITIES EXHIBITING VARIABLE LEVELS OF STARTUP ACTIVITY

Abstract

Microbial electrochemical technologies (MET) require the establishment of anode biofilms to generate electrical current. The factors driving bioanode formation and their variability during startup remain unclear, leading to a lack of effective strategies to initiate larger-scale systems. Accordingly, our objective was to characterize the electrochemical properties and microbial community structure of a large set of replicate bioanodes during their first cycle of current generation. To do this, we operated eight bioanode replicates at each of two fixed electrode potentials [−0.15 V and +0.15 V vs. standard hydrogen electrode (SHE)] for one fed-batch cycle. We found that startup time decreased and maximum current generation increased at +0.15 V compared to −0.15 V, but at both potentials the bioanode replicates clustered into three distinct activity levels based on when they initiated current. Despite a large variation in current generation across the eight +0.15 V bioanodes, bioanode resistance and abundance of *Geobacter* species remained quite similar, differing by only 10% and 12%, respectively. At −0.15 V, current production strongly followed *Geobacter* species abundance and bioanode resistance, wherein the largest abundance of *Geobacter* was associated with the lowest charge transfer resistance. Our findings show that startup variability occurs at both applied potentials, but the underlying electrochemical and microbial factors driving variability are dependent on the applied potential.

This chapter has been published as

Ortiz-Medina, J.F., Call, D.F. Electrochemical and Microbiological Characterization of Bioanode Communities Exhibiting Variable Levels of Startup Activity. *Front. Energy Res.* **2019**, 7,103.

3.1 Introduction

Microbial electrochemical technologies (METs) convert organic material, such as wastewater, into electricity, hydrogen gas, or commodity chemicals.[1] Over the past few decades, these technologies have advanced from lab- to demonstration-scales.[2] A challenge facing larger-scale systems is the unpredictable and erratic behavior during the initiation of current or what is frequently referred to as reactor startup.[3,4] Identifying the underlying reasons for this behavior and how to improve startup is therefore paramount for the success of these technologies.

Despite the important role that electricity-generating microorganisms, or exoelectrogens, play in initiating current, most of our knowledge of their function and composition comes from bioanodic communities operated over long time scales.[5] The most common enrichment procedure used to study these communities is to operate them throughout several cycles (in a batch system) until a stable current output is reached.[3,6] Typically after at least one month of operation, bioanodes converge to similar electrochemical properties and community structure regardless of the inoculum source and operational conditions such as the anode potential.[3,7,8] Most of these studies agree that exoelectrogens with efficient pathways of extracellular electron transfer (EET), such as members of the genus *Geobacter*, play a pivotal role in generating current and decreasing anode charge transfer resistance.[9,10]

Bioanode properties during startup are less understood. Understanding startup behavior is important because many pilot-scale systems have reported significant delays (e.g., months) to

initiate current.[4,11,12] It is frequently observed, but not discussed, in long-term studies that a high degree of variable electrochemical performance across replicates occurs during startup,[7,13] but the underlying factors driving the variation remain unclear. This can ultimately influence the predictability and reproducibility of bioanodes over the long term, as shown in several studies that observe this erratic behavior.[4,14–16] Insufficient replicates is an additional factor leading to this unpredictability, as it obscures a possible consensus on startup time, expected current, and influence of the microbial community. This causes conflicting results from which decisions about optimal electrochemical conditions for bioanode startup are determined, such as which fixed anode potential to choose.[8,17–19] The initial enrichment stage of bioanodes is further complicated by the fact that different outcomes during acclimation are influenced by both stochastic and deterministic factors, which are dictated by microbial community dynamics.[13]

The objective of this study was to characterize the electrochemical behavior and community structure of bioanode communities during startup as a function of anode potential. Two anode potentials were selected in order to create two different energy-harvesting conditions for the bioanodes. A lower anode potential of −0.15 V [vs. standard hydrogen electrode (SHE)] was chosen to impart a lower driving force for extracellular electron transfer (EET), and a higher potential of +0.15 V, which increases the EET rate, was selected to represent conditions under which the microorganisms could better exploit the available energy.[20] Eight replicates at each anode potential were included in order to assess factors associated with startup variability, and all reactors were inoculated with the same enrichment culture (domestic wastewater) and electron donor (acetate). At the end of the first cycle, the bioanode electrochemical properties were measured using cyclic voltammetry and electrochemical impedance spectroscopy (EIS) and the community profile analyzed using high-throughput Illumina sequencing. Our findings show that

startup variability occurs at both applied potentials, but the underlying electrochemical and microbial factors driving the variability are dependent on the applied potential.

3.2 Materials and methods

3.2.1. Reactor assembly and configuration

Microbial electrolysis cells (MECs) were based on a polycarbonate circular chamber design (28 mL empty volume) as previously described.[21] This configuration fixed the electrode spacing across the replicates (2.3 ± 0.1 cm between anode and cathode). We selected a single-chamber design for this study because compared to two-chamber designs using membrane separators, it lowers resistance and eliminates detrimental pH gradients. The electrodes and their pretreatment were based on previous methods.[8,22] Briefly, the anodes were graphite plates (2 × 2 cm; GraphiteStore.com, Inc., Northbrook, IL) pretreated by polishing with sandpaper (grit type 400), soaked in a 1 M HCl solution overnight, and rinsed and stored in DI water until used. The cathodes were stainless steel mesh (4 cm diameter; Type 304, mesh size 50 × 50; McMaster-Carr, Elmhurst, IL). The current collectors were titanium wire (anode) and stainless steel wire (cathode). Each MEC was adjusted until the contact resistance between electrodes and current collectors was < 0.7 Ω. To fix the anode potentials, Ag/AgCl reference electrodes (~200 mV vs. SHE) were installed equidistant between the anode and cathode. All reference electrodes were checked against a calibrated saturated calomel electrode (SCE) to ensure that the difference in potential between them and the SCE was < 1 mV.

3.2.2 Microbial enrichment and chronoamperometry

To perform the microbial enrichment, effluent from the primary clarifier of a domestic wastewater treatment plant (~300 mg/L COD) was mixed in equal proportions with 100 mM

phosphate buffer, 1 g/L sodium acetate (780 mg/L COD) as the electron donor, and 10 mL/L of both Wolfe's trace vitamin and mineral solutions.[22] The contribution of acetate and wastewater to the total COD was 84% and 16%, respectively. We amended our MECs with acetate to promote the growth of exoelectrogens and reduce diversion of electrons to other pathways, such as fermentation. Enhancing exoelectrogen growth allowed us to better understand differences across bioreactors that initiated current quickly, slowly, or not at all and is consistent with other lab-scale investigations[10,15,18,23] and amendment practices in some larger-scale systems.[4,24–26] Cathodically-generated H_2 gas may have been present and consumed as an electron donor as well by the microbial communities; thus, our design best represents applied systems operating without a membrane separator (e.g., MEC-amended anaerobic digesters).[27,28] The reactors were connected to a potentiostat (Bio-Logic Science Instruments, Knoxville, TN) and operated at different fixed anode potentials (E_{AN}): −0.15 V or +0.15 V (both vs. SHE) or open circuit voltage (OCV). These potentials were chosen because they provide different scenarios of energy harvesting by microorganisms based on EET kinetics. The lower potential (−0.15 V) represents a smaller driving force that yields slower EET rates. The higher potential (+0.15 V) enables higher EET rates, and in turn more optimized energy harvesting from the available energy.[20] Eight replicates for each of the three anode treatments were operated. Preliminary tests were conducted to assess when maximum current was reached for each E_{AN}. These values were 5.5 days for −0.15 V and 5.0 days for +0.15 V. Bioanodes at OCV were operated for 5.0 days. All reactors were operated at a constant 30°C.

3.2.3 Electrochemical characterization

To characterize the electrochemical properties of the bioanodes, cyclic voltammograms (CVs) were collected at a scan rate of 1 mV/s, ranging from −0.3 V to +0.5 V vs SHE. A single CV cycle was performed to avoid a prolonged effect of varying the potential on the subsequent microbial community analysis. Electrochemical impedance spectroscopy (EIS) was conducted to determine the total and component resistances of the bioanodes. The bioanodes were operated for 30 minutes at their respective enrichment E_{AN} (−0.15 V or +0.15 V) and the frequency was varied from 0.1 MHz to 10 mHz with a 10 mV perturbation amplitude. Both CVs and EIS were performed at the end of the chronoamperometry measurements. To initially characterize the reactors and ensure that all replicates agreed within 10%, both techniques were likewise performed at the start of the experiments with the reactors filled with 50 mM phosphate buffer and no inoculum. The same techniques were conducted in an identical manner on the OCV controls, but with the anode potential held at OCV during EIS instead of one of the two E_{AN}. Depending on the bioanode impedance behavior, data from the EIS tests were fitted using equivalent circuits similar to single and double-time constant models (**Appendix A**), which have been used previously.[29,30] The resistances in the model were attributed to solution resistance (R_s) and charge transfer resistances (R_{ct}, $R_{ct,2}$). Model fitting was performed using the function Z-Fit on the EC-Lab software, version 11.10, by minimizing the Chi-Square values of each system.

3.2.4 Microbial community visualization and analysis

After the electrochemical analyses were completed, the MECs were disassembled and the bioanodes processed for further analysis. To observe the extent of microbial colonization of the anodes, one piece of every electrode was visualized using scanning electron microscopy (SEM).

The samples were placed in a 2.5% glutaraldehyde solution overnight, dehydrated in ethanol, and dried for 2 h at 30°C.[31] Before imaging, the samples were coated with a gold/palladium layer for 2 min at 12 mA under an argon atmosphere. The sample was visualized using a Hitachi S-3200N variable pressure scanning electron microscope (Hitachi High-Technologies, Japan) with an accelerating voltage of 5 kV and a working distance of 23 mm.

To analyze the microbial community composition and diversity, samples from the anodic biofilm and the suspension were obtained. Anodic biofilm was scraped using a sterile blade. For the suspension samples, 10 ml of reactor effluent was collected in 15 ml centrifuge tubes, then centrifuged at 4000 rpm for 20 min. DNA from the biofilm and suspension pellets was extracted using a PowerSoil® DNA isolation kit (MO BIO Laboratories, Carlsbad, CA) following the manufacturer's instructions. The V3 and V4 regions of the 16S rRNA gene were amplified using the forward primer 5' TCGTCGGCAGCGTCAGATGTGTATAAGAGACAGCCTACGGGNG-GCWGCAG 3' and the reverse primer 5' GTCTCGTGGGCTCGGAGATGTGTATAAGAGA-CAGGACTACHVGGGTATCTAATCC 3' for Illumina sequencing, using the protocol provided by the company.[32] The samples were sequenced using the Illumina MiSeq platform (Illumina Inc., San Diego, CA), with a paired-end sequencing of 300 base pairs (bp) length. The sequencing data was deposited into the GenBank database of the National Center of Biotechnology Information (NCBI), under the BioProject accession number PRJNA559682.

To establish the composition and compare microbial communities, the software QIIME was utilized.[33] After alignment, the samples were clustered into operational taxonomic units (OTU) by performing open-reference picking with the UCLUST algorithm, using 97% sequence similarity as the threshold and following the default commands available at the developers' website.[34] After OTU classification at the genus level, the generated data was further processed in

the R platform. Shannon (H) diversity indexes were calculated to assess the diversity of the studied samples, while Principal Component Analysis (PCA) plots were constructed to visualize the relationship between community composition and bioanode performance. Both were generated in R with the help of the vegan[35] and phyloseq packages.[36]

3.3 Results and discussion

3.3.1 Current generation during bioanode initiation

We first examined current densities (I_A) over time during the startup period. Despite identical inoculum, reactor design, and operating conditions, I_A was highly variable across the eight replicates for each E_{AN} (**Fig. 3.1**). To quantify variability, we defined startup time as the point when the bioanodes reached 0.1 A/m^2 [dashed line in **Fig. 3.1A and B**; selected based on similar thresholds used in other MET startup studies [23,37]]. Bioanodes that did not reach this value after five (+0.15 V) or 5.5 days (−0.15 V) were defined as inactive. Based on this definition, three bioanodes were inactive at −0.15 V and one was inactive at +0.15 V. The remaining bioanodes clustered into two levels: 1) high-activity, which reached the 0.1 A/m^2 threshold the fastest, and 2) low-activity, which were the slowest to reach the threshold (**Fig. 3.1B**).

Considering only the high- and low-activity bioanodes, there were appreciable differences during the startup period within and across each E_{AN}. At +0.15 V, the high-activity bioanodes required 3.91 ± 0.06 days and the low-activity bioanodes required 4.28 ± 0.10 days to reach the startup threshold. At −0.15 V, the high- and low-activity reactors took significantly longer to reach the threshold than those at +0.15 V (*t*-test, $p < 0.05$), requiring 4.60 ± 0.03 and 5.32 ± 0.16 days, respectively. Maximum I_A followed a similar trend as the startup time, wherein bioanodes at +0.15 V reached higher maximum I_A than those at −0.15 V for all activity levels. Bioanode startup

activity level largely agreed with the maximum current behavior. The exception was one bioanode at +0.15 V, which classified as high-activity with respect to startup time but did not reach the same I_A as the other high-activity bioanodes. This bioanode ended the cycle at the same level of current as the +0.15 V low-activity bioanodes.

The startup behavior of METs varies widely across the literature, and our results are consistent with some, but not all, prior reports. The high degree of startup variability that we observed is often not discussed (or reported) in other studies that use triplicate or duplicate reactors, even though there is a clear need to operate enough replicates to characterize possible outcomes.[7] Zhou et al.,[13] which is one of the only studies to use more than triplicate reactors, reported a wide range of startup times (~1–12 days) across 14 replicates, which is consistent with our findings. The effect of E_{AN} on startup varies across studies. Using a microbial fuel cell (MFC) with a cloth separator between the electrodes, Zhang et al.[14] showed that wastewater-inoculated reactors at +0.2 V started up more quickly than those at −0.2 V. Faster startup at less negative potentials has been reported in other studies as well, in both single-chamber[17] and double-chamber systems.[37,38] While one explanation for this behavior is the higher energy harvested due to higher EET rates,[20] a selection of exoelectrogens with more efficient EET mechanisms at higher potential has also been proposed.[37] Conversely, Torres et al.,[18] using a double-chamber system with multiple anodes in one chamber, observed a faster startup and higher maximum current density at more negative anode potentials. They attributed this behavior to the selection of microorganisms (e.g., *Geobacter sulfurreducens*) that could harvest energy and transfer electrons efficiently at such negative potentials. However, it is unclear if their unique multi-anode configuration played a role in their findings. Kumar et al.,[39] comparing single- and double-chamber MECs with the same inoculum, medium, and under continuous operation, observed that the single-chamber MEC displayed a

higher level of electrochemical activity at less negative potentials (0 V vs. SHE). Both configurations have inherent differences, such as cathodically-generated H_2 that can serve as an electron donor in single-chamber systems[40,41] and pH gradients in double-chamber reactors[42] that may influence bioanode enrichment and startup time. Reactor configurations thus play an additional factor that needs to be considered during research on startup behavior.

3.3.2 Cyclic voltammetry

To investigate the electrochemical properties of the bioanodes, we used cyclic voltammetry at the end of the startup cycle. Cyclic voltammetry reveals electron transfer kinetics between microorganisms and the electrode across a range of bioanode potentials, as well as possible electron transfer mechanisms.[43] The CVs clustered according to the activity levels defined above and had limiting currents ($i_{l,a}$) that were generally proportional to the maximum current densities recorded during startup (**Fig. 3.2**). The CVs of bioanodes that did not reach the startup threshold closely followed the OCV control. All other bioanodes generated a sigmoidal shaped CV regardless of E_{AN}, which is indicative of a self-regenerating electron transfer process that is typical in mediatorless, exoelectrogenic biofilms.[9,14,44] These same bioanodes showed a similar midpoint potential ($E_{1/2}$) at −0.18 ± 0.01 V (dashed vertical line in **Fig. 3.2**) and potential (E_p; *ca*. –0.1 V) where maximum oxidative current (i_p) was reached, which further confirms the presence of a primary electron transfer pathway utilized by the biofilm across E_{AN} and levels of activity. This behavior is frequently associated with bioanodes dominated by *Geobacter* spp., which normally show sigmoidal-shaped voltammograms and midpoint potentials between −0.16 V and −0.22 V due to the outer membrane cytochromes expressed by these organisms.[8,45,46] This suggests that

Geobacter spp. were primarily involved in extracellular electron transfer on our bioanodes during startup.

The most notable effect of E_{AN} was observed in the CV behavior of the high-activity bioanodes. Although bioanodes at both E_{AN} showed similar sigmoidal curves and i_p values, after the sweeping potential increased beyond E_p, the current produced by the two high-activity bioanodes enriched at –0.15 V dropped sharply by ~25% (**Fig. 3.2A**). Current slightly increased with potential, but did not exceed i_p. In contrast, the bioanodes enriched at +0.15 V did not show the same drop in current; current remained similar to i_p after passing E_p (**Fig. 3.2B**). Both behaviors at similar E_{AN} in other studies have been consistently observed in full grown biofilms.[8,9,37,47] One explanation for this difference is that at +0.15 V, electron transfer rates operated near their maximum because this potential provided a larger driving force for electron flow through the cell.[20] This is consistent with previous reports that at potentials beyond which i_p occurs, electron transfer rates do not increase substantially because they are kinetically limited by intracellular electron carriers (e.g., NAD^+/NADH).[9,20,48] At –0.15 V, the bioanodes were subject to a lower driving force, and in turn lower electron turnover rates.

It is known that biofilms dominated by *Geobacter* spp. express different pathways, regulated by inner membrane cytochromes, to allow growth using electron acceptors at different potentials. This has been demonstrated by the presence of different oxidation peaks as a function of E_{AN}.[47,49] One electron transfer pathway, the CbcL-dependent pathway, operates at redox potentials below –0.10 V,[50] whereas at E_{AN} above this value, the ImcH-dependent pathway is expressed to harvest additional energy.[51] The CbcL pathway has been reported to contribute significantly (at least 60%) to electron transfer, even in bioanodes formed at higher E_{AN} and its deletion shifts the midpoint potential to values around –0.1 V.[50] It is thus possible that the

bioanodes at –0.15 V expressed a pathway that was not adapted to EET at more positive E_{AN}, which is consistent with the current drop after i_p. Differences in the expression and activity of these two pathways are therefore the likely reasons for the different CV profiles at –0.15 V and +0.15 V.

3.3.3 Electrochemical impedance spectroscopy

Bioanode impedance profiles, which characterize the biofilm-electrode interface in terms of resistance and capacitance elements, were dependent on activity level for the bioanodes enriched at −0.15 V, but not +0.15 V (**Fig. 3.3**). The majority of the bioanode profiles (all except the high-activity −0.15 V bioanodes) reflected a single characteristic impedance semi-circle. Those profiles could be fitted to an equivalent circuit that considers the solution resistance (R_s) and a single charge transfer resistance (R_{ct}) circuit.[30] For all bioanodes (both −0.15 V and +0.15 V), R_s was 13 ± 4 Ω, which is low relative to the majority of the R_{ct} values. Other observable phenomena in the high frequency region of the semi-circle were perceived as too small (**Appendix A**) because including them during model fitting did not change the values of the other calculated resistances by more than 5%.

The impedance of the −0.15 V bioanodes decreased as the current recorded at the end of the startup period increased (**Fig. 3.3A**). The corresponding R_{ct} ranged from 24 Ω to 3.4 ×10^4 Ω between the bioanodes with the highest and the lowest current density, respectively. The high-activity bioanodes at −0.15 V had impedances that were up to 90% lower than the low-activity bioanodes (**Fig. 3.3A**). They generated Nyquist plots with double semicircles (**Appendix A**) that can be attributed to two charge transfer processes.[52] Such processes can be better distinguished in the phase angle Bode plot as two local minimums that become one as activity decreases and

impedance increases (**Appendix A**). Relative to the abiotic controls (i.e., prior to introducing the microorganisms), impedance of the low-activity bioanodes was lower and the inactive bioanodes was higher. The latter result suggests that electron transfer to the anode was slowed or inhibited. This may have been caused by growth of non-conductive biofilms[53] or presence of substances such as polysaccharides[54] that changed the anode surface conductivity. The similar impedance profile of these bioanodes and the OCV control (where microorganisms are present but not respiring on the anode) lends support for this hypothesis.

Bioanodes enriched at +0.15 V produced similar impedance profiles of single semi-circles, regardless of the startup current or the electrochemical activity reflected in the CVs (**Fig. 3.3B**). Total impedance did not increase dramatically in the low frequency region as was observed for the bioanodes at –0.15 V (**Appendix A**), and the phase angle only increased slightly relative to the initial response of the graphite anode (**Appendix A**). The average charge transfer resistances (R_{ct}), calculated by the aforementioned model fitting, were 3,140 ± 330 Ω and 2,140 ± 580 Ω for the high- and low-activity bioanodes, respectively. The differences in resistance cannot be explained by differences in the bioanode design, materials, connections, etc., because the impedance of each anode prior to inoculation was not related to the final activity obtained at both E_{AN} (**Appendix A**). Thus, higher current production at +0.15 V did not correlate with lower total resistance.

To better visualize the relationship between R_{ct} and bioanode activity level, R_{ct} of each bioanode was divided by the respective initial R_{ct} (calculated before inoculation). Plotting I_A against normalized charge transfer resistance (R_{ct}^*) yielded a linear relationship for the high- and low-activity (R^2 = 97%) bioanodes at −0.15 V (**Fig. 3.4**). Bioanodes at +0.15 V did not show a clear trend in terms of decrease in R_{ct}, and high-activity bioanodes had similar R_{ct}^* values as most of the low-activity bioanodes, but they had a much larger I_A (**Fig. 3.4**). Their larger maximum

current output in CVs indicates that despite appreciable resistance, these communities were highly efficient at transferring electrons to the anode.

3.3.4 Microbial colonization of the anodes

We visualized the bioanode surfaces to qualitatively assess relationships between the electrochemical characteristics described above and biofilm coverage. To do this, we captured SEM images of the bioanodes at the end of the startup cycle. At −0.15 V, the high-activity bioanodes were fully covered with a homogenous layer of microorganisms (**Fig. 3.5A**), and the low-activity bioanodes had little to no coverage (data not shown). At +0.15 V, biofilm coverage was patchy and heterogenous (**Fig. 3.5B**), with no clear difference between high- and low-activity bioanodes. Inactive bioanodes at both potentials showed a less defined colonization pattern (**Fig. 3.5C**), which was similar to the OCV controls (**Fig. 3.5D**).

Bioanode surface coverage was consistent with the EIS results. A more complete coverage of the anode minimizes charge transfer resistance.[46] This was observed in the high-activity bioanode impedance spectra at −0.15 V (**Fig. 3.3**). Thin biofilms and limited surface coverage are associated with larger charge transfer resistance, which was observed in the high- and low-activity bioanodes at +0.15 V. This implies that even though bioanode resistance was larger at +0.15 V, the per-cell EET rates at that potential were greater than at −0.15 V. Improved kinetics and optimization of energy-harvesting pathways at more positive anode potentials support this observation.[52,55] Overall, these results show that bioanode growth and activity occurs differently depending on E_{AN}.

3.3.5 Microbial community composition

Across low- and high-activity levels at both E_{AN}, sequences matching to *Geobacter* had the highest relative abundance in the biofilms (**Fig. 3.6**). The relative abundance of this genus was generally higher in bioanodes that produced the highest $I_{A,}$ which is more noticeable at −0.15 V (**Fig. 3.6A)** than +0.15 V (**Fig. 3.6B)**. A similar trend was found in suspension samples obtained from the bioreactors, where *Geobacter* abundance was generally related to the maximum I_A (**Appendix A**). *Geobacter* species are frequently enriched in METs supplied acetate as the electron donor, regardless of E_{AN}, and consist of several known exoelectrogens.[8] The use of single chamber MECs in this study may have contributed to the enrichment of this genus, as some species are able to utilize hydrogen gas (H_2) produced at the cathode as an additional electron donor.[40,41] Several other genera were present in the bioanodes, some of which may have participated in current generation. Genera, including *Sedimentibacter*, *Fusibacter*, *Pseudomonas*, and an unknown genus of the family Comamonadaceae, were detected. While the latter were found in the OCV controls, both *Sedimentibacter* and *Fusibacter* were not highly abundant (**Appendix A**). Comamonadaceae were present in the inoculum, although at a low abundance of around 2.5% (**Apendix A**). In the high-activity bioanodes, there was a greater abundance of *Pseudomonas* species at +0.15 V than −0.15 V. Some *Pseudomonas* species are exoelectrogenic, producing current through the use of electron shuttles.[56] A greater abundance of these bacteria at +0.15 V than −0.15 V is consistent with prior reports regarding the influence of E_{AN} on the thermodynamic favorability of electron transport mechanisms.[17,48]

To better visualize the relationship between community composition and bioanode performance, a principal component analysis (PCA) biplot was constructed (**Fig. 3.7**). In this plot, genera are represented as vectors, and the points depict each bioanode and its corresponding

current output at the end of the startup cycle. Points located along the axis of a vector contain a higher relative abundance of those respective genera, and the length of the vector indicates possible influence of the corresponding microorganism on the distribution of samples.[57] The genus *Geobacter* was the primary influence affecting bioanode activity level at both E_{AN}. Its vector aligns well with the horizontal axis that explains more than 90% of the observed variation. Bioanodes with the highest activity levels are closest to this vector. In contrast, samples corresponding to inactive bioanodes are located in the opposite direction of this vector, indicating a lower presence of *Geobacter* spp. The other enriched microorganisms, *Sedimentibacter* and *Fusibacter* spp., had a stronger influence on the low- and high-activity bioanodes at +0.15 V than −0.15 V. These microorganisms have been detected in METs exhibiting stable electrochemical performance.[58] Although their function in an electrically conductive biofilm is unclear, their presence in early biofilm formation suggests a possible role during startup. In contrast, vectors of microorganisms such as Comamonadaceae and *Pseudomonas* spp. are directed towards inactive reactors and the OCV controls.

In all bioanodes, a higher abundance of *Geobacter* resulted in lower community diversity. By plotting the Shannon index (H), an indicator of microbial diversity, against the current density recorded at the end of the startup cycle, we found that diversity at both E_{AN} decreased as I_A increased (**Fig. 3.8**); however, the rate of decrease was much faster at −0.15 V than +0.15 V. This result can be explained by the greater selection pressure at −0.15 V. The thermodynamic driving force for EET is lower at –0.15 V than +0.15 V; thus it favors microorganisms that can regulate electron transfer pathways to capture energy under challenging thermodynamic conditions.[20] Microorganisms that use electron transport mechanisms, such as electron shuttles, that have more positive midpoint potentials than −0.15 V are limited by thermodynamic constraints.[18]

Comparatively, at +0.15 V, the thermodynamics are favorable for a wider range of microorganisms and/or electron transfer mechanisms.[18]

The more selective nature of –0.15 V is one possible reason why there was a higher number of inactive bioanodes at –0.15 V. Since the driving force for energy harvesting is lower at –0.15 V than +0.15 V, external forces that influence bioanode colonization and respiration, such as alternative electron acceptors, may have a stronger impact on biofilm development than at +0.15 V. We hypothesize that under those conditions, competition of *Geobacter* spp. with other microorganisms that are able to use the same electron donor and breathe on traces of other electron acceptors such as oxygen becomes more pronounced.[59,60] The relatively low abundance of *Geobacter* in inactive reactor bioanodes and suspension supports this hypothesis.

Coupling the microbial community data with the electrochemical properties described above, several interesting observations can be made. First, the relative abundance of *Geobacter* was closely linked with bioanode electrochemical behavior at −0.15 V, but not +0.15 V. From the low- to high-activity bioanodes at +0.15 V, the relative abundance of *Geobacter* deviated by only 12% and ranged from 44.5% to 62.3%. This trend matches well with the impedance data, wherein the total resistance across these same bioanodes varied by 10%. In contrast, at −0.15 V the relative abundance of *Geobacter* increased from 25.1% to 90.0% across these same activity levels, resulting in a total deviation of at least 53% compared to the average of all activity levels. Total bioanode resistance followed this pattern, with a 91% decrease in resistance between the low- to high-activity bioanodes. One possible explanation for why impedance did not vary with activity level for the +0.15 V bioanodes is that that potential selected for an EET pathway (i.e., from the terminal cytochrome to electrode) that was highly optimized for electron transfer to the anode. In that case, the rate of electron flow would depend on internal electron transfer processes (i.e.,

electron transport prior to EET) which would be a function of the "maturity", or activity level, of those internal pathways during startup.

3.4. Conclusions

Our overall objective was to determine the impact of two anode potentials on the electrochemical and microbial characteristics of bioanodes during the first cycle of current generation. Within this objective, we also assessed the variability in these characteristics across a large (n = 8) set of replicates for each potential. We found that the anode potential [E_{AN}; –0.15 V, +0.15 V vs. standard hydrogen electrode (SHE)] had a strong impact on the amount of time required to initiate current, the electrochemical properties [measured by cyclic voltammograms (CVs) and electrochemical impedance spectroscopy (EIS)], and the resulting microbial community composition. Even though variability across replicates was large, three distinct bioanode activity levels (defined based on the time required to reach a current density threshold) emerged within each E_{AN}. Bioanodes fixed at −0.15 V required more time to initiate current, and total resistance was closely related to the startup current and abundance of *Geobacter* species in the biofilm. Bioanodes at +0.15 V initiated current faster and had less variability in total resistance and *Geobacter* abundance across bioanode activity levels. SEM images of the bioanodes were consistent with the electrochemical profiles. Highly active bioanodes at −0.15 V had homogeneous biofilm coverage whereas sparse colonization at +0.15 V was consistent with the higher total resistance at that potential. A larger decrease in community diversity with current production at −0.15 V indicated that this potential was more selective for *Geobacter* spp., whereas the more favorable exploitation of energy at +0.15 V allowed for a greater diversity of other microorganisms. Further studies are needed in order to gain a deeper insight of microbial dynamics

within the community that forms during the startup phase as a function of E_{AN}. Filling this knowledge gap may allow the design of more robust and predictable METs for practical applications.

Chapter 3 References

(1) Wang, H.; Ren, Z. J. A Comprehensive Review of Microbial Electrochemical Systems as a Platform Technology. *Biotechnol. Adv.* **2013**, *31* (8), 1796–1807. https://doi.org/10.1016/j.biotechadv.2013.10.001.

(2) Janicek, A.; Fan, Y.; Liu, H. Design of Microbial Fuel Cells for Practical Application: A Review and Analysis of Scale-up Studies. *Biofuels* **2014**, *5* (1), 79–92. https://doi.org/10.4155/bfs.13.69.

(3) Paitier, A.; Godain, A.; Lyon, D.; Haddour, N.; Vogel, T. M.; Monier, J. M. Microbial Fuel Cell Anodic Microbial Population Dynamics during MFC Start-Up. *Biosens. Bioelectron.* **2017**, *92* (September 2016), 357–363. https://doi.org/10.1016/j.bios.2016.10.096.

(4) Cusick, R. D.; Bryan, B.; Parker, D. S.; Merrill, M. D.; Mehanna, M.; Kiely, P. D.; Liu, G.; Logan, B. E. Performance of a Pilot-Scale Continuous Flow Microbial Electrolysis Cell Fed Winery Wastewater. *Appl. Microbiol. Biotechnol.* **2011**, *89* (6), 2053–2063. https://doi.org/10.1007/s00253-011-3130-9.

(5) Logan, B. E. Exoelectrogenic Bacteria That Power Microbial Fuel Cells. *Nat. Rev. Microbiol.* **2009**, *7* (5), 375–381. https://doi.org/10.1038/nrmicro2113.

(6) Hutchinson, A. J.; Tokash, J. C.; Logan, B. E. Analysis of Carbon Fiber Brush Loading in Anodes on Startup and Performance of Microbial Fuel Cells. *J. Power Sources* **2011**, *196* (22), 9213–9219. https://doi.org/10.1016/j.jpowsour.2011.07.040.

(7) Yates, M. D.; Kiely, P. D.; Call, D. F.; Rismani-Yazdi, H.; Bibby, K.; Peccia, J.; Regan, J. M.; Logan, B. E. Convergent Development of Anodic Bacterial Communities in Microbial Fuel Cells. *ISME J.* **2012**, *6* (11), 2002–2013. https://doi.org/10.1038/ismej.2012.42.

(8) Zhu, X.; Yates, M. D.; Hatzell, M. C.; Ananda Rao, H.; Saikaly, P. E.; Logan, B. E. Microbial Community Composition Is Unaffected by Anode Potential. *Environ. Sci. Technol.* **2014**, *48* (2), 1352–1358. https://doi.org/10.1021/es404690q.

(9) Marsili, E.; Sun, J.; Bond, D. R. Voltammetry and Growth Physiology of *Geobacter sulfurreducens* Biofilms as a Function of Growth Stage and Imposed Electrode Potential. *Electroanalysis* **2010**, *22* (7–8), 865–874. https://doi.org/10.1002/elan.200800007.

(10) Ter Heijne, A.; Schaetzle, O.; Gimenez, S.; Navarro, L.; Hamelers, B.; Fabregat-Santiago, F. Analysis of Bio-Anode Performance through Electrochemical Impedance Spectroscopy. *Bioelectrochemistry* **2015**, *106*, 64–72. https://doi.org/10.1016/j.bioelechem.2015.04.002.

(11) Hiegemann, H.; Herzer, D.; Nettmann, E.; Lübken, M.; Schulte, P.; Schmelz, K.-G.; Gredigk-Hoffmann, S.; Wichern, M. An Integrated 45 L Pilot Microbial Fuel Cell System at a Full-Scale Wastewater Treatment Plant. *Bioresour. Technol.* **2016**, *218*, 115–122. https://doi.org/10.1016/j.biortech.2016.06.052.

(12) Escapa, A.; San-Martín, M. I.; Mateos, R.; Morán, A. Scaling-up of Membraneless Microbial Electrolysis Cells (MECs) for Domestic Wastewater Treatment: Bottlenecks and Limitations. *Bioresour. Technol.* **2015**, *180*, 72–78. https://doi.org/10.1016/j.biortech.2014.12.096.

(13) Zhou, J.; Liu, W.; Deng, Y.; Jiang, Y.-H.; Xue, K.; He, Z.; Van Nostrand, J. D.; Wu, L.; Yang, Y.; Wang, A. Stochastic Assembly Leads to Alternative Communities with Distinct Functions in a Bioreactor Microbial Community. *MBio* **2013**, *4* (2), 8. https://doi.org/10.1128/mBio.00584-12.

(14) Zhang, F.; Xia, X.; Luo, Y.; Sun, D.; Call, D. F.; Logan, B. E. Improving Startup Performance with Carbon Mesh Anodes in Separator Electrode Assembly Microbial Fuel Cells. *Bioresour. Technol.* **2013**, *133*, 74–81. https://doi.org/10.1016/j.biortech.2013.01.036.

(15) Yanuka-Golub, K.; Reshef, L.; Rishpon, J.; Gophna, U. Community Structure Dynamics during Startup in Microbial Fuel Cells - The Effect of Phosphate Concentrations. *Bioresour. Technol.* **2016**, *212*, 151–159. https://doi.org/10.1016/j.biortech.2016.04.016.

(16) Escapa, A.; San-Martín, M. I.; Mateos, R.; Morán, A. Scaling-up of Membraneless Microbial Electrolysis Cells (MECs) for Domestic Wastewater Treatment: Bottlenecks and Limitations. *Bioresour. Technol.* **2015**, *180*, 72–78. https://doi.org/10.1016/j.biortech.2014.12.096.

(17) Finkelstein, D. A.; Tender, L. M.; Zeikus, J. G. Effect of Electrode Potential on Electrode-Reducing Microbiota. *Environ. Sci. Technol.* **2006**, *40* (22), 6990–6995. https://doi.org/10.1021/es061146m.

(18) Torres, C. I.; Krajmalnik-Brown, R.; Parameswaran, P.; Marcus, A. K.; Wanger, G.; Gorby, Y. A.; Rittmann, B. E. Selecting Anode-Respiring Bacteria Based on Anode Potential: Phylogenetic, Electrochemical, and Microscopic Characterization. *Environ. Sci. Technol.* **2009**, *43* (24), 9519–9524. https://doi.org/10.1021/es902165y.

(19) Wagner, R. C.; Call, D. F.; Logan, B. E. Optimal Set Anode Potentials Vary in Bioelectrochemical Systems. *Environ. Sci. Technol.* **2010**, *44* (16), 6036–6041. https://doi.org/10.1021/es101013e.

(20) Korth, B.; Harnisch, F. Spotlight on the Energy Harvest of Electroactive Microorganisms: The Impact of the Applied Anode Potential. *Front. Microbiol.* **2019**, *10* (June), 1–9. https://doi.org/10.3389/fmicb.2019.01352.

(21) Call, D. F.; Logan, B. E. Hydrogen Production in a Single Chamber Microbial Electrolysis Cell Lacking a Membrane. *Environ. Sci. Technol.* **2008**, *42* (9), 3401–3401.

(22) Call, D. F.; Logan, B. E. A Method for High Throughput Bioelectrochemical Research Based on Small Scale Microbial Electrolysis Cells. *Biosens. Bioelectron.* **2011**, *26* (11), 4526–4531. https://doi.org/10.1016/j.bios.2011.05.014.

(23) Liu, G.; Yates, M. D.; Cheng, S.; Call, D. F.; Sun, D.; Logan, B. E. Examination of Microbial Fuel Cell Start-up Times with Domestic Wastewater and Additional Amendments. *Bioresour. Technol.* **2011**, *102* (15), 7301–7306. https://doi.org/10.1016/j.biortech.2011.04.087.

(24) Dekker, A.; Ter Heijne, A.; Saakes, M.; Hamelers, H. V. M.; Buisman, C. J. N. Analysis and Improvement of a Scaled-up and Stacked Microbial Fuel Cell. *Environ. Sci. Technol.* **2009**, *43* (23), 9038–9042. https://doi.org/10.1021/es901939r.

(25) Liang, P.; Duan, R.; Jiang, Y.; Zhang, X.; Qiu, Y.; Huang, X. One-Year Operation of 1000-L Modularized Microbial Fuel Cell for Municipal Wastewater Treatment. *Water Res.* **2018**, *141*, 1–8. https://doi.org/10.1016/j.watres.2018.04.066.

(26) Brown, R. K.; Harnisch, F.; Wirth, S.; Wahlandt, H.; Dockhorn, T.; Dichtl, N.; Schröder, U. Evaluating the Effects of Scaling up on the Performance of Bioelectrochemical Systems Using a Technical Scale Microbial Electrolysis Cell. *Bioresour. Technol.* **2014**, *163*, 206–213. https://doi.org/10.1016/j.biortech.2014.04.044.

(27) Feng, Y.; Zhang, Y.; Chen, S.; Quan, X. Enhanced Production of Methane from Waste Activated Sludge by the Combination of High-Solid Anaerobic Digestion and Microbial Electrolysis Cell with Iron-Graphite Electrode. *Chem. Eng. J.* **2015**, *259*, 787–794. https://doi.org/10.1016/j.cej.2014.08.048.

(28) Guo, X.; Liu, J.; Xiao, B. Bioelectrochemical Enhancement of Hydrogen and Methane Production from the Anaerobic Digestion of Sewage Sludge in Single-Chamber Membrane-Free Microbial Electrolysis Cells. *Int. J. Hydrogen Energy* **2013**, *38* (3), 1342–1347. https://doi.org/10.1016/j.ijhydene.2012.11.087.

(29) Martin, E.; Savadogo, O.; Guiot, S. R.; Tartakovsky, B. Electrochemical Characterization of Anodic Biofilm Development in a Microbial Fuel Cell. *J. Appl. Electrochem.* **2013**, *43* (5), 533–540. https://doi.org/10.1007/s10800-013-0537-2.

(30) Srikanth, S.; Marsili, E.; Flickinger, M. C.; Bond, D. R. Electrochemical Characterization of *Geobacter sulfurreducens* Cells Immobilized on Graphite Paper Electrodes. *Biotechnol. Bioeng.* **2008**, *99* (5), 1065–1073. https://doi.org/10.1002/bit.21671.

(31) Katuri, K. P.; Werner, C. M.; Jimenez-Sandoval, R. J.; Chen, W.; Jeon, S.; Logan, B. E.; Lai, Z.; Amy, G. L.; Saikaly, P. E. A Novel Anaerobic Electrochemical Membrane Bioreactor (AnEMBR) with Conductive Hollow-Fiber Membrane for Treatment of Low-Organic Strength Solutions. *Environ. Sci. Technol.* **2014**, *48* (21), 12833–12841. https://doi.org/10.1021/es504392n.

(32) Illumina Inc. 16S Metagenomic Sequencing Library Preparation http://support.illumina.com/content/dam/illumina-support/documents/documentation/chemistry_documentation/16s/16s-metagenomic-library-prep-guide-15044223-b.pdf (accessed Aug 21, 2017).

(33) Caporaso, J. G.; Kuczynski, J.; Stombaugh, J.; Bittinger, K.; Bushman, F. D.; Costello, E. K.; Fierer, N.; Peña, A. G.; Goodrich, J. K.; Gordon, J. I.; et al. QIIME Allows Analysis of High- Throughput Community Sequencing Data. *Nat. Publ. Gr.* **2010**, *7* (5), 335–336. https://doi.org/10.1038/nmeth0510-335.

(34) QIIME. pick_open_reference_otus.py - Perform open-reference OTU picking http://qiime.org/scripts/pick_open_reference_otus.html (accessed Apr 27, 2017).

(35) Oksanen, J.; Blanchet, F. G.; Friendly, M.; Kindt, R.; Legendre, P.; McGlinn, D.; Minchin, P. R.; O'Hara, R. B.; Simpson, G. L.; Solymos, P.; et al. Package "Vegan." *Community Ecol. Packag.* **2017**, 1–263.

(36) McMurdie, P. J.; Holmes, S. Phyloseq: An R Package for Reproducible Interactive Analysis and Graphics of Microbiome Census Data. *PLoS One* **2013**, *8* (4). https://doi.org/10.1371/journal.pone.0061217.

(37) Commault, A. S.; Lear, G.; Packer, M. A.; Weld, R. J. Influence of Anode Potentials on Selection of *Geobacter* Strains in Microbial Electrolysis Cells. *Bioresour. Technol.* **2013**, *139*, 226–234. https://doi.org/10.1016/j.biortech.2013.04.047.

(38) Wang, X.; Feng, Y.; Ren, N.; Wang, H.; Lee, H.; Li, N.; Zhao, Q. Accelerated Start-up of Two-Chambered Microbial Fuel Cells: Effect of Anodic Positive Poised Potential. *Electrochim. Acta* **2009**, *54* (3), 1109–1114. https://doi.org/10.1016/j.electacta.2008.07.085.

(39) Kumar, A.; Leech, D.; Siggins, A.; Katuri, K.; Mahony, T.; O'Flaherty, V.; Lens, P. Catalytic Response of Microbial Biofilms Grown under Fixed Anode Potentials Depends on Electrochemical Cell Configuration. *Chem. Eng. J.* **2013**, *230*, 532–536. https://doi.org/10.1016/j.cej.2013.06.044.

(40) Lee, H. S.; Rittmann, B. E. Significance of Biological Hydrogen Oxidation in a Continuous Single-Chamber Microbial Electrolysis Cell. *Environ. Sci. Technol.* **2010**, *44* (3), 948–954. https://doi.org/10.1021/es9025358.

(41) Call, D. F.; Wagner, R. C.; Logan, B. E. Hydrogen Production by *Geobacter* Species and a Mixed Consortium in a Microbial Electrolysis Cell. *Appl. Environ. Microbiol.* **2009**, *75* (24), 7579–7587. https://doi.org/10.1128/AEM.01760-09.

(42) Rozendal, R. A.; Hamelers, H. V. M.; Buisman, C. J. N. Effects of Membrane Cation Transport on pH and Microbial Fuel Cell Performance. *Environ. Sci. Technol.* **2006**, *40* (17), 5206–5211. https://doi.org/10.1021/es060387r.

(43) Fricke, K.; Harnisch, F.; Schröder, U. On the Use of Cyclic Voltammetry for the Study of Anodic Electron Transfer in Microbial Fuel Cells. *Energy Environ. Sci.* **2008**, *1* (1), 144. https://doi.org/10.1039/b802363h.

(44) Katuri, K. P.; Kavanagh, P.; Rengaraj, S.; Leech, D. *Geobacter sulfurreducens* Biofilms Developed under Different Growth Conditions on Glassy Carbon Electrodes: Insights Using Cyclic Voltammetry. *Chem. Commun.* **2010**, *46* (26), 4758–4760. https://doi.org/10.1039/c003342a.

(45) Katuri, K. P.; Rengaraj, S.; Kavanagh, P.; O'Flaherty, V.; Leech, D. Charge Transport through *Geobacter sulfurreducens* Biofilms Grown on Graphite Rods. *Langmuir* **2012**, *28* (20), 7904–7913. https://doi.org/10.1021/la2047036.

(46) Marsili, E.; Rollefson, J. B.; Baron, D. B.; Hozalski, R. M.; Bond, D. R. Microbial Biofilm Voltammetry: Direct Electrochemical Characterization of Catalytic Electrode-Attached Biofilms. *Appl. Environ. Microbiol.* **2008**, *74* (23), 7329–7337. https://doi.org/10.1128/AEM.00177-08.

(47) Zhu, X.; Yates, M. D.; Logan, B. E. Set Potential Regulation Reveals Additional Oxidation Peaks of *Geobacter sulfurreducens* Anodic Biofilms. *Electrochem. commun.* **2012**, *22* (1), 116–119. https://doi.org/10.1016/j.elecom.2012.06.013.

(48) Wei, J.; Liang, P.; Cao, X.; Huang, X. A New Insight into Potential Regulation on Growth and Power Generation of *Geobacter sulfurreducens* in Microbial Fuel Cells Based on Energy Viewpoint. *Environ. Sci. Technol.* **2010**, *44* (8), 3187–3191. https://doi.org/10.1021/es903758m.

(49) Peng, L.; Zhang, X. T.; Yin, J.; Xu, S. Y.; Zhang, Y.; Xie, D. T.; Li, Z. L. *Geobacter sulfurreducens* Adapts to Low Electrode Potential for Extracellular Electron Transfer. *Electrochim. Acta* **2016**, *191*, 743–749. https://doi.org/10.1016/j.electacta.2016.01.033.

(50) Zacharoff, L.; Chan, C. H.; Bond, D. R. Reduction of Low Potential Electron Acceptors Requires the CbcL Inner Membrane Cytochrome of *Geobacter sulfurreducens*. *Bioelectrochemistry* **2016**, *107*, 7–13. https://doi.org/10.1016/j.bioelechem.2015.08.003.

(51) Levar, C. E.; Hoffman, C. L.; Dunshee, A. J.; Toner, B. M.; Bond, D. R. Redox Potential as a Master Variable Controlling Pathways of Metal Reduction by *Geobacter sulfurreducens*. *ISME J.* **2017**, *11* (3), 741–752. https://doi.org/10.1038/ismej.2016.146.

(52) Ramasamy, R. P.; Gadhamshetty, V.; Nadeau, L. J.; Johnson, G. R. Impedance Spectroscopy as a Tool for Non-Intrusive Detection of Extracellular Mediators in Microbial Fuel Cells. *Biotechnol. Bioeng.* **2009**, *104* (5), 882–891. https://doi.org/10.1002/bit.22469.

(53) Dheilly, A.; Linossier, I.; Darchen, A.; Hadjiev, D.; Corbel, C.; Alonso, V. Monitoring of Microbial Adhesion and Biofilm Growth Using Electrochemical Impedancemetry. *Appl. Microbiol. Biotechnol.* **2008**, *79* (1), 157–164. https://doi.org/10.1007/s00253-008-1404-7.

(54) Kouzuma, A.; Meng, X. Y.; Kimura, N.; Hashimoto, K.; Watanabe, K. Disruption of the Putative Cell Surface Polysaccharide Biosynthesis Gene SO3177 in *Shewanella oneidensis* MR-1 Enhances Adhesion to Electrodes and Current Generation in Microbial Fuel Cells. *Appl. Environ. Microbiol.* **2010**, *76* (13), 4151–4157. https://doi.org/10.1128/AEM.00117-10.

(55) Borole, A. P.; Aaron, D.; Hamilton, C. Y.; Tsouris, C. Understanding Long-Term Changes in Microbial Fuel Cell Performance Using Electrochemical Impedance Spectroscopy. *Environ. Sci. Technol.* **2010**, *44* (7), 2740–2745. https://doi.org/10.1021/es9032937.

(56) Rabaey, K.; Boon, N.; Siciliano, S. D.; Verhaege, M.; Verstraete, W. Biofuel Cells Select for Microbial Consortia That Self-Mediate Electron Transfer. *Appl. Environ. Microbiol.* **2004**, *70* (9), 5373–5382. https://doi.org/10.1128/AEM.70.9.5373-5382.2004.

(57) Ramette, A. Multivariate Analyses in Microbial Ecology. *FEMS Microbiol. Ecol.* **2007**, *62*, 142–160. https://doi.org/10.1111/j.1574-6941.2007.00375.x.

(58) Lesnik, K. L.; Liu, H. Establishing a Core Microbiome in Acetate-Fed Microbial Fuel Cells. *Appl. Microbiol. Biotechnol.* **2014**, *98* (9), 4187–4196. https://doi.org/10.1007/s00253-013-5502-9.

(59) Ren, L.; Zhang, X.; He, W.; Logan, B. E. High Current Densities Enable Exoelectrogens to Outcompete Aerobic Heterotrophs for Substrate. *Biotechnol. Bioeng.* **2014**, *111* (11), 2163–2169. https://doi.org/10.1002/bit.25290.

(60) Hasany, M.; Mardanpour, M. M.; Yaghmaei, S. Biocatalysts in Microbial Electrolysis Cells: A Review. *Int. J. Hydrogen Energy* **2016**, *41* (3), 1477–1493. https://doi.org/10.1016/j.ijhydene.2015.10.097.

Figures

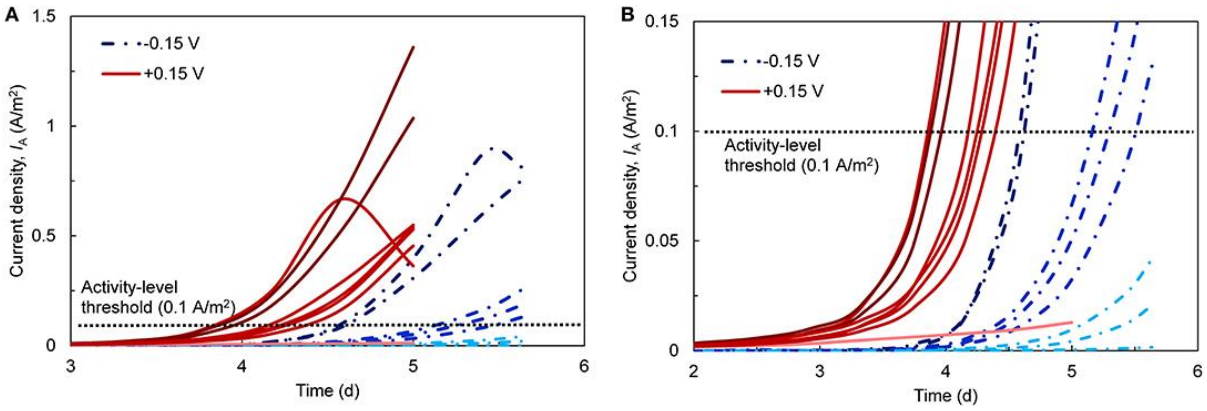

Figure 3.1. A) Current densities (I_A; normalized to anode surface area) over time during the startup phase of the bioanodes. Eight replicates (red lines) were started with an applied anode potential [E_{AN}; reported vs the standard hydrogen electrode (SHE)] of +0.15 V and another eight (blue, segmented lines) were started at −0.15 V. The dark, medium, and light shading of the lines corresponds to high-, low-activity, and inactive bioanodes, respectively. The horizontal dotted line denotes the current density threshold (0.1 A/m^2) selected to define the bioanode activity level. B) A closer view of the bioanode startup current densities with respect to the activity threshold.

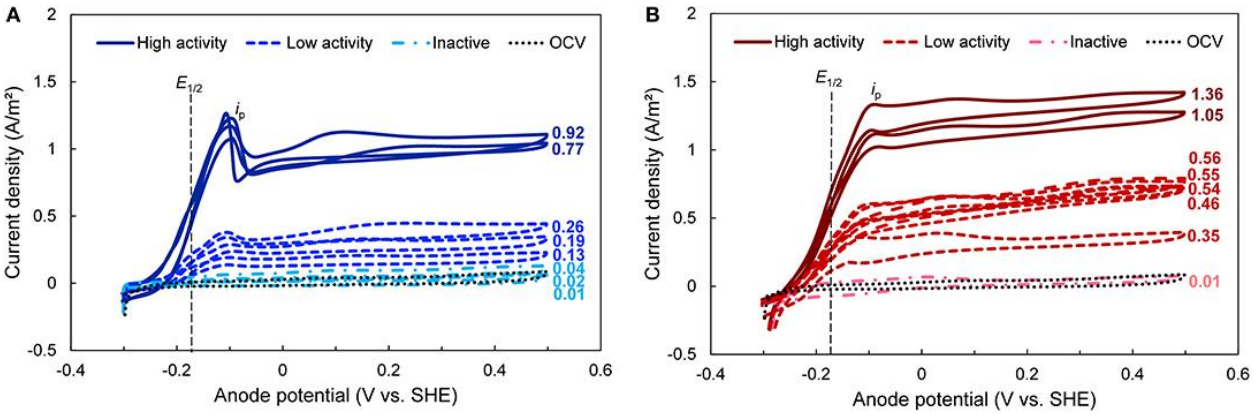

Figure 3.2. Cyclic voltammograms (CVs) taken at the end of the startup period for bioanodes fixed at A) E_{AN} = –0.15 V and B) E_{AN} = +0.15 V. All curves in the same plot are replicates. High-, low-activity, and inactive bioanode levels are defined based on the time required to reach the startup current threshold (**Fig. 3.1**). Numbers next to each curve represent the current density recorded at the end of the startup cycle. $E_{1/2}$ – Midpoint potential (vertical black dashed line); i_p – peak current obtained during the potential sweep; OCV – open circuit voltage (dotted black line).

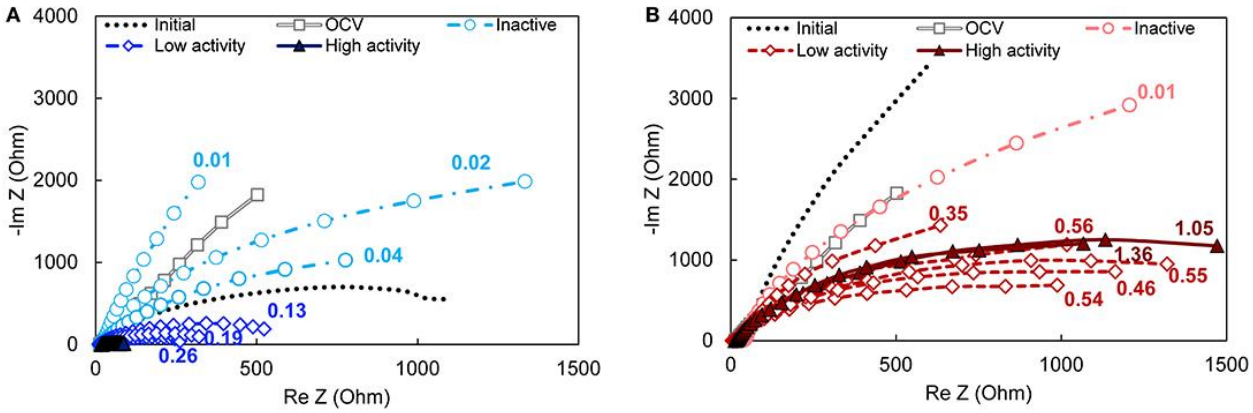

Figure 3.3. Nyquist plots of bioanodes fixed at a) E_{AN} = –0.15 V and b) E_{AN} = +0.15 V taken at the end of the startup cycle. All curves in the same plot are replicates. The magnitude of impedance is lower when the ratio of the shown curve is lower, which translates into lower total resistance. High-, low-activity, and inactive bioanode levels are defined based on the time required to reach the startup current threshold (**Fig. 3.1**). The numbers next to each curve are the current density recorded at the end of the startup period. OCV – open circuit voltage (gray double line with squares); Initial – prior to inoculation (dotted line).

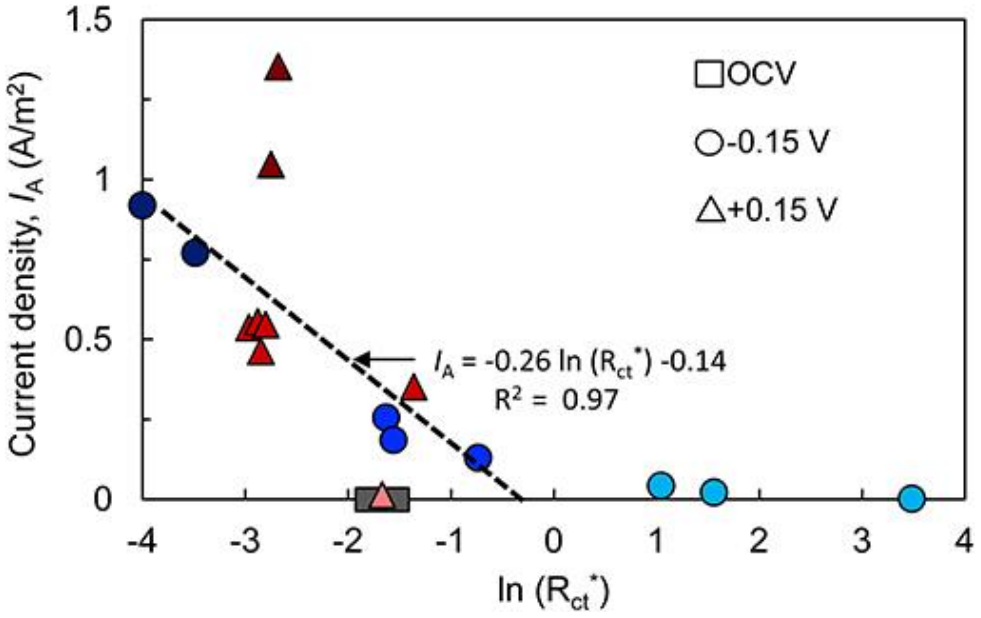

Figure 3.4. Relationship between bioanode charge transfer resistance (R_{ct}^*; normalized to each bioanode's resistance prior to introducing microorganisms) and current density (I_A). Both metrics were recorded at the end of the startup cycle. Points with the same shape represent replicate bioanodes fixed at –0.15 V (circles) and +0.15 V (triangles). The points are shaded to reflect bioanode activity level (dark – high-activity; medium – low-activity; light – inactive). OCV – open circuit voltage bioanodes (squares). The linear regression of high- and low-activity bioanode points at -0.15 V is shown as a dotted line.

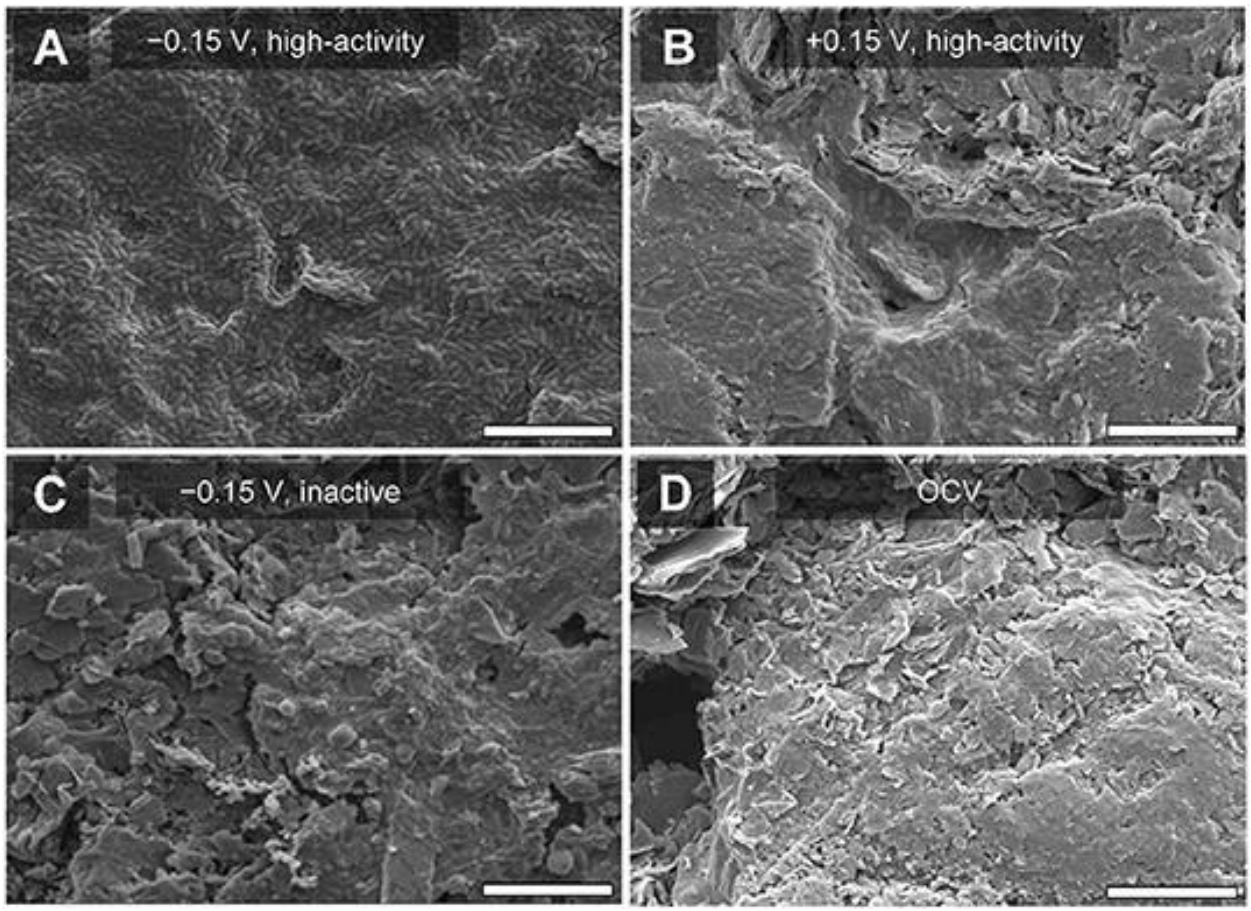

Figure 3.5. Scanning electron microscopy (SEM) images of bioanodes at the end of the startup cycle. A) High-activity bioanode at –0.15 V showing uniform and complete surface coverage of microorganisms, B) high-activity bioanode at +0.15 V with similar cell morphology as A), but less surface coverage, C) low-activity bioanode at –0.15 V, with mixed cell morphology and lower coverage relative to A), and D) bioanode at open circuit voltage (OCV). White bar at the bottom of each figure represents a distance of 10 μm.

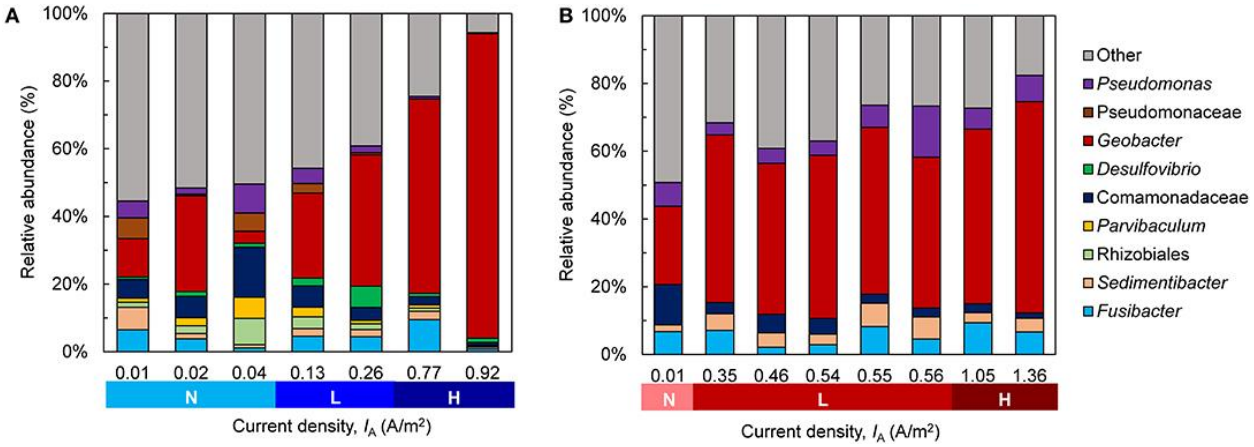

Figure 3.6. Community composition of the bioanode biofilms fixed at A) –0.15 V and B) +0.15 V. The replicates for each anode potential are ordered from lowest to highest current density (I_A) recorded at the end of the startup cycle and are categorized according to their activity level during the startup cycle [Inactive (N), low-activity (L), high-activity (H)]. Genera with a relative abundance less than 5% are grouped into "Other".

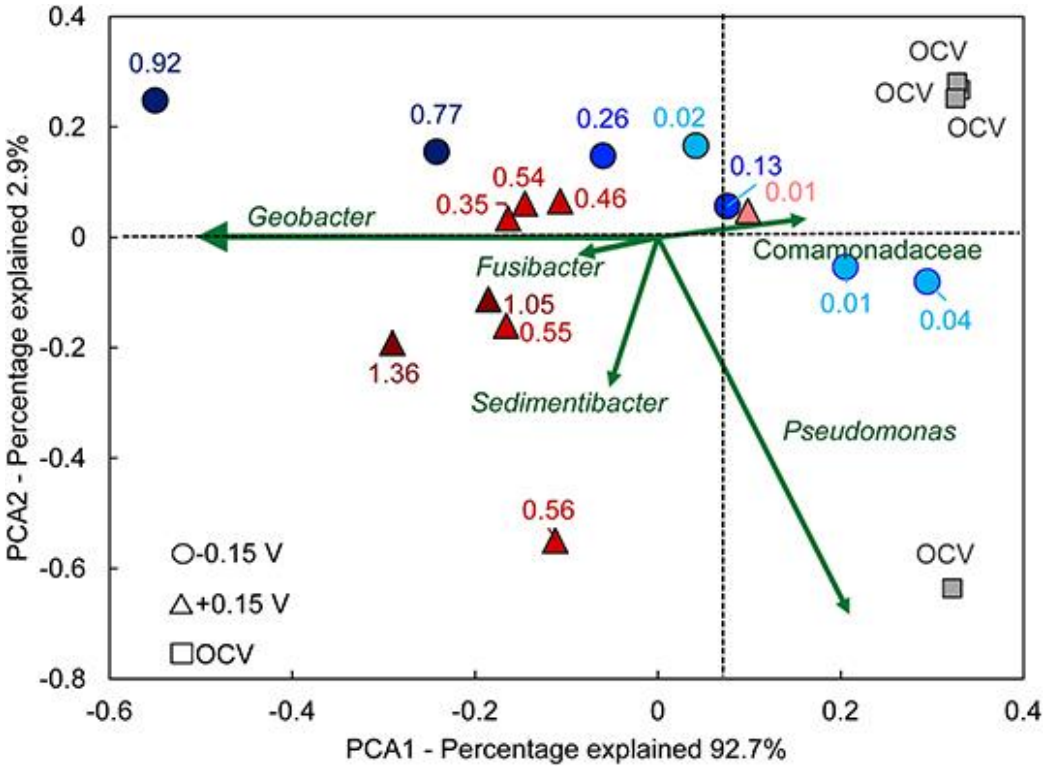

Figure 3.7. Principal Component Analysis (PCA) biplot of anode biofilm microbial communities. Points with the same shape represent replicate bioanodes fixed at –0.15 V (circles) and +0.15 V (triangles). The points are shaded to reflect bioanode activity level (dark – high-activity; medium – low-activity; light – inactive). The numbers next to each curve are the current density recorded at the end of the startup period. Green vectors symbolize the eigenvector of the corresponding genus. Samples that are located in the direction of an eigenvector contain that particular genus, with an increased relative abundance the farther they are located from the center. OCV – open circuit voltage bioanodes (squares).

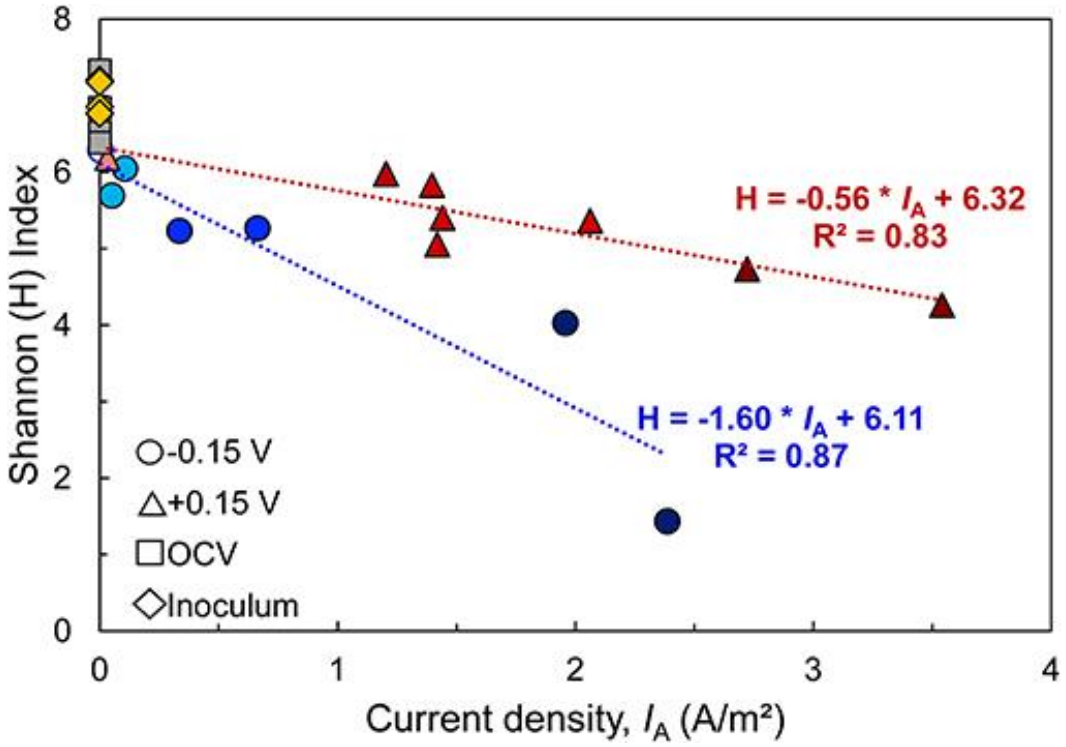

Figure 3.8. Relationship between microbial diversity [estimated by the Shannon Diversity index (H)] and bioanode current density (I_A) recorded at the end of the startup cycle. A higher H index represents a more diverse microbial community. Linear regression of replicates from each fixed potential are represented by dashed lines (blue: –0.15 V, red: +0.15 V), along with regression equation and coefficient of determination (R^2). Points with the same shape represent replicate bioanodes fixed at –0.15 V (circles) and +0.15 V (triangles). The points are shaded to reflect bioanode activity level (dark – high-activity; medium – low activity; light – inactive). Communities from wastewater inoculum are shown as yellow rhombi and the open circuit (OCV) controls are represented as gray squares.

CHAPTER 4

NITROGEN GAS FIXATION AND CONVERSION TO AMMONIUM USING MICROBIAL ELECTROLYSIS CELLS

Abstract

Ammonia (NH_3) is an important industrial chemical that is produced using the energy- and carbon-intensive Haber-Bosch process. Recovering NH_3 from microorganisms that fix nitrogen gas (N_2) may provide a sustainable alternative because their specialized nitrogenase enzymes can reduce N_2 to ammonium (NH_4^+) without the need for high temperature and pressure. This study explored the possibility of converting N_2 into NH_4^+ using anaerobic, single-chamber microbial electrolysis cells (MECs). N_2 fixation rates [based on an acetylene gas (C_2H_2) to ethylene gas (C_2H_4) conversion assay] of a microbial consortium increased significantly when the applied voltage between the anode and cathode increased from 0.7 V to 1.0 V and reached a maximum of ~40 nmol C_2H_4/(min-mg protein), which is comparable to model aerobic N_2-fixing bacteria. The presence of NH_4^+, which can inhibit the activity of the nitrogenase enzyme, did not significantly reduce N_2 fixation rates. Upon addition of methionine sulfoximine, an NH_4^+ uptake inhibitor, NH_4^+ was recovered at rates approaching 5.2×10^{-12} mol NH_4^+/(s-cm^2), normalized to the anode surface area. Relative to the electrical energy consumed, the normalized energy demand (in MJ/mol NH_4^+) was negative because of the energy-rich methane gas recovered in the MEC. Including the substrate energy resulted in total energy demands as low as 24 MJ/mol. Community analysis results of the anode biofilms revealed that *Geobacter* species predominated in both the presence and absence of NH_4^+, suggesting that they played a key role in current generation and N_2 fixation. This study shows that MECs may provide a new route for generating NH_4^+.

This chapter has been published as

Ortiz-Medina, J.F., Grunden, A.M., Hyman, M.R., Call, D.F. Nitrogen Gas Fixation and Conversion to Ammonium Using Microbial Electrolysis Cells. *ACS Sustainable Chem. Eng.* **2019**, **7**,3, 3511-3519.

4.1 Introduction

Ammonia (NH_3) is a widely used chemical in the industrial, commercial, and agricultural sectors. Increasing from roughly 100 million ton NH_3 per year in 2008 to 150 million ton NH_3 per year in 2017, NH_3 is the second most produced chemical in the world.[1] Demand for NH_3 is expected to increase as the population grows[1]. The majority (~80%) of NH_3 produced is used in fertilizers. It is also an ingredient in other products such as explosives, pharmaceuticals, refrigerants, and cleaning products and is receiving growing interest as an alternative transportation fuel.

Most NH_3 is produced through the Haber-Bosch process, an energy- and carbon-intensive technology. In this process, nitrogen (N_2) and hydrogen (H_2) gases are converted into NH_3 under high temperatures (350-550°C) and pressures (150-300 atm).[2] It consumes 1.5-2.5% of global energy annually and is responsible for roughly 2.5% of global carbon dioxide (CO_2) emissions.[3] Alternatives to Haber-Bosch include a growing list of methods involving electrochemistry, photocatalysis, plasma-induction, and metallic complex catalysis.[2] Many of these technologies suffer from low conversion efficiencies, expensive catalysts, and low selectivity.[2] Electrochemical methods in which N_2 is reduced on anode electrodes have been examined for a wide range of electrolytes and catalysts.[4] Finding resilient and selective catalysts remains a challenge for these methods,[4] and high temperatures (which impart an energy penalty) are still preferred due to slow

kinetics at ambient temperatures.[4] Bioelectrochemical approaches in which an enzyme (e.g., nitrogenase) is attached to an electrode overcome many of the limitations of abiotic systems. However, the irreversible damage of these enzymes upon oxygen (O_2) exposure, the requirement for soluble electron shuttles such as methyl viologen, and long-term enzyme stability are major limitations.[5]

Using whole-cell N_2-fixing microorganisms (called diazotrophs), rather than just the isolated nitrogenase enzyme, is an alternative route to generate NH_3. These naturally occurring microorganisms have nitrogenase enzymes that break the strong N≡N bond under ambient conditions.[6] Many microorganisms in nitrogen-deficient environments rely on these enzymes to provide fixed nitrogen for growth (e.g., amino acids) or to support the growth of other organisms. Agricultural practices leverage the latter function from symbiotic diazotrophs in the farming of legumes.[7] Free-living diazotrophs, which do not require a symbiont, have been engineered to excrete ammonium (NH_4^+; the protonated form of NH_3; $pK_a = 9.3$) to concentrations as high as 30 mM.[8] One inherent limitation of aerobic diazotrophs, including model *Azotobacter* species, is that their terminal electron acceptor (i.e., O_2) can also inhibit nitrogenase function.[9] Increasing growth and respiration by using higher O_2 concentrations can therefore reduce N_2 fixation activity. Driving high N_2 fixation rates remains a challenge for moving these biological approaches forward.

One possible route to drive the microbial conversion of N_2 into NH_4^+ is to combine the fields of electrochemistry and microbiology. Research in electromicrobiology has shown that electrically active microorganisms, many of which are known diazotrophs, are highly responsive to electrical driving forces.[10] In anaerobic microbial electrolysis cells (MECs), an applied voltage drives the conversion of organic material into electrical current by anode respiring microorganisms (exoelectrogens), resulting in the production of energy-rich gases, for example, H_2 and CH_4.[11]

Community analyses of anode biofilms have revealed that *Geobacter* species predominate in these systems.[12] These bacteria are also prolific N_2-fixing microorganisms, which is one explanation for their abundance in nitrogen-limited bioremediation sites.[13,14] N_2 fixation has been previously documented in microbial electrochemical technologies (METs),[15–17] but the generation and recovery of NH_4^+ have yet to be shown.

As MEC anodes are typically highly populated with *Geobacter* species, operation occurs under completely anaerobic conditions (where O_2 cannot inhibit nitrogenase function), and applied voltages (> 0.2 V) drive anode respiration rates, we hypothesized 1) that we could use voltage to drive N_2 fixation, and 2) NH_4^+ could be recovered from N_2-fixing exoelectrogenic communities. To test these hypotheses, we measured the current densities of MECs with only N_2 gas as the nitrogen source at two applied voltages ($E_{AP,}$ 0.7 V and 1.0 V). We estimated N_2 fixation rates using the acetylene (C_2H_2) reduction assay, which is a standard method for assessing nitrogenase activity.[18] To determine the impact of NH_4^+, which is known to slow or inhibit N_2 fixation, identical MECs with NH_4^+ and a N_2 headspace were operated in parallel. To explore the possibility of recovering NH_4^+, an NH_4^+ uptake inhibitor was added and the resulting NH_4^+ generation rates recorded. A microbial community analysis was conducted on the anode biofilms in order to identify the microorganisms associated with N_2 fixation in the MEC. Finally, an assessment of energy demands to generate NH_4^+ in the MEC was performed.

4.2 Materials and Methods

4.2.1 MEC design and operation

Serum-bottle MECs were assembled as previously described.[19] Briefly, graphite plate anodes (A_A = 4.5 cm^2) and stainless steel mesh cathodes (A_C = 3.9 cm^2) spaced 1.5 cm apart, were

connected to titanium and stainless steel wire current collectors, respectively, and inserted through stoppers. The electrode assembly was installed in glass serum bottles (75 mL), sealed using aluminum caps, and sterilized by autoclaving. The MECs were inoculated with effluent from an active MEC. The growth medium consisted of phosphate buffered medium (PBM) as previously described.[19] Ammonium chloride (NH_4Cl) was not included unless specified. Sodium acetate (1 g/L) was supplied as the electron donor and carbon source. The MEC headspace was purged with ultra-high- purity N_2 gas prior to each cycle. Two treatments (both operated in triplicate) were examined: 1) MECs without NH_4^+ added, and 2) MECs with NH_4^+ (0.31 g NH_4Cl/L). The MECs were connected to a power supply (3645A DC Power Supply, Circuit Specialists, Inc., Tempe, AZ), and a voltage (E_{AP}) of 0.7 V was applied between the anode and cathode. After 16 cycles, E_{AP} was increased to 1.0 V. Current was determined by recording the voltage over a 10 Ω resistor. The MECs were operated in fed-batch mode, wherein the medium was emptied when the current density (I_A; normalized to A_A) dropped below 0.2 A m^{-2} and then replaced with new medium. All MECs were operated at 30 ^oC.

4.2.2 Nitrogenase activity assay

Nitrogenase activity was measured by subjecting the MECs to an acetylene gas (C_2H_2) reduction assay (ARA). This method serves as a proxy for N_2 fixation because 1) the nitrogenase enzyme converts C_2H_2 to ethylene gas (C_2H_4), 2) this conversion does not occur abiotically, 3) neither C_2H_2 nor C_2H_4 inhibits nitrogenase activity, and 4) C_2H_4 can be readily quantified by gas chromatography (GC).[18] The ARA was used when current stabilized for both E_{AP} = 0.7 V and 1.0 V. After replacing the medium of the MECs and purging with N_2 gas, C_2H_2 (obtained from calcium carbide) was injected in the headspace, giving a final concentration of 10% (v/v gas phase). After

applying a voltage, headspace samples (100 µL) were taken at regular intervals using a gas-tight syringe (Hamilton, Reno, NV). Samples were injected into a GC (Shimadzu GC-14A, Kyoto, Japan) equipped with a flame ionization detector and a stainless steel column [PoraPak N (80/100 mesh); 6 ft x 1/8 in]. Headspace pressure was measured using a pressure gauge and then converted to moles of C_2H_4 using the ideal gas law. The total moles of C_2H_4 were determined from the headspace and dissolved aqueous compositions.

4.2.3 Ammonium quantification and inhibition

To determine NH_4^+ concentrations, MEC medium (0.5 mL) was extracted at several points during a batch cycle and filtered (0.22 µm). Dissolved NH_4^+ concentrations were determined using the Low Range AmVer™ Salicylate Test N'Tube™ method (Hach Company, Loveland, CO), with a working range of 0.01-2.50 mg NH_3-N L^{-1}. Accuracy of the method was verified using NH_4^+ standards, which deviated by no more than 0.01 mg NH_3-N L^{-1}.

To encourage NH_4^+ excretion from the microorganisms, the NH_4^+ uptake inhibitor methionine sulfoximine (MSX) was added. This inhibitor acts on the enzyme glutamine synthetase, which catalyzes the assimilation of NH_4^+ into amino acids. It is commonly used to recover NH_4^+ from free-living diazotrophs.[20] An MSX concentration of 5 mM was selected, which falls within the range used in other studies.[21–23] Once the MEC was filled with fresh, MSX-containing medium, samples (0.5 mL) were taken over the course of a batch cycle at both E_{AP}. In initial tests, MSX generated a previously undocumented false positive for NH_4^+ (~7 mg NH_3-N/L) with the quantification method stated above. A two-stage trap was therefore used to separate the NH_4^+ from the MSX (full details available in the Supporting Information; **Appendix B**).

4.2.4 Microbial community analysis

To identify the anode microbial community, the anode biofilm was scraped using a sterile razor blade (~200 µg per electrode). Genomic DNA was extracted using a PowerSoil® DNA isolation kit (MO BIO Laboratories, Carlsbad, CA) following the manufacturer instructions. The prokaryotic V3 and V4 regions of the 16S rRNA gene were amplified using polymerase chain reaction (PCR), with the forward primer 5' TCGTCGGCAGCGTCAGATGTGTATAAGAGAC-AGCCTAYGGGRBGCASCAG 3' and the reverse primer 5' GTCTCGTGGGCTCGGAGATGT-GTATAAGAGACAGGGACTACNNGGGTATCTAAT 3'. These primers are based on the sequences used by Yu et al.[24] and included the required Illumina adapters for sequencing. After purification and barcoding, the final amplicons were sequenced using Illumina MiSeq equipment (Illumina Inc., San Diego, CA) with a paired-end sequencing of 300 base pairs (bp) in length. The sequencing results were further processed and the operational taxonomic units (OTU) assigned using the QIIME software.[25]

4.2.5 Coulombic efficiency

The Coulombic efficiency (C_E, %) was calculated as

$$C_E = \frac{M \int_0^{t_b} I dt}{FnV\Delta S} \qquad (1)$$

where the current, I (A) is integrated over the duration of the batch cycle (t_b), M represents the molar mass of sodium acetate (82 g/mol), F is Faraday's constant (96,500 C per mol e^-), n is the number of electrons per mol of acetate oxidized (8 mol e^-/mol acetate), V (mL) is the medium volume in the MEC (20 mL), and ΔS (g/L) is the amount of acetate consumed during a batch cycle. Previous studies using this MEC design have shown that nearly all acetate (1 g/L) is

consumed once the current falls below 0.10 mA (or 0.22 A/m^2).[12] All acetate was therefore assumed to be completely consumed by the end of each cycle (ΔS = 1 g/L).

4.2.6 Energy demand

To determine the energy demand of NH_4^+ production, the electrical energy consumed, substrate energy consumed, and energy produced as gas (i.e., CH_4) were calculated. The amount of energy added to the circuit by the power source, adjusted for losses across the resistor, W_E, is given by eq 2,

$$W_E = \sum_1^n (I\, E_{AP}\, \Delta t - I^2\, R_{EX}\, \Delta t) \qquad (2)$$

where I is measured at n points over the course of a batch cycle, Δt (s) is the time interval between each measurement, and R_{EX} = 10 Ω is the external resistor. The amount of energy added by the substrate is,

$$W_S = \Delta G_S\, n_S \qquad (3)$$

where $\Delta G_S = 844.1$ kJ/mol is the Gibbs energy of combustion of the substrate (acetate in this case)[26] and n_S is the number of moles of substrate consumed during a batch cycle. The amount of energy available in the produced gas depends on the gas composition. This was determined using a GC (details available in Appendix B). At the end of the experiments, the MECs in this study produced only CH_4. Hydrogen gas, a side product of the nitrogenase, was not detected, and was likely consumed by hydrogenotrophic methanogens.[27] The theoretical energy content of the recovered CH_4 was calculated as

$$W_{CH_4} = \Delta G_{CH_4}\, n_{CH_4} \qquad (4)$$

where $\Delta G_{CH_4} = 817.97$ kJ/mol and n_{CH_4} the number of CH_4 moles produced during a batch cycle.[28] The specific energy demand of NH_4^+ production, $E_{NH_4^+}$, is the ratio of the energy inputs (electricity and substrate) and outputs (CH_4) to the moles of NH_4^+ generated, or

$$E_{NH_4^+} = \frac{W_E + W_S - W_{CH_4}}{n_{NH_4^+}} \qquad (5)$$

where $n_{NH_4^+}$ is the moles of NH_4^+ recovered in a batch cycle. To determine the electrical energy demand, W_S is removed from eq 5, and for the substrate energy demand, W_E is removed. The amount of usable energy associated with the recovered CH_4 will depend on the conversion efficiency of the technology used to generate electrical energy (i.e., fuel cell versus a combustion engine). In some cases, we adjusted the W_{CH_4} values using a conversion efficiency of 32.9% (an average efficiency of typical biogas converting technologies).[29] Energy demand values that include this conversion efficiency are shown in parentheses next to the non-adjusted values.

4.3 Results and discussion

4.3.1 Electrical current generation during N_2 fixation

We first determined current density (I_A) and coulombic efficiency (C_E) when only N_2 was provided as a nitrogen source. After inoculating the serum-bottle MECs containing medium without fixed nitrogen, purging the headspace with N_2 gas and applying a constant whole-cell voltage (E_{AP} = 0.7 V), current generation began within five days. Four cycles later (15 days), I_A reached a reproducible maximum of 3.0 ± 0.15 A/m^2 (**Fig. 4.1A**). Current densities were stable for more than 10 cycles operated at this E_{AP}, with no significant difference (ANOVA, $p > 0.05$) relative to the average of 3.1 ± 0.27 A/m^2 over that time period (**Fig. 4.1B**). This result is consistent with prior reports of METs operating with little to no fixed nitrogen from 15 to 200 days.[15,30] To

determine if the lack of a fixed nitrogen source impacted I_A, we operated identical MECs, but with NH_4Cl (5.8 mM NH_4^+) added to the medium. Current generation in those reactors began within five days and reached 3.1 ± 0.31 A/m^2 after stabilizing. Over the course of 12 cycles, I_A in the presence versus absence of NH_4^+ deviated 9.3% on average, but the difference between treatments was not significant (*t*-test, $p > 0.05$). When E_{AP} was increased to 1.0 V, I_A increased in the absence and presence of NH_4^+ to 4.8 ± 0.27 A/m^2 and 5.2 ± 0.27 A/m^2, respectively. The lack of a fixed nitrogen source did not negatively impact C_E. With only N_2 present, C_E averaged 89 ± 1%, and was slightly lower (83 ± 1%) with NH_4^+ present at E_{AP} = 0.7 V. At E_{AP} = 1.0 V, C_E decreased relative to E_{AP} = 0.7 V, but remained similar in the absence (71 ± 3%) versus presence (67 ± 2%) of NH_4^+. The near identical I_A and C_E values of the MECs with and without NH_4^+ and similarities to prior reports of MECs (2.1 – 4.2 A/m^2 for E_{AP} = 0.7 V)[19,31] highlight that the absence of dissolved NH_4^+ (a condition that encourages N_2 fixation[32]) does not negatively impact current production over time.

4.3.2 N_2 fixation rates

In order to quantify N_2 fixation rates, we conducted the acetylene gas (C_2H_2) reduction assay (ARAs). When C_2H_2 was added to the MECs at the start of a cycle, ethylene (C_2H_4) accumulated at a constant rate for the first 50 hours at both E_{AP} (**Fig. 4.2**). At E_{AP} = 0.7 V, the MECs generated C_2H_4 at a rate of 7.7 ± 1.1 nmol C_2H_4/min in the absence of NH_4^+ and 3.0 ± 0.8 nmol C_2H_4/min when NH_4^+ was added (based on linear regression of C_2H_4 generation over time). These two rates were significantly different (*t*-test, $p < 0.05$). Increasing E_{AP} to 1.0 V increased C_2H_4 production rates in both treatments to 26 ± 2.4 nmol C_2H_4/min (without NH_4^+) and 20 ± 3.7 nmol C_2H_4/min (with NH_4^+). These rates were not significantly different (*t*-test, $p > 0.05$),

indicating that NH_4^+ did not have an impact on N_2 fixation. The increase in C_2H_4 production rates between applied voltages was significant (*t*-test, $p < 0.05$) regardless of NH_4^+ presence. The more than threefold increase in C_2H_4 generation rates between E_{AP} = 0.7 V and E_{AP} = 1.0 V was notable considering that I_A increased by less than two-fold.

The minimal reduction in C_2H_4 generation rates when NH_4^+ was added was an interesting result because NH_4^+ is known to repress nitrogenase gene expression.[32] Depending on the microorganism and the growth conditions, this threshold can vary. Values as low as 0.2 mM have been reported to completely repress nitrogenase activity in the model microorganism *Azotobacter vinelandii*.[32] For several *Azospirillum* species, concentrations as low as 0.05 mM NH_4^+ reduced nitrogenase activity.[33] In a community with *Geobacter* spp., 0.5 mM NH_4^+ repressed the expression of *nifD*, one of the genes encoding nitrogenase.[34] Since the N_2 fixation activity in the presence of NH_4^+ was not fully shutdown in our MECs, it is possible that the bulk NH_4^+ concentrations could not completely repress the nitrogenase genes. The concentration may have been too low or diffusion limitations may have prevented nitrogenase inhibition by NH_4^+ throughout the entire biofilm. Partial nitrogenase repression has been observed in free-living diazotrophs at varying NH_4^+ concentrations.[33,35] The fact that N_2 fixation occurred in the presence of NH_4^+ may have important implications for wastewater-treating METs. Typical domestic wastewater NH_4^+ concentrations (0.8 – 3.6 mM NH_4^+)[36] are lower than what was used here. N_2 fixation may therefore be occurring in wastewater-fed METs.

To confirm that anode respiration was linked with N_2 fixation, we also conducted the ARA on the MECs during open circuit voltage (OCV; no current flow) (**Fig. 4.2**). No C_2H_4 was detected during the same period as the MECs in closed circuit mode (60 h). Further evidence that anode respiration was required is that, after approximately 50 h in the closed-circuit MECs (when current

generation approached zero), the C_2H_4 generation rate dropped sharply. At that point, acetate was depleted and anode respiration ceased. Outside the electromicrobiology field, some studies have noted correlations between microbial N_2 fixation rates and respiration rates,[37–39] while others have not.[40–42] An inherent challenge when using aerobic N_2-fixing microorganisms is that increasing O_2 concentrations has the dual effect of increasing respiration rates but also potentially inhibiting O_2-sensitive nitrogenases.[38,40–42] Our work here, where O_2 is not present, lends support for the hypothesis that respiration rates (as measured by I_A) are linked to N_2 fixation rates. We also conducted additional tests in which acetate was replaced with H_2 (45% headspace concentration) as the sole electron donor to determine N_2 fixation rates associated with H_2 consuming microorganisms (E_{AP} = 0.7 V; **Appendix B**). C_2H_4 generation dropped significantly from approximately 20 µmol C_2H_4 recovered at 45 h with acetate (**Fig. 4.2**) to below detection with H_2 at the same time point. Current densities also decreased to below 0.1 A/m^2. These results suggest that acetate oxidation was the primary source of reducing power for N_2 fixation.

To allow comparison with free-living diazotrophs, we normalized our C_2H_4 generation rates to the total anode protein density (150 ± 3 µg/cm^2, protein assay details available in the Supporting Methods). At E_{AP} = 1.0 V, the normalized rate was 39 ± 3.7 nmol C_2H_4/(min-mg protein). Free-living, aerobic diazotrophs such as *Azotobacter* species have reached N_2 fixation rates of 35 to 100 nmol C_2H_4/(min-mg protein). Obtaining normalized rates comparable to *Azotobacter* species is an important finding because they are some of the best studied free-living diazotrophs. The rates of other microorganisms such as cyanobacteria (e.g., *Anabaena* spp.) and anaerobic free-living bacteria (e.g., *Azospirillum* spp.) range from 0.11 to 6.5 nmol C_2H_4/(min-mg protein).[18,43] Regarding species that are similar to exoelectrogenic bacteria, suspended cultures of the anaerobic, metal-reducing bacteria *G. metallireducens* and *Magnetospirillum magnetotacticum*

obtained rates of 12 and 22 nmol C_2H_4/(min-mg protein), respectively.[44] Therefore, the increase in E_{AP} proved to be an effective way to stimulate N_2 fixation rates that are comparable with many other free-living diazotrophs.

In METs, there are limited reports of N_2 fixation measurements. Wong et al.[15] enriched an exoelectrogenic community on a high-surface area granular graphite anode poised at +0.2 V vs. Ag/AgCl. By making some assumptions about the electrode surface area used in their study (calculation available in the Supporting Information), we estimate an anode normalized rate of 0.40 nmol C_2H_4/(min-cm^2) compared to 5.9 nmol C_2H_4/(min-cm^2) in our MECs at E_{AP} = 1.0 V. One possible explanation for the higher rates reported here is that acetate, rather than glucose, was provided as an electron donor. Acetate-fed METs typically generate higher current than glucose and favor the growth of known diazotrophic exoelectrogens, such as *Geobacter* species.[45] Zhou et al.[16] isolated an exoelectrogenic bacterium belonging to the genus *Azospirillum*, which reached rates of 1.75 nmol C_2H_4/(min-10^8 cells);[16] however, N_2 fixation during anode respiration was not examined.

4.3.3 Ammonium production

To test the hypothesis that NH_4^+ can be recovered in the MEC, we first measured NH_4^+ concentrations over time while current was generated. In the standard growth medium without NH_4^+ added, little (< 10 µM) to no NH_4^+ was detected over the course of a batch cycle (limit of detection = 3 µM) (**Fig. 4.3**). To eliminate the possibility that NH_4^+ was generated through an abiotic reaction of H_2 and N_2 at the cathode, abiotic reactors were operated at E_{AP} = 1.0 V with a H_2/N_2 [50/50 (v/v)] headspace composition. No NH_4^+ was detected over the same period as the biotic experiments (**Appendix B**). Abiotic NH_4^+ production was therefore ruled out.

To encourage NH_4^+ release from the microorganisms during N_2 fixation, we added the NH_4^+ uptake inhibitor methionine sulfoximine (MSX). In the presence of MSX (5 mM), NH_4^+ concentrations increased steadily over time at both E_{AP} and reached final concentrations of 70 µM (E_{AP} = 0.7 V) and 260 µM (E_{AP} = 1.0 V). Theoretically, we estimate that 10% of the NH_4^+ that was generated during N_2 fixation was recovered, regardless of E_{AP}. We determined this based on the assumption that one mole of NH_4^+ is produced for every two moles of C_2H_4 generated during the ARA (a commonly used conversion factor).[46] This would result in up to 3 mM NH_4^+ after 60 h at E_{AP} = 1.0 V and correspond to a rate of around 40 µM NH_4^+/h, which is roughly 10-fold larger than the actual rate (4.2 ± 0.7 µM NH_4^+/h). One explanation for this difference may be that the MSX concentration was too low to fully inhibit the glutamine synthase enzymes. Other studies have used MSX concentrations as low as 0.35 µM or as high as 0.11 M, depending on the microorganism examined.[47,48] Since there are no reports in the literature on the application of MSX to exoelectrogenic biofilms, we used a concentration that was consistent with other studies on free living diazotrophs such as *Azotobacter chrococcum*.[23] As a reference, using the same chemical inhibitor (0.35-200 µM) with the cyanobacterium *Anabaena*, NH_4^+ generation rates from 10 to 150 µM NH_4^+/h were reported.[20,47] In comparison, Ahmad and Hellebust[21] did not notice a significant effect of MSX, suggesting the existence of an alternate NH_4^+ assimilation pathway. The lower NH_4^+ generation rates are therefore likely due to differences in susceptibility to MSX among microorganisms and biofilm growth on the anode that would reduce MSX mass transfer to the microorganisms compared with suspended growth in those other studies.

Relative to other bioelectrochemical technologies at ambient conditions, the MEC NH_4^+ generation rates are quite comparable. Normalized to the anode surface area, the MEC rates increased from 1.3×10^{-12} mol NH_4^+/(s-cm^2) at E_{AP} = 0.7 V up to 5.2×10^{-12} mol NH_4^+/(s-cm^2) at E_{AP}

= 1.0 V. Knoche et al.,[10] in the only study to date that reports bioelectrochemical NH_4^+ excretion, immobilized cells of *Anabaena variabilis* SA-1 onto indium tin oxide electrodes and applied cyclic voltammetry, producing up to 4.7 µM NH_4^+ at a rate of 2.6×10^{-12} mol/(s-cm^2).[10] Milton et al.[5] used a fuel cell with electrode-immobilized nitrogenase and hydrogenase enzymes instead of whole-cell microorganisms. Their system generated 2.3×10^{-11} mol NH_4^+/(s-cm^2) after applying 60 mC of charge over two hours. However, an electron mediator (methyl viologen) was required to shuttle electrons to/from both enzymes. Recently, Rago et al.[17] enriched a biocathodic microbial community to perform N_2 fixation at a fixed applied potential of -0.7 V vs SHE . While this is a more direct approach for N_2 conversion to NH_4^+, the maximum current density detected in their system was around 0.01 A/m^2, at least two orders of magnitude lower than the current generated in this study. Since our work shows a link between N_2 fixation rates and current density, it is unlikely that biocathode-driven N_2 fixation was a major contributor to our observed N_2 fixation rates.

4.3.4 Microbial community analysis

To identify the microorganisms in the MECs, genomic DNA from the anode biofilms was extracted and the 16S rRNA genes were amplified and sequenced. Among the bacteria, *Geobacter* was the most prevalent genus with a relative abundance of 43.7 ± 2.3 % in the absence of NH_4^+ (**Fig. 4.4**). This genus is frequently detected in exoelectrogenic biofilms that use acetate as the electron donor.[12,49] Many *Geobacter* spp. are also diazotrophs, including *G. sulfurreducens*, *G. metallireducens,* and *G. uraniireducens*.[13,14,44] In the presence of NH_4^+, *Geobacter* spp. abundance was similar (43.5 ± 6.8 %; **Fig. 4.4**), suggesting that the requirement for N_2 fixation did not negatively impact their ability to colonize the anode. Except for *Methanocorpusculum* spp.

(discussed below), all genera with an average relative abundance > 5% did not significantly vary in abundance in the presence versus absence of NH_4^+ (*t*-test, $p > 0.05$). This finding is supported by the relatively high N_2 fixation rates recorded in the presence of NH_4^+ (**Fig. 4.2**) and another study that showed *Geobacter*-rich environments maintained similar transcript levels of key N_2 fixation genes when NH_4^+ concentrations increased from 0 to 350 µM.[34]

Other Bacteria identified in the anode include species belonging to the genus *Aminiphilus*, as well as the *Blvii28* group. The former genus is known to ferment several amino acids, generating products such as acetate.[50] This function suggests a possible syntrophy with *Geobacter* spp., as *Aminiphilus* spp. are frequently found in acetate-fed METs with relative abundances as high as 43%.[51] The latter has also been found in wastewater-inoculated systems such as up-flow anaerobic sludge beds, anaerobic biofilm membrane bioreactors, and anaerobic digesters, where they likely ferment carbohydrates and generate H_2.[52–54] Only a single member of this group, *Acetobacteroides hydrogenigenes*, has been successfully isolated.[55] For both genera, the diazotrophic and exolectrogenic capabilities remain unknown.

Within the archaea, methanogenic microorganisms including *Methanocorpusculum* spp. (6.2 ± 3.4 %) and an unknown genus belonging to the family *Methanobacteriaceae* were detected (8.3 ± 2.8 %) in the absence of NH_4^+. These genera contain hydrogenotrophic methanogens that require H_2 and CO_2 to generate CH_4.[56,57] Their presence explains why CH_4 was recovered instead of H_2, which commonly occurs in single-chamber MECs.[27] Some members of the *Methanobacteriaceae* have been reported to fix N_2.[58] It is plausible that they contributed to the observed N_2 fixation rates and NH_4^+ production in the MEC. Methanogen N_2 fixation rate estimates reported in the literature, which range between 0.7 to 15 nmol C_2H_4/(min-mg protein),[59] would only account for about 1.8 – 38% of our normalized rates. Coupling this estimate with the

significantly lower C_2H_4 generation rates when we supplied the MECs with H_2 (**Appendix B**) suggests that methanogens were not the primary N_2 fixers in the MECs. For *Methanocorpusculum* spp., nitrogenase-like gene sequences, but with no experimentally established diazotrophic behavior, have been reported.[60] The significant decrease (*t*-test, $p < 0.05$) in abundance of this genus when NH_4^+ was absent supports that these microorganisms may not grow as well when required to fix N_2. Elucidating the contribution of *Geobacter* spp. and methanogens to N_2 fixation in METs is warranted.

4.3.5 Energy demand

The energy needed to drive NH_4^+ production in the MECs consists of electrical and substrate (i.e., acetate in this study) inputs. It is important to note that these inputs also produce energy-rich gases (H_2 and CH_4) in the MEC.[26,27] This is recoverable energy that can be used to offset some of the energy demands. The MECs in this study generated CH_4 (no H_2 detected), which is due to methanogenic consumption of cathodic electrons and/or H_2.[27] The MECs generated 0.27 ± 0.02 mmol CH_4 per cycle, regardless of E_{AP}. The energy recovered was 136-162 MJ/(mol NH_4^+) at E_{AP} = 0.7 V (45-53 MJ/mol when adjusted for CH_4 conversion to electricity) and 37-47 MJ/mol (12-15 MJ/mol) at E_{AP} = 1.0 V. Considering only the electrical energy input, the energy demand ranged from -92 to -65 MJ/mol (E_{AP} = 0.7 V) and from -14 to -7.1 MJ/mol (E_{AP} = 1.0 V) because the recovered energy was greater than the consumed electrical energy. These values become positive if adjusted to account for CH_4 conversion into electricity (16-25 MJ/mol for E_{AP} = 0.7 V and 14-17 MJ/mol for E_{AP} = 1.0 V). Conventional and emerging N_2 fixation technologies do not generate energy. Recovering energy-rich gas in MECs may therefore impart an energy advantage over other approaches. Relative to only the substrate energy, the energy demands ranged from -

0.041 to 0.051 MJ/mol, indicating that the majority of the substrate energy was converted to CH_4. The substrate energy is an important factor that increases the net energy demand (around 150 MJ/mol at E_{AP} = 0.7 V and 37 MJ/mol at E_{AP} = 1.0 V). This energy expenditure can be reduced or eliminated by utilizing waste sources low in nitrogen such as industrial wastewater (e.g., pulp and paper wastewater).[15] Taking into account both the electrical and substrate energy inputs, the energy demands were 51-84 MJ/mol (166-175 MJ/mol) at E_{AP} = 0.7 V and 24-34 MJ/mol (55-58 MJ/mol) at E_{AP} = 1.0 V. The decrease in demand when E_{AP} increased can be explained by a larger increase in NH_4^+ production rates relative to the increase in energy input. It may be possible to obtain higher generation rates at higher voltages, but voltages above 1.2 V should be avoided to minimize unwanted abiotic water electrolysis. A further consideration is the requirement to separate and recover NH_4^+ from the MEC. While the evaluation of NH_4^+ extraction technologies is outside the scope of the present study, there are several methods that could be used. For example, driving NH_4^+ transport across a cation-exchange membrane has already been shown in METs. Alternatively, NH_4^+ conversion to NH_3 gas in a separate alkaline cathode chamber conditions may also be a possibility.[61,62]

Relative to other NH_3 generation technologies, the MEC energy demand was large because only small amounts of NH_4^+ were recovered when the inhibitor was used. Based on the N_2 fixation rate estimates reported here, if 100% recovery was achieved (assuming NH_4^+ is the main product), the energy demand could be lowered by an order of magnitude to about 3.2 MJ/mol at E_{AP} = 1.0 V (~5.6 MJ/mol if CH_4 conversion to electricity is considered). Engineering high NH_4^+-producing exoelectrogenic strains similar to the approach used by Barney et al.[8] to develop an aerobic *Azotobacter* spp. that accumulated up to 30 mM NH_4^+ at a rate of 200 μM h^{-1} may be an approach to further reduce energy requirements.[8,63,64] Additionally, optimizing the MEC design and

materials could also help reduce the energy demand through, for example, using large surface area electrodes, minimizing electrode spacing, and optimizing N_2 gas transfer to the biofilm.

4.3.6 Implications

Based on the obtained results, the use of an MET offers an alternative to NH_4^+ using diazotrophic, exoelectrogenic bacteria. Compared with other methods that require expensive materials (e.g., platinum, gold, ruthenium), high temperatures and/or pressures, sunlight, or rely on non-renewable catalysts, the MEC used here generates NH_4^+ under ambient conditions, with inexpensive electrode materials (e.g., graphite, stainless steel), and self-renewing microbial catalysts.[11,26,45]. Our findings suggest that multiple N_2 fixation pathways may occur in the MEC (**Fig. 4.5**). Diazotrophic exoelectrogenic bacteria fix N_2 while consuming organic matter and respiring on the anode. The electrons transferred to the anode result in the cathodic generation of H_2 that can be further converted to CH_4 via methanogenesis. Methanogens may also fix N_2, although likely to a lesser degree than the exoelectrogens. To further optimize the technology, identifying and engineering promising N_2-fixing exoelectrogens will be needed, rather than relying on chemical inhibitors. We justify the use of an NH_4^+ uptake inhibitor here to explore the potential for NH_4^+ generation from the MEC, but it is not a long-term, sustainable approach. There are promising diazotrophic exoelectrogens (e.g., *G. sulfurreducens*) that may yield new NH_4^+-excreting, engineered strains[13,14,44]. On the basis of the high relative abundance of *Geobacter* spp. in our MEC anode biofilms, we hypothesize that these microorganisms were the primary contributors to the high current and N_2 fixation rates in the MECs[15,30]. Further studies must assess the capability of N_2 fixation and NH_4^+ production by pure cultures of *Geobacter* species, as well as determine the N_2 fixation capabilities of other microorganisms such as methanogens.

4.4 Conclusions

This study explored the possibility of converting N_2 gas into NH_4^+ using single-chamber microbial electrolysis cells (MECs). We showed that MEC N_2 fixation rates can approach those reported for model aerobic diazotrophs such as *Azotobacter* species. Increasing the electrical input from an applied voltage of 0.7 V to 1.0 V resulted in a significant increase in N_2 fixation rates. The addition of an NH_4^+ uptake inhibitor resulted in generation rates up to 5.2×10^{-12} mol NH_4^+/(s-cm^2), normalized to the anode surface area. While the energy demands of this proof-of-concept study were larger than commercially available processes (i.e., Haber-Bosch), the possibility of recovering multiple products, including H_2, CH_4, and NH_4^+ may provide a unique niche for this technology.

Chapter 4 References

(1) Erisman, J. W.; Sutton, M. A.; Galloway, J.; Klimont, Z.; Winiwarter, W. How a Century of Ammonia Synthesis Changed the World. *Nat. Geosci.* **2008**, *1* (10), 636–639. https://doi.org/10.1038/ngeo325.

(2) Cherkasov, N.; Ibhadon, A. O.; Fitzpatrick, P. A Review of the Existing and Alternative Methods for Greener Nitrogen Fixation. *Chem. Eng. Process. Process Intensif.* **2015**, *90*, 24–33. https://doi.org/10.1016/j.cep.2015.02.004.

(3) Zhou, F.; Azofra, L. M.; Ali, M.; Kar, M.; Simonov, A. N.; McDonnell-Worth, C.; Sun, C.; Zhang, X.; MacFarlane, D. R. Electro-Synthesis of Ammonia from Nitrogen at Ambient Temperature and Pressure in Ionic Liquids. *Energy Environ. Sci.* **2017**, *10* (12), 2516–2520. https://doi.org/10.1039/C7EE02716H.

(4) Giddey, S.; Badwal, S. P. S.; Kulkarni, A. Review of Electrochemical Ammonia Production Technologies and Materials. *Int. J. Hydrogen Energy* **2013**, *38* (34), 14576–14594. https://doi.org/10.1016/j.ijhydene.2013.09.054.

(5) Milton, R. D.; Cai, R.; Abdellaoui, S.; Leech, D.; De Lacey, A. L.; Pita, M.; Minteer, S. D. Bioelectrochemical Haber-Bosch Process: An Ammonia-Producing H_2/N_2 Fuel Cell. *Angew. Chemie Int. Ed.* **2017**, *56* (10), 2680–2683. https://doi.org/10.1002/anie.201612500.

(6) Saikia, S. P.; Jain, V. Biological Nitrogen Fixation with Non-Legumes: An Achievable Target or a Dogma? *Curr. Sci.* **2007**, *92* (3), 317–322.

(7) Van Kessel, C.; Hartley, C. Agricultural Management of Grain Legumes: Has It Led to an Increase in Nitrogen Fixation? *F. Crop. Res.* **2000**, *65* (2–3), 165–181. https://doi.org/10.1016/S0378-4290(99)00085-4.

(8) Barney, B. M.; Plunkett, M. H.; Natarajan, V.; Mus, F.; Knutson, C. M.; Peters, J. W. Transcriptional Analysis of an Ammonium-Excreting Strain of *Azotobacter vinelandii* Deregulated for Nitrogen Fixation. *Appl. Environ. Microbiol.* **2017**, *83* (20), 1–22. https://doi.org/10.1128/AEM.01534-17.

(9) Gallon, J. R. The Oxygen Sensitivity of Nitrogenase: A Problem for Biochemists and Micro-Organisms. *Trends Biochem. Sci.* **1981**, *6* (C), 19–23. https://doi.org/10.1016/0968-0004(81)90008-6.

(10) Knoche, K. L.; Aoyama, E.; Hasan, K.; Minteer, S. D. Role of Nitrogenase and Ferredoxin in the Mechanism of Bioelectrocatalytic Nitrogen Fixation by the Cyanobacteria *Anabaena variabilis* SA-1 Mutant Immobilized on Indium Tin Oxide (ITO) Electrodes. *Electrochim. Acta* **2017**, *232*, 396–403. https://doi.org/10.1016/j.electacta.2017.02.148.

(11) Logan, B. E.; Rabaey, K. Conversion of Wastes into Bioelectricity and Chemicals by Using Microbial Electrochemical Technologies. *Science.* **2012**, *337* (6095), 686–690. https://doi.org/10.1126/science.1217412.

(12) Zhu, X.; Yates, M. D.; Hatzell, M. C.; Ananda Rao, H.; Saikaly, P. E.; Logan, B. E. Microbial Community Composition Is Unaffected by Anode Potential. *Environ. Sci. Technol.* **2014**, *48* (2), 1352–1358. https://doi.org/10.1021/es404690q.

(13) Methe, B. A.; Webster, J.; Nevin, K.; Butler, J.; Lovley, D. R. DNA Microarray Analysis of Nitrogen Fixation and Fe(III) Reduction in *Geobacter sulfurreducens*. *Appl. Environ. Microbiol.* **2005**, *71* (5), 2530–2538. https://doi.org/10.1128/AEM.71.5.2530-2538.2005.

(14) Holmes, D. E.; O'Neil, R. A.; Chavan, M. A.; N'Guessan, L. A.; Vrionis, H. A.; Perpetua, L. A.; Larrahondo, M. J.; DiDonato, R.; Liu, A.; Lovley, D. R. Transcriptome of *Geobacter uraniireducens* Growing in Uranium-Contaminated Subsurface Sediments. *ISME J.* **2009**, *3* (2), 216–230. https://doi.org/10.1038/ismej.2008.89.

(15) Wong, P. Y.; Cheng, K. Y.; Kaksonen, A. H.; Sutton, D. C.; Ginige, M. P. Enrichment of Anodophilic Nitrogen Fixing Bacteria in a Bioelectrochemical System. *Water Res.* **2014**, *64* (1), 73–81. https://doi.org/10.1016/j.watres.2014.06.046.

(16) Zhou, S.; Han, L.; Wang, Y.; Yang, G.; Zhuang, L.; Hu, P. *Azospirillum humicireducens* Sp. Nov., a Nitrogen-Fixing Bacterium Isolated from a Microbial Fuel Cell. *Int. J. Syst. Evol. Microbiol.* **2013**, *63* (Pt 7), 2618–2624. https://doi.org/10.1099/ijs.0.046813-0.

(17) Rago, L.; Zecchin, S.; Villa, F.; Goglio, A.; Corsini, A.; Cavalca, L.; Schievano, A. Bioelectrochemical Nitrogen Fixation (e-BNF): Electro-Stimulation of Enriched Biofilm Communities Drives Autotrophic Nitrogen and Carbon Fixation. *Bioelectrochemistry* **2018**, *125*, 105–115. https://doi.org/10.1016/J.BIOELECHEM.2018.10.002.

(18) Hardy, R. W. F.; Burns, R. C.; Holsten, R. D. Applications of the Acetylene-Ethylene Assay for Measurement of Nitrogen Fixation. *Soil Biol. Biochem.* **1973**, *5* (1), 47–81. https://doi.org/10.1016/0038-0717(73)90093-X.

(19) Call, D. F.; Logan, B. E. A Method for High Throughput Bioelectrochemical Research Based on Small Scale Microbial Electrolysis Cells. *Biosens. Bioelectron.* **2011**, *26* (11), 4526–4531. https://doi.org/10.1016/j.bios.2011.05.014.

(20) Colnaghi, R.; Green, A.; He, L.; Rudnick, P.; Kennedy, C. Strategies for Increased Ammonium Production in Free-Living or Plant Associated Nitrogen Fixing Bacteria. *Plant Soil* **1997**, 145–154. https://doi.org/10.1023/A:1004268526162.

(21) Ahmad, I.; Hellebust, J. A. Effects of Methionine Sulfoximine on Growth and Nitrogen Assimilation of the Marine Microalga *Chlorella autotrophica*. *Mar. Biol.* **1985**, *86* (1), 85–91. https://doi.org/10.1007/BF00392582.

(22) Ronzio, R. A.; Rowe, W. B.; Meister, A. Studies on the Mechanism of Inhibition of Glutamine Synthetase By Methionine Sulfoximine. *Biochemistry* **1969**, *8* (3), 1066–1075. https://doi.org/10.1021/bi00831a038.

(23) Cejudo, F. J.; de la Torre, A.; Paneque, A. Short-Term Ammonium Inhibition of Nitrogen Fixation in *Azotobacter*. *Biochem. Biophys. Res. Commun.* **1984**, *123* (2), 431–437. https://doi.org/10.1016/0006-291X(84)90248-1.

(24) Yu, Y.; Lee, C.; Kim, J.; Hwang, S. Group-Specific Primer and Probe Sets to Detect Methanogenic Communities Using Quantitative Real-Time Polymerase Chain Reaction. *Biotechnol. Bioeng.* **2005**, *89* (6), 670–679. https://doi.org/10.1002/bit.20347.

(25) Caporaso, J. G.; Kuczynski, J.; Stombaugh, J.; Bittinger, K.; Bushman, F. D.; Costello, E. K.; Fierer, N.; Peña, A. G.; Goodrich, J. K.; Gordon, J. I.; et al. QIIME Allows Analysis of High-Throughput Community Sequencing Data. *Nat. Methods* **2010**, *7* (5), 335–336. https://doi.org/10.1038/nmeth.f.303.

(26) Logan, B. E.; Call, D.; Cheng, S.; Hamelers, H. V. M.; Sleutels, T. H. J. A.; Jeremiasse, A. W.; Rozendal, R. A. Microbial Electrolysis Cells for High Yield Hydrogen Gas Production from Organic Matter. *Environ. Sci. Technol.* **2008**, *42* (23), 8630–8640. https://doi.org/10.1021/es801553z.

(27) Call, D.; Logan, B. E. Hydrogen Production in a Single Chamber Microbial Electrolysis Cell Lacking a Membrane. *Environ. Sci. Technol.* **2008**, *42* (9), 3401–3406. https://doi.org/10.1021/es8001822.

(28) Villano, M.; Monaco, G.; Aulenta, F.; Majone, M. Electrochemically Assisted Methane Production in a Biofilm Reactor. *J. Power Sources* **2011**, *196* (22), 9467–9472. https://doi.org/10.1016/j.jpowsour.2011.07.016.

(29) U.S. Environmental Protection Agency; Combined Heat and Power Partnership. Opportunities for Combined Heat and Power at Wastewater Treatment Facilities : Market Analysis and Lessons from the Field. **2011**.

(30) Belleville, P.; Strong, P. J.; Dare, P. H.; Gapes, D. J. Influence of Nitrogen Limitation on Performance of a Microbial Fuel Cell. *Water Sci. Technol.* **2011**, *63* (8), 1752–1757. https://doi.org/10.2166/wst.2011.111.

(31) Ren, L.; Siegert, M.; Ivanov, I.; Pisciotta, J. M.; Logan, B. E. Treatability Studies on Different Refinery Wastewater Samples Using High-Throughput Microbial Electrolysis Cells (MECs). *Bioresour. Technol.* **2013**, *136*, 322–328. https://doi.org/10.1016/j.biortech.2013.03.060.

(32) Laane, C.; Krone, W.; Konings, W.; Haaker, H.; Veeger, C. Short-Term Effect of Ammonium Chloride on Nitrogen Fixation by *Azotobacter vinelandii* and by Bacteroids of *Rhizobium leguminosarum*. *Eur. J. Biochem.* **1980**, *103* (1), 39–46. https://doi.org/10.1111/j.1432-1033.1980.tb04286.x.

(33) Hartmann, A.; Fu, H.; Burris, R. H. Regulation of Nitrogenase Activity by Ammonium Chloride in *Azospirillum* spp. *J. Bacteriol.* **1986**, *165* (3), 864–870. https://doi.org/10.1128/jb.165.3.864-870.1986.

(34) Mouser, P. J.; N'Guessan, A. L.; Elifantz, H.; Holmes, D. E.; Williams, K. H.; Wilkins, M. J.; Long, P. E.; Lovley, D. R. Influence of Heterogeneous Ammonium Availability on Bacterial Community Structure and the Expression of Nitrogen Fixation and Ammonium Transporter Genes during in Situ Bioremediation of Uranium-Contaminated Groundwater. *Environ. Sci. Technol.* **2009**, *43* (12), 4386–4392. https://doi.org/10.1021/es8031055.

(35) Bottomley, P. J.; Grillo, J. F.; Van Baalen, C.; Tabita, F. R. Synthesis of Nitrogenase and Heterocysts by *Anabaena* sp. CA in the Presence of High Levels of Ammonia. *J. Bacteriol.* **1979**, *140* (3), 938–943.

(36) Tchobanoglous, G. *Wastewater Engineering. Treatment, Disposal and Reuse*, 3rd Editio.; McGraw-Hill, 1991.

(37) Hurek, T.; Reinhold-Hurek, B.; Turner, G. L.; Bergersen, F. J. Augmented Rates of Respiration and Efficient Nitrogen Fixation at Nanomolar Concentrations of Dissolved O2 in Hyperinduced *Azoarcus* sp. Strain BH72. *J. Bacteriol.* **1994**, *176* (15), 4726–4733. https://doi.org/10.1128/jb.176.15.4726-4733.1994.

(38) Linkerhägner, K.; Oelze, J. Cellular ATP Levels and Nitrogenase Switchoff upon Oxygen Stress in Chemostat Cultures of *Azotobacter vinelandii*. *J. Bacteriol.* **1995**, *177* (18), 5289–5293. https://doi.org/10.1128/jb.177.18.5289-5293.1995.

(39) Linkerhägner, K.; Oelze, J. Nitrogenase Activity and Regeneration of the Cellular ATP Pool in *Azotobacter vinelandii* Adapted to Different Oxygen Concentrations. *J. Bacteriol.* **1997**, *179* (4), 1362–1367. https://doi.org/10.1128/jb.179.4.1362-1367.1997.

(40) Zhang, Y.; Pohlmann, E. L.; Roberts, G. P. Effect of Perturbation of ATP Level on the Activity and Regulation of Nitrogenase in *Rhodospirillum rubrum*. *J. Bacteriol.* **2009**, *191* (17), 5526–5537. https://doi.org/10.1128/JB.00585-09.

(41) Kuhla, J.; Oelze, J. Dependence of Nitrogenase Switch-off upon Oxygen Stress on the Nitrogenase Activity in Azotobacter vinelandii. *J. Bacteriol.* **1988**, *170* (11), 5325–5329. https://doi.org/10.1128/jb.170.11.5325-5329.1988.

(42) Post, E.; Kleiner, D.; Oelze, J. Whole Cell Respiration and Nitrogenase Activities in *Azotobacter vinelandii* Growing in Oxygen Controlled Continuous Culture. *Arch. Microbiol.* **1983**, *134* (1), 68–72. https://doi.org/10.1007/BF00429410.

(43) Fay, P. Oxygen Relations of Nitrogen Fixation in Cyanobacteria. *Microbiol. Rev. Rev.* **1992**, *56* (2), 340–373.

(44) Bazylinski, D. A.; Dean, A. J.; Schuler, D.; Phillips, E. J. P.; Lovley, D. R. N_2-Dependent Growth and Nitrogenase Activity in the Metal-Metabolizing Bacteria, *Geobacter* and *Magnetospirillum* Species. *Environ. Microbiol.* **2000**, *2* (3), 266–273. https://doi.org/10.1046/j.1462-2920.2000.00096.x.

(45) Logan, B. E.; Regan, J. M. Electricity-Producing Bacterial Communities in Microbial Fuel Cells. *Trends Microbiol.* **2006**, *14* (12), 512–518. https://doi.org/10.1016/j.tim.2006.10.003.

(46) Staal, M.; Lintel-Hekkert, S. te; Harren, F.; Stal, L. Nitrogenase Activity in Cyanobacteria Measured by the Acetylene Reduction Assay: A Comparison between Batch Incubation and on-Line Monitoring. *Environ. Microbiol.* **2001**, *3* (5), 343–351. https://doi.org/10.1046/j.1462-2920.2001.00201.x.

(47) Ramos, J. L.; Guerrero, M. G.; Losada, M. Sustained Photoproduction of Ammonia from Dinitrogen and Water by the Nitrogen-Fixing Cyanobacterium *Anabaena* sp. Strain ATCC. *Appl. Environ. Microbiol.* **1984**, *48* (1), 114–118.

(48) Gordon, J. K.; Brill, W. J. Derepression of Nitrogenase Synthesis in the Presence of Excess NH4+. *Biochem. Biophys. Res. Commun.* **1974**, *59* (3), 967–971. https://doi.org/10.1016/S0006-291X(74)80074-4.

(49) Torres, C. I.; Krajmalnik-Brown, R.; Parameswaran, P.; Marcus, A. K.; Wanger, G.; Gorby, Y. A.; Rittmann, B. E. Selecting Anode-Respiring Bacteria Based on Anode Potential: Phylogenetic, Electrochemical, and Microscopic Characterization. *Environ. Sci. Technol.* **2009**, *43* (24), 9519–9524. https://doi.org/10.1021/es902165y.

(50) Diaz, C.; Baena, S.; Fardeau, M.-L.; Patel, B. K. C. *Aminiphilus circumscriptus* Gen. Nov., Sp. Nov., an Anaerobic Amino-Acid-Degrading Bacterium from an Upflow Anaerobic Sludge Reactor. *Int. J. Syst. Evol. Microbiol.* **2007**, *57* (8), 1914–1918. https://doi.org/10.1099/ijs.0.63614-0.

(51) Lesnik, K. L.; Liu, H. Establishing a Core Microbiome in Acetate-Fed Microbial Fuel Cells. *Appl. Microbiol. Biotechnol.* **2014**, *98* (9), 4187–4196. https://doi.org/10.1007/s00253-013-5502-9.

(52) Wang, Y.; Wang, Q.; Li, M.; Yang, Y.; He, W.; Yan, G.; Guo, S. An Alternative Anaerobic Treatment Process for Treatment of Heavy Oil Refinery Wastewater Containing Polar Organics. *Biochem. Eng. J.* **2016**, *105*, 44–51. https://doi.org/10.1016/j.bej.2015.08.012.

(53) Li, N.; He, L.; Lu, Y.-Z.; Zeng, R. J.; Sheng, G.-P. Robust Performance of a Novel Anaerobic Biofilm Membrane Bioreactor with Mesh Filter and Carbon Fiber (ABMBR) for Low to High Strength Wastewater Treatment. *Chem. Eng. J.* **2017**, *313*, 56–64. https://doi.org/10.1016/j.cej.2016.12.073.

(54) Latif, M. A.; Mehta, C. M.; Batstone, D. J. Enhancing Soluble Phosphate Concentration in Sludge Liquor by Pressurised Anaerobic Digestion. *Water Res.* **2018**, *145* (60), 660–666. https://doi.org/10.1016/j.watres.2018.08.069.

(55) Su, X.-L.; Tian, Q.; Zhang, J.; Yuan, X.-Z.; Shi, X.-S.; Guo, R.-B.; Qiu, Y.-L. *Acetobacteroides hydrogenigenes* Gen. Nov., Sp. Nov., an Anaerobic Hydrogen-Producing Bacterium in the Family Rikenellaceae Isolated from a Reed Swamp. *Int. J. Syst. Evol. Microbiol.* **2014**, *64* (Pt 9), 2986–2991. https://doi.org/10.1099/ijs.0.063917-0.

(56) Oren, A. The Family Methanocorpusculaceae. In *The Prokaryotes: Other Major Lineages of Bacteria and The Archaea*; Rosenberg, E., DeLong, E. F., Lory, S., Stackebrandt, E., Thompson, F., Eds.; Springer Berlin Heidelberg: Berlin, Heidelberg, 2014; pp 225–230. https://doi.org/10.1007/978-3-642-38954-2_314.

(57) Oren, A. The Family Methanobacteriaceae. In *The Prokaryotes*; Rosenberg, E., DeLong, E. F., Lory, S., Stackebrandt, E., Thompson, F., Eds.; Springer Berlin Heidelberg: Berlin, Heidelberg, 2014; pp 165–193. https://doi.org/10.1007/978-3-642-38954-2_411.

(58) Leigh, J. Nitrogen Fixation In Methanogens: The Archaeal Perspective. *Curr. Issues Mol. Biol.* **2000**, *2* (4), 125–131. https://doi.org/10.21775/cimb.002.125.

(59) Lobo, A. L.; Zinder, S. H. Nitrogen Fixation by Methanogenic Bacteria. In *Biological Nitrogen Fixation*; 1992; pp 191–211.

(60) Dos Santos, P. C.; Fang, Z.; Mason, S. W.; Setubal, J. C.; Dixon, R. Distribution of Nitrogen Fixation and Nitrogenase-like Sequences amongst Microbial Genomes. *BMC Genomics* **2012**, *13* (1), 162. https://doi.org/10.1186/1471-2164-13-162.

(61) Zhang, C.; Ma, J.; He, D.; Waite, T. D. Capacitive Membrane Stripping for Ammonia Recovery (CapAmm) from Dilute Wastewaters. *Environ. Sci. Technol. Lett.* **2018**, *5* (1), 43–49. https://doi.org/10.1021/acs.estlett.7b00534.

(62) Tarpeh, W. A.; Barazesh, J. M.; Cath, T. Y.; Nelson, K. L. Electrochemical Stripping to Recover Nitrogen from Source-Separated Urine. *Environ. Sci. Technol.* **2018**, *52* (3), 1453–1460. https://doi.org/10.1021/acs.est.7b05488.

(63) Bageshwar, U. K.; Srivastava, M.; Pardha-Saradhi, P.; Paul, S.; Gothandapani, S.; Jaat, R. S.; Shankar, P.; Yadav, R.; Biswas, D. R.; Kumar, P. A.; et al. An Environmentally Friendly Engineered *Azotobacter* Strain That Replaces a Substantial Amount of Urea Fertilizer While Sustaining the Same Wheat Yield. *Appl. Environ. Microbiol.* **2017**, *83* (15), 1–14. https://doi.org/10.1128/AEM.00590-17.

(64) Bali, A.; Blanco, G.; Hill, S.; Kennedy, C. Excretion of Ammonium by a *NifL* Mutant of *Azotobacter Vinelandii* Fixing Nitrogen. *Appl. Environ. Microbiol.* **1992**, *58* (5), 1711–1718.

Figures

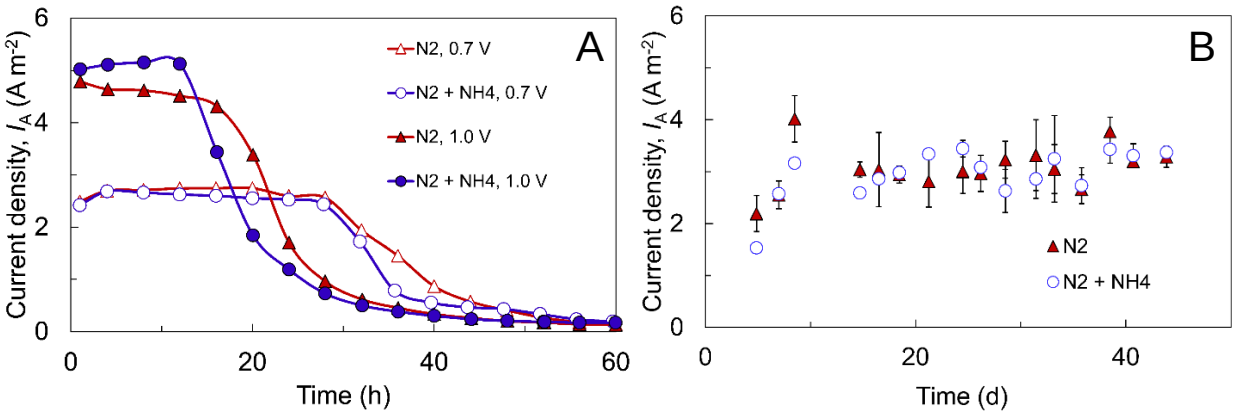

Figure 4.1. A) Current densities (I_A; normalized to anode surface area) of the microbial electrolysis cells (MECs) at E_{AP} = 0.7 V and 1.0 V under an atmosphere of 100% N_2 with and without NH_4^+ added (5.8 mM) to the medium. A representative cycle (cycle 16; 40 days after inoculation) is shown. Each line represents the average current of triplicate MECs. The error bars are omitted to improve clarity. Abiotic MECs (not shown) did not generate current. B) Current densities over several cycles at E_{AP} = 0. 7 V. Error bars show the deviation of maximum current density per cycle among triplicates.

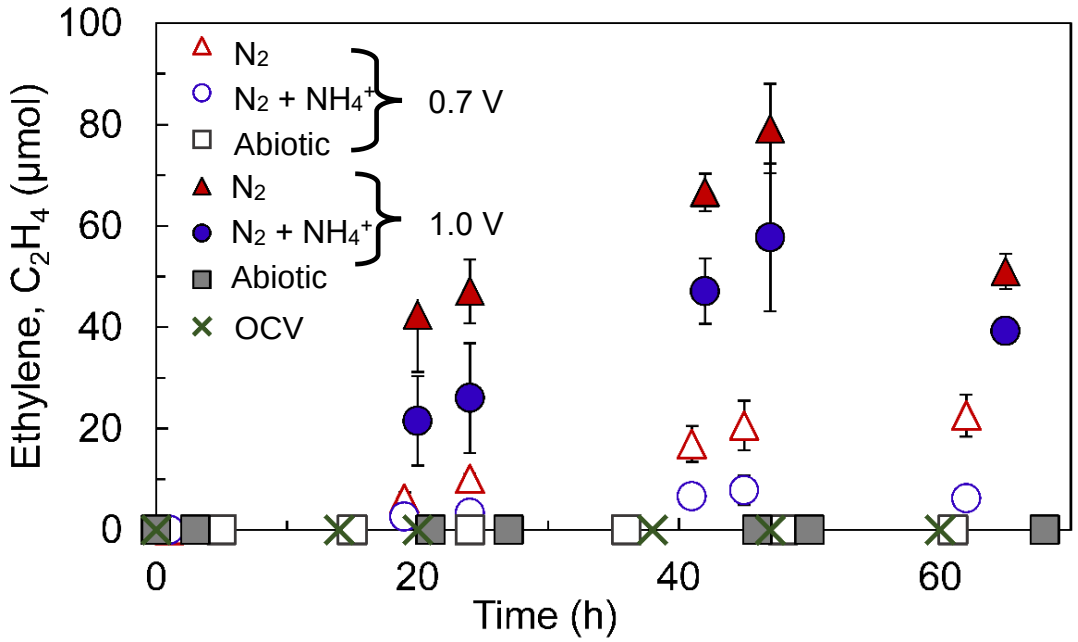

Figure 4.2. N_2 fixation rates during current generation in the microbial electrolysis cells (MECs) at E_{AP} = 0.7 V and E_{AP} =1.0 V. To estimate N_2 fixation rates, the acetylene gas reduction assay was performed, wherein the nitrogenase enzyme within the microorganisms reduces acetylene to ethylene gas (C_2H_4; y-axis). MECs were purged with 100% N_2 and operated without fixed nitrogen (N_2) or with NH_4^+ added (N_2 + NH_4^+). Results are shown for cycle 17 (E_{AP} = 0.7 V) and 18 (E_{AP} = 1.0 V). Abiotic controls are identical MECs but lack microorganisms, and open circuit voltage (OCV) controls are biotic MECs without current flow. Error bars represent the standard deviation of triplicate MECs.

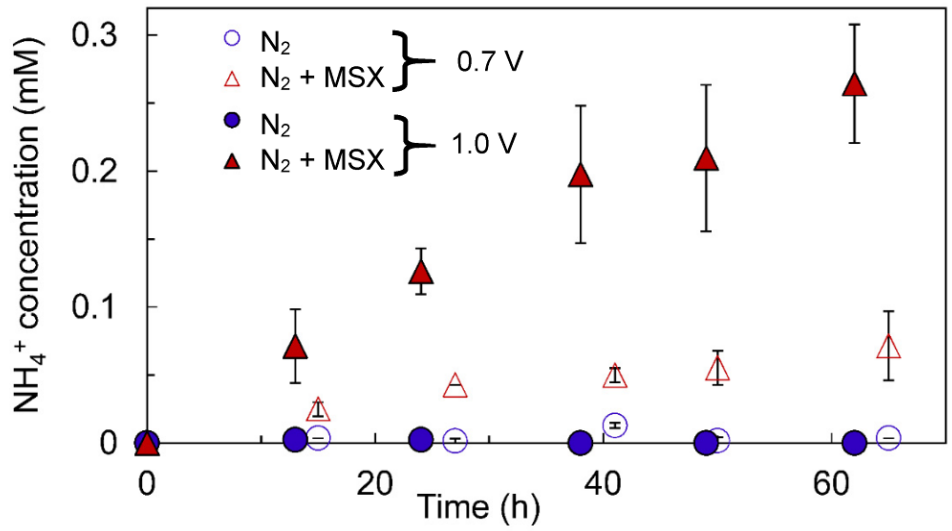

Figure 4.3. NH_4^+ generation in the microbial electrolysis cells (MECs) at an applied voltage (E_{AP}) of 0.7 V and 1.0 V with and without an NH_4^+ uptake inhibitor [methionine sulfoximine (MSX)] added to the medium. All MECs were operated with a 100% N_2 atmosphere and no NH_4^+ added. One complete MEC cycle is shown (~60 h). Error bars show the standard deviation of triplicate MECs.

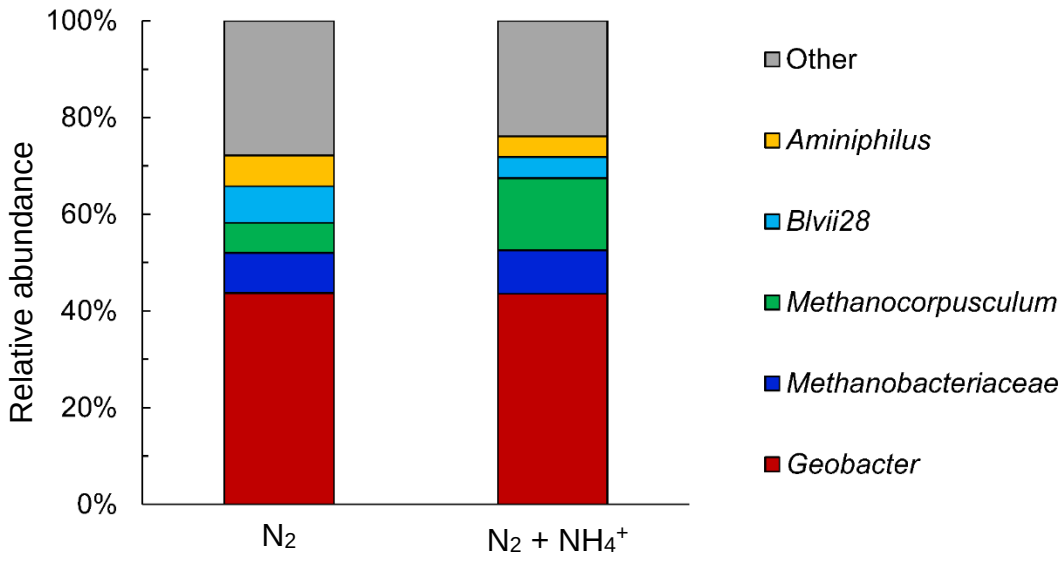

Figure 4.4. Microbial community composition of anode biofilms in the presence and absence of NH_4^+. Percentages show the average relative abundance of genera from triplicate anode biofilms. Dominant biofilm genera (relative abundance > 5%) are shown individually, while the rest are grouped as "Other".

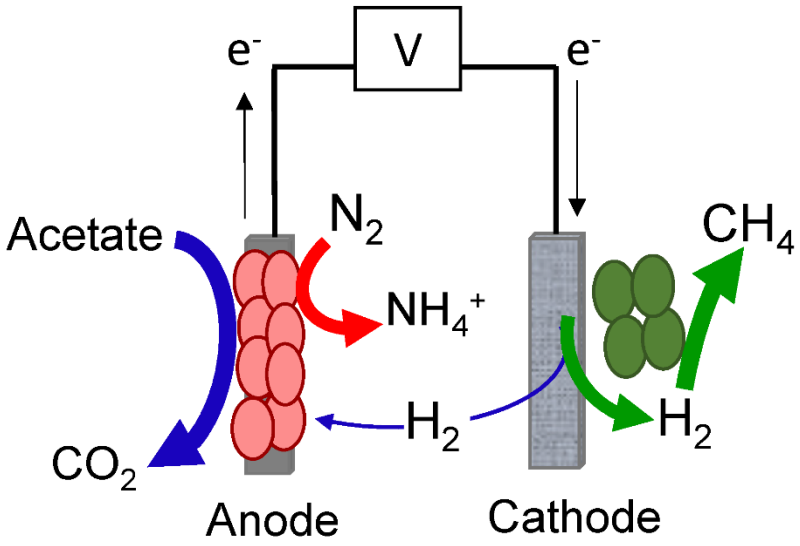

Figure 4.5. Graphical representation of N_2 fixation in the microbial electrolysis cell (MEC). Oxidation (consumption) of acetate provides the required electrons (e^-) for N_2 fixation by the exoelectrogenic bacteria (pink circles). The exoelectrogens transfer the electrons to the anode during respiration. An external voltage (V) drives electrons to the cathode where they produce H_2 gas. H_2 can be consumed by the exoelectrogens to provide electrons for further N_2 fixation and/or converted to CH_4 by methanogens (green circles).

CHAPTER 5

ANALYSIS OF THE TRANSCRIPTOME OF ANODE-RESPIRING *GEOBACTER SULFURREDUCENS* TO REVEAL GENE EXPRESSION CHANGES DURING NITROGEN FIXATION

Abstract

Nitrogen gas (N_2) fixation in anode respiring bacteria such as *Geobacter sulfurreducens* is a complex, multi-step process whose regulation and expression at the genetic level need to be better understood to optimize ammonium (NH_4^+) production in microbial electrolysis cells (MECs). In this chapter, I hypothesized that expression of genes associated with N_2 fixation and NH_4^+ assimilation in *G. sulfurreducens* during anode respiration would be dependent on the anode potential and presence of dissolved NH_4^+. To test this hypothesis, I obtained gene expression levels (via RNA sequencing) from a pure culture of *G. sulfurreducens* growing on anodes fixed at different potentials (E_{AN}) and in the presence of different concentrations of NH_4^+. I found that the presence of NH_4^+ decreased the expression of genes associated with N_2 fixation, such as *nifH*, and *nifD* and *nifK*, which encode the structural subunits of the nitrogenase complex. This result was expected due to the known sensitivity of nitrogenases to NH_4^+. The anode potential had a dramatic and unexpected impact on the expression levels of N_2 fixation genes. At the low E_{AN} [−0.15 V vs. standard hydrogen electrode (SHE)], nitrogenase genes were significantly up-regulated, as were genes associated with NH_4^+ uptake and transport, such as glutamine and glutamate synthetases. Considering that −0.15 V provides less energy to the cells relative to +0.15 V (based on thermodynamic predictions), my results suggest that the cells responded to this highly energy-constrained environment by increasing expression of N_2 fixation pathways. These findings have

important implications for understanding regulatory pathways of N_2 fixation and will allow identification of target genes or operational strategies to enhance NH_4^+ production in MECs.

Significance

A key knowledge gap towards the development of an NH_4^+-generating microbial electrochemical technology (MET) is the mechanism of microbial N_2 fixation in response to electrochemical process control. The results of this chapter are significant because they provide fundamental insight into N_2 fixation pathways in the exoelectrogen *G. sulfurreducens*. Most notably, my findings suggest that targeting NH_4^+ assimilation and transport genes may permit excretion of this compound during anode respiration. Additionally, controlling the anode potential to enable increased expression of N_2 fixation genes may provide an operational approach to enhance N_2 fixation rates.

5.1 Introduction

Biological nitrogen gas (N_2) fixation is considered a promising alternative to generate ammonium (NH_4^+) due to the capacity of microorganisms to perform this process under atmospheric conditions. Many bacteria belonging to the family Geobacteraceae possess N_2 fixation genes, which allow them to survive in conditions when fixed nitrogen is limited.[1] Several species in this family are classified as electrochemically active bacteria (EAB), or exoelectrogens, due to their ability to transfer electrons extracellularly to insoluble electron acceptors during respiration. Among those microorganisms, extensively studied EAB such as *Geobacter metallireducens* and *G. sulfurreducens* are capable of performing N_2 fixation, either through nitrogenase activity in the wild type strains or by the manipulation of genes, such as *nifD*, that encode nitrogenase subunits.[1,2]

As discussed in Chapter 4, one advantage of using EAB for N_2 fixation and NH_4^+ production is that their respiration rates can be increased through the application of an external applied voltage. However, in that chapter NH_4^+ recovery was only possible with the addition of a chemical inhibitor, which may pose an economic and environmental challenge for sustainable production of NH_4^+. Developing a bacterial strain capable of excreting NH_4^+ may provide a sustainable approach to recovering NH_4^+. This approach has been performed previously on model aerobic diazotrophs, such as *Azotobacter* species, through genetic manipulation and mutation of NH_4^+ uptake genes.[3,4] The resulting mutant strains are able to excrete NH_4^+ at concentrations close to 30 mM.[5] However, due to the O_2 sensitivity of nitrogenase enzymes, it is challenging to increase and sustain NH_4^+ production in microorganisms such as *Azotoacter* that require O_2 as a terminal electron acceptor. Generating an efficient strain of a diazotrophic, exoelectrogenic bacteria that operates under the anaerobic conditions of an MET is thus an attractive strategy for sustainably producing NH_4^+.

There are several N_2 fixation pathways and regulatory controls that are common across diazotrophs. Due to the high energetic and metabolic requirements, N_2 fixation is tightly regulated by several regulatory motifs that activate hierarchically (a "regulatory cascade") only when nitrogen limiting conditions are present and the process can proceed under favorable conditions (e.g., absence of O_2).[6] Expression of N_2 fixation and NH_4^+ assimilation genes are dependent on sigma factor 54 of the RNA polymerase (σ^{54}) encoded by RpoN[7] which is normally present in diazotrophic microorganisms.[8] In well characterized, free-living diazotrophs, regulation of transcription is normally performed by the general nitrogen regulation system (Ntr), which comprises the proteins GlnB (or its homolog GlnK), GlnD, NtrB and NtrC, with the latter two acting as a two-component His-Asp phosphorelay sensory system in which NtrB, a histidine

kinase, phosphorylates NtrC after the other proteins sense low levels of bioavailable nitrogen.[9] Through this system, Ntr controls the expression of the *nifLA* promoter, which encodes the transcriptional activator NifA and the anti-activator protein NifL. NifA acts as the master regulator of N_2 fixation that ultimately allows transcription initiation by the RNA polymerase-σ^{54} complex. NifL forms a complex with NifA when enough fixed nitrogen is present or inhibitory oxygen levels are sensed, preventing transcription of N_2 fixation genes and adding an extra component to the regulatory cascade (**Fig. 5.1A**).[6]

While this regulatory process is well conserved and characterized in diazotrophic Alpha, Beta and Gamma-Proteobacteria, N_2 fixation and its regulatory controls are different and less understood for Delta-proteobacteria, particularly within the genus *Geobacter*. Nitrogenase genes such as *nifD* are generally similar to other diazotrophic bacteria and are well-conserved among species within Geobacteraceae.[10] N_2 fixation and NH_4^+ assimilation genes are also dependent on the regulon RpoN; however, the expression of these genes appears to be controlled by two two-component His-Asp phosphorelay systems instead of one.[11] The first regulator, the GnfL/GnfM system, acts similarly to the NtrB/NtrC system in other organisms by initially sensing fixed nitrogen (NH_4^+) concentrations, where GnfL (also a histidine kinase) phosphorylates GnfM when NH_4^+ levels are low. GnfM also acts as the master regulator to initiate transcription, a theory supported by the absence of NifA homologues in *Geobacter*.[11] The second phosphorelay system, GnfK/GnfR, supports the expression of N_2 fixation genes by means of an anti-termination mechanism (**Fig. 5.1B**). A deeper understanding is thus needed to know which genes can be targeted to overcome regulatory limitations and optimize N_2 conversion into NH_4^+ in these organisms.

Microbial electrolysis cells (MECs) offer a controlled, anaerobic environment where diazotrophic EAB grow. The anode, acting as electron acceptor for EAB, can be adjusted by external electrochemical factors such as external voltage (E_{AP}) or a fixed anodic potential (E_{AN}),[12,13] leading to different respiration rates and electron transfer responses that are attributed to the expression of different electron transferring proteins and pathways. While the CbcL-dependent pathway has been reported to be the main contributor (at least 60%) to electron transfer in *Geobacter*-enriched anodes,[14] at E_{AN} above −0.10 V vs. standard hydrogen electrode (SHE), the ImcH-dependent pathway is expressed to harvest additional energy.[15] For this reason, biocatalytic activity of organisms such as *G. sulfurreducens* largely remains unchanged, although biomass and current generation increase with a more positive E_{AN} due to the higher electron transfer rates and the expression of additional pathways for electron transfer.[16,17] Subsequently, it is important to know which processes and metabolic pathways are favored due to the changes in available energy and electron transfer mechanisms. Additionally, both N_2 fixation and extracellular electron transfer are vulnerable to O_2 exposure, therefore, cells must develop mechanisms to protect cells from oxidative stress caused by this gas. Diazotrophic EAB such as *G. sulfurreducens* contain genes that encode enzymes to scavenge oxygen radicals and provide protection from oxidative stress,[18] while also being able to respire on O_2 under low concentrations (~5%).[19] Although performing N_2 fixation in MECs offers the advantage that this system is maintained under anaerobic conditions, the presence of trace amounts of O_2 needs to be accounted for in case it is present in larger scale iterations of this technology.[20]

The aforementioned processes involve the transfer of electrons that are obtained from the electron donor. After reducing equivalents are generated through respiration, some electrons are redirected to biomass production, while others are utilized in the reduction of N_2.[21] Energy may

also be spent in the production of stress response mechanisms, such as the presence of O_2, which inhibits nitrogenase and acts as a repressor of nitrogen fixation even in aerobic microorganisms.[22] Therefore, besides the required regulation of each process (e.g., the double phosphorelay system for N_2 fixation control), strong regulatory pathways that serve as links between processes must ensure that distribution of energy and electrons is optimized.

Unlike other diazotrophic microorganisms, RpoN in *Geobacter* species appears to control a handful of constitutive genes, regardless of nitrogen availability. Genome analysis suggests that RpoN is involved in conductive pili (nanowire) biosynthesis,[7] while also being the primary sigma factor to regulate energy metabolism and maintain redox homeostasis.[23] It is therefore, the factor responsible for shifting respiratory pathways in *G. sulfurreducens* when an insoluble electron acceptor, such as an electrode, is utilized instead of fumarate (the most common soluble electron acceptor for this bacterium).[23] The role of RpoN-directed regulation thus suggests metabolic interactions within *Geobacter sp.* occur between N_2 fixation, biomass generation through NH_4^+ uptake and extracellular electron transfer. The interactions of these pathways can be better understood by comparing the expression levels of genes involved in diverse microbial functions. To achieve this, the bacterial transcriptome [all transcribed messenger RNA (mRNA)] can be extracted, sequenced, and analyzed to detect differences in expression levels depending on the growth conditions. For exoelectrogenic bacteria, transcriptome analysis has been performed previously to study changes in metabolic pathways due to anode respiration. In pure cultures of *G. sulfurreducens* respiring on anodes, anode respiration lead to higher expression levels (upregulation) of several genes found to be involved in extracellular electron transfer.[24,25] While similar studies have been performed to find processes that are involved in regulation of N_2 fixation, information about gene expression under simultaneous N_2 fixation and anode respiration is scarce.

Therefore, the overarching objective of this chapter was to analyze the transcriptome of *G. sulfurreducens* growing under different electrochemical and environmental conditions. Doing so would permit assessment of changes in gene expression during different conditions of anode respiration and N_2 fixation, and lead to a better understanding of the regulation of diazotrophic pathways that occurs in *G. sulfurreducens*.

5.2 Materials and methods

5.2.1 Reactor assembly and operation

Gas-tight microbial electrolysis cells (MECs) were utilized to grow electrochemically active bacteria (**Fig. 5.2**). They consisted of 100 ml glass bottles, with gas-tight rubber stoppers (DWK Life Sciences, Germany). A graphite plate (A_A = 4.5 cm^2) was utilized as anode, whereas stainless steel mesh (A_C = 3.9 cm^2) was utilized as a cathode. Both electrodes were connected to current collectors (titanium and stainless-steel wires, respectively) and inserted through the rubber stopper. To guarantee reproducibility of replicates, a plastic screw was used to join the electrodes and ensure a similar distance between them (2 cm). A silver-silver chloride (Ag/AgCl) reference electrode (~+200 mV vs. SHE) was inserted through the rubber stopper and placed between the anode and cathode.

After assembly, MECs were inoculated with a pure culture of *G. sulfurreducens* strain PCA. This organism was chosen because it is a model exoelectrogenic microorganism that can fix N_2, its genome is sequenced,[18] and it has been proven amenable for bacterial transformation, offering the possibility of eventual NH_4^+ production and optimization through gene editing.[2] *G. sulfurreducens* cultures were grown in a phosphate buffered medium as previously described,[26] with sodium acetate as electron donor (1 g/L), sodium fumarate as electron acceptor (8 g/L), and

without ammonium chloride (NH_4Cl) added to the medium. Once cells achieved early stationary phase (OD_{600} ~ 0.5), 10 ml of culture per reactor were harvested by centrifugation (4,000 rpm for 20 min), and the pellet was resuspended in 100 ml of PBM, with 2 g/L of sodium acetate (to ensure a longer and stable maximum current period during MEC operation) but with no fumarate added. Unless specified, NH_4Cl was omitted from the medium. After addition of media and inocula to the MECs, they were operated in batch mode at 30 ºC and were connected to a potentiostat (Bio-Logic Science Instruments, Knoxville, TN) under the treatments shown in **Table 5.1**. These treatments were chosen to study the effects of applied potential (E_{AN}), NH_4^+ concentration in the medium, and O_2 addition on gene expression and metabolic pathways of *G. sulfurreducens*. Current density (I_A) was measured to track metabolic activity of the cultures and estimate electron transfer rates, and media was replaced once I_A was stable for at least three days (or when I_A started to decrease) to avoid stress responses due to the lack of substrate. MECs were operated for three batches to allow biofilm formation in the anode. For the third batch, reactors operated for two days after refeeding before harvesting the anode and extracting RNA to ensure constant current generation and stable respiration rates.

5.2.2 RNA extraction and sequencing

Once MECs demonstrated stable respiration rates, anode biofilms were harvested for RNA extraction. Two days after the beginning of the third batch, anodes were removed and placed directly in RNAprotect Bacteria Reagent (QIAGEN) to preserve total RNA. The anode was vigorously scraped using a sterile razor sharp to remove the biofilm cells, which were deposited in the aforementioned solution and incubated for 5 min. After centrifuging the samples (5,000 g for 10 min at 4 ºC), the supernatant was removed, and the pellets were stored at −80 ºC until RNA

was extracted. RNA extraction was performed using the RNAeasy Mini Kit (QIAGEN) following the manufacturer's instructions to lyse cells using lysozyme and proteinase K, as well as adding DNAse I to remove DNA contamination. At least 3 µg of total RNA per sample, all with an A_{260}/A_{280} purity of 2 or higher, were sent to the Genomic Sciences Laboratory (GSL) at North Carolina State University. The RNA samples were subjected to ribodepletion, where ribosomal RNA (rRNA) was removed from the samples using the RiboMinus Transcriptome Isolation kit for bacteria followed by the RiboMinus Concentration Module (Thermo Fisher Scientific, Waltham, MA). Although only a fractional depletion of ribosomal RNA (rRNA) was achieved (~60% removal), RNA libraries were successfully prepared using the NEBNext Ultra RNA library prep kit for Illumina (New England BioLabs Inc., Ipswich, MA). The average library size was 430 base pairs (bp) with an average insert size of 305 bp. The pooled libraries were sequenced using the Illumina NovaSeq 6000 SP platform, with a read length of 150 paired end (PE). Around 20-25 million sequencing reads per sample were obtained in order to account for the remaining rRNA and increase the resolution of the mRNA profiles.

After the sequencing data were obtained, sequencing results were filtered using the Trimmomatic tool to remove adapters and low-quality reads.[27] They were subsequently aligned to existing genes using the Bowtie2 software tool, using the genome of *G. sulfurreducens* PCA from Ensembl Genome platform as a reference.[28] Counts of successful alignments and generation of gene tables were performed using the HTSeq software tool.[29] Gene tables were analyzed on the R platform, utilizing the DESeq2 package to perform statistical and differential expression analysis.[30] Genes of the tested treatments were considered to be differentially expressed against the reference treatment ("NP"; No NH_4^+ added, +0.15 V E_{AN}) when log2-fold expression levels were higher than 2.0, and when the adjusted *p*-value was less than 0.05 to minimize false discovery rates (FDR).

5.3 Results and discussion

5.3.1 Current density profiles of MECs

The purpose of utilizing gas-tight microbial electrolysis cells (MECs) with a bigger volume than in the previous studies described in this dissertation was to obtain robust and reproducible gene expression profiles as a function of two key variables: (1) applied potential (E_{AN}) and (2) concentration of fixed nitrogen (NH_4^+). After inoculation with pure cultures of *G. sulfurreducens*, all reactors displayed similar current density (I_A) profiles (**Fig. 5.3**), where bacterial colonization of the anode was reflected in a steady increase in I_A (defined as the startup or enrichment phase) due to extracellular electron transfer and consumption of electron donor (i.e., acetate) until maximum I_A was reached. Subsequent replenishment of growth medium caused I_A to reach similar densities that were maintained for at least seven days, implying successful biofilm formation on the anode. Even though I_A profiles were similar among all treatments, especially in regards to E_{AN} (**Figs. 5.3A** and **5.3B**), it is worth noting that the presence of NH_4^+ (**Figs. 5.3C** and **5.3D**) was associated with a decrease in current over time, which is also reflected in the maximum current achieved in treatments amended with NH_4^+ (**Table 5.2**). While this decrease in current may be associated with microbial stress, the concentration of NH_4^+ (5.8 mM) that we used is frequently used in growth media for MEC studies involving *Geobacter* species,[31] and both concentrations that we used are below values (> 15 mM NH_4^+) that are reported to cause a significant decrease in current and biomass in MECs.[32] It has been reported that large current densities can occur when low to no fixed nitrogen is present,[33] which agrees with our results.

The presence of O_2 in the MECs caused unpredictable (5% O_2, "OP") and undetectable (21% O_2, "AP") current generation. As such, start-up times and maximum current in reactors with 5% O_2 generally were longer and displayed more variability (**Table 5.2**), with I_A profiles

appreciably different from the other treatments (**Appendix C**). Regarding MECs with atmospheric levels of O_2, current generation was very low and reactors never achieved 0.1 A/m^2, which was expected given the vulnerability of *G. sulfurreducens* to aerobic conditions.

5.3.2 Transcriptome data summary

Gene expression profiles of *G. sulfurreducens* under N_2 fixation conditions in MECs were compared across five treatments (**Table 5.1**). When discussing changes in gene expression, we defined the transcriptome of reactors operating at E_{AN} = +0.15 V and no NH_4^+ added ("NP") as the reference. From the approximately 3,430 genes that were identified during analysis, a total of 290, 193 and 304 genes were differentially expressed under the conditions of low E_{AN} ("NN"), the addition of 5.8 mM NH_4^+ ("LP"), and the addition of 11.6 mM NH_4^+ ("HP"), respectively (**Table 5.3**). We defined differential expression as a 2-fold change > 2.00 and a *p*-value < 0.05. Based on this definition, differentially expressed genes are those that are responsive to either the change in E_{AN} or the presence of NH_4^+ (classified as up-regulated or down-regulated with respect to "NP"), while non-differentially expressed genes are constitutively-expressed genes and/or are unaffected by anode potential or NH_4^+. We grouped differentially expressed genes by metabolic function (e.g., N_2 fixation, electron transfer activity, etc.) based on gene ontology and assigned annotations for *G. sulfurreducens* PCA from the Gene Ontology (GO) and Ensembl databases.[34,35] Several genes had a significant difference in expression with respect to the reference treatment ($p < 0.05$), but the change did not reach the log2-fold threshold, which is shown in the respective volcano plots for expression distribution (**Appendix C**). Many of those genes displayed high normalized gene counts [expressed in reads per kilobase per million mapped reads (RPKM)], which implies that those genes possessed high levels of expression under a specific treatment. As such, we decided

to include those genes in the discussion below in order to better understand the impact of our treatments on exoelectrogenic N_2 fixation.

For the 5% O_2 ("OP", **Table 5.2**) treatment, current generation and transcriptome profiles were erratic and unreproducible. No genes for that treatment were differentially expressed. Possible reasons for this result include: (1) difficulty maintaining a uniform gas composition within the MECs, as O_2 was directly injected to the headspace instead of employing a standardized mixture, and (2) differences in O_2 exposure throughout the anode biofilm. Since we did not have a high degree of confidence in this treatment and the resulting transcriptome profile, we omit discussion of this treatment in the following section.

5.3.3 Gene expression under N_2 fixation conditions

The expression of several genes related to N_2 fixation increased when the cells were operated at the negative potential (E_{AN} = −0.15 V; **Fig. 5.4**) in the absence of NH_4^+. Although only two genes that are critical to N_2 fixation (*nifEN* and *nifV;* involved in nitrogenase assembly) were upregulated by more than two log2-fold, other genes showed a high number of counts when E_{AN} was negative, including genes encoding the nitrogenase enzyme (*nifD*, *nifH* and *nifK*). Genes such as *gnfK* and *gnfR*, which are involved in regulating and expressing the required genes for N_2 fixation under low fixed nitrogen conditions,[11] were upregulated at −0.15 V, supporting the hypothesis that N_2 fixation increased at the negative anode potential. Although moderately expressed, the counts of *amtB* were also higher at −0.15 V. This gene encodes an NH_4^+ transporter that is expressed when low or limiting concentrations of NH_4^+ are present to better help the cell scavenge this nutrient from the environment.[36] Gene counts for the molybdenum (Mo) transport system genes at −0.15 V were also higher (**Appendix C)**. It has been shown that *Geobacter* sp.

increase expression of this system under N_2 fixing conditions to acquire Mo from the environment,[37] which is consistent with the increased demand of this element, as it is an essential component of the Mo-Fe nitrogenase in *G. sulfurreducens*.[11] It is worth noting that other regulatory genes involved in N_2 fixation did not display a difference with respect to E_{AN}, such as *draG* and *draT*, which are responsible for biochemically modulating nitrogenase reductase activity in response to high fixed nitrogen in diazotrophic microorganisms.[38] Although these regulatory genes are adjacent in *G. sulfurreducens* to other N_2 fixation genes which were differentially expressed (such as *NifEN*), there is little information on their function and importance in regulating N_2 fixation.

Regarding NH_4^+ assimilation, relevant genes such as *glnA*, *nfnA*, and *gltS* possessed both high numbers of counts and were upregulated at $E_{AN} = -0.15$ V (**Fig. 5.4**). The gene *glnA*, which encodes the enzyme glutamine synthetase, is crucial for enabling NH_4^+ (either generated through N_2 fixation or that is present in the medium) to react with the amino acid glutamate (one amino group) and form glutamine (two amino groups). The genes *nfnA* and *gltS* encode an electron carrier-dependent glutamate synthase that utilizes glutamine as a substrate to recycle glutamate (via removal an amino group), effectively acting as an NH_4^+ assimilation and transport mechanism as well as an additional nitrogen sensing system.[39,40] Glutamate is sometimes produced by bacteria when osmotic regulation is required in response to a change in solute concentrations in the cell's environment,[41] as well as a decrease in pH. Due to higher nitrogenase activity at −0.15 V (based on gene expression profiles), higher intracellular NH_4^+ concentrations would be expected.[42] Therefore, a counter-ion such as glutamate may be needed to balance charges and to provide a reactant to convert NH_4^+ into glutamine to avoid osmotic stress.[43] Glutamate formation may also alleviate H^+ buildup from oxidation of H_2 (consumed via uptake hydrogenases) generated as a

byproduct of the nitrogenase.[42] Another function of glutamate, which could be related to the high expression of *nfnA* and *gltS*, is to act as an electron sink under low availability of electron acceptors. It has been reported that other organisms, such as the fungi *Aspergillus nidulans* and the bacterium *Clostridium thermocellum*, produce amino acids (among them glutamate) under low oxygen levels (i.e., fermentative conditions) to reduce the accumulation of reduced electron carriers such as NADH and NADPH.[44–46] As *gltS* encodes a NADPH-dependent glutamate synthase, it is possible that a similar process is taking place in *G. sulfurreducens*, as a low E_{AN} offers lower electron transfer rates that may lead to accumulation of electron carriers.

We also examined the expression of genes related to extracellular electron transfer in *G. sulfurreducens* as a function of anode potential since those genes are involved in current generation in MECs. Genes related to electron transfer shared a major portion of the overall expression profile, where 14 genes were up-regulated and 11 down-regulated when E_{AN} became negative (**Fig. 5.5**). This change in expression was expected because electron transfer kinetics and activity depend on E_{AN} in METs,[17] and exoelectrogenic bacteria can adapt electron transfer pathways to changes in E_{AN}.[17] When normalized counts were calculated for genes that are known to possess electron transfer activity, we found that the expression of several genes was significantly higher at E_{AN} = −0.15 V, including flavoproteins, periplasmic proteins and some outer-membrane cytochromes (OMCs) (**Fig. 5.6A**). Flavoproteins such as *etfB* (and presumably, adjacent genes GSU2795 and GSU2799) are likely involved in anode respiration, as they become upregulated in *G. sulfurreducens* growing on electrodes.[47] OMCs are usually required by *Geobacter* species to transfer electrons to insoluble electron acceptors, such as iron, manganese, uranium, or anodes in microbial electrochemical technologies (METs).[21,24,48] Among them, *omcE* was heavily expressed at the negative E_{AN}. This cytochrome is required for iron (III) oxide reduction[49] and has also been

shown to be involved in anode respiration,[47,50] although its structure, properties, and exact function during electron transfer remain to be elucidated.[51] Interestingly, the genes of other well-characterized OMCs that are commonly expressed during anode respiration, such as *omcB* and *omcS*,[48,50] were not found to be differentially expressed in response to E_{AN}. Although it has been previously discussed that different OMCs are expressed depending on E_{AN}, a more positive potential favors the expression of a higher variety of OMCs.[52] Therefore, it is surprising that only *omcE* showed high expression levels and was upregulated at $E_{AN} = -0.15$ V, suggesting that this OMC may have a connection with N_2 fixation. It is important to note that other genes associated with electron transfer in *G. sulfurreducens* and are responsive to E_{AN}, such as *cbcL* and *imcH*,[15,52,53] were not differentially expressed in our experiments. *cbcL* expression was 1.09 Log2-fold lower at $E_{AN} = -0.15$ V, which agrees with another study[52] but contradicts others that established that the *cbcL*-associated electron transfer pathway had higher activity at potentials below −0.1 V.[15,53] Even though *pilA* is not classified within the "electron transfer activity" category, it encodes a critical component for electron transfer to anodes in *G. sulfurreducens.*[54] The expression of *pilA* during $E_{AN} = -0.15$ V was up-regulated (log2-fold change = 2.48), which suggests a higher electron transfer activity, even though I_A was similar between E_{AN} (**Table 5.3**).

Other genes of interest with high expression counts at −0.15 V included the H_2-dependent growth transcriptional repressor gene *hgtR* (upregulated at −0.15 V) and genes belonging to the *hyb* gene cluster (**Fig. 5.6B**). HgtR represses genes that are involved in biosynthesis and energy generation when *Geobacter* species use H_2 as an electron donor.[55] The high expression of this gene can be attributed to two possible reasons: (1) the MEC chosen for this study is a single-chamber reactor where H_2 generated at the cathode is available for uptake by the anode biofilm, and (2) nitrogenase produces H_2 as a by-product of N_2 fixation, which can serve as an electron donor.[56]

As nitrogenase-related genes had higher expression levels at −0.15 V (implying that N_2 fixation was greater at that potential), it is likely that *hgtR* was highly expressed due to H_2 produced by the nitrogenase. Expression of *hgtR* may have diverted electrons from central carbon metabolism and biosynthesis towards N_2 fixation at that potential. The fact that both HgtR and N_2 fixation genes are mediated by RpoN[7,55] lends support to a relationship between these processes.

Regarding hydrogenase genes, the *hyb* cluster comprises genes that synthesize a periplasmic-oriented, nickel-dependent hydrogenase Hyb, which is essential for *G. sulfurreducens* to use H_2 as an electron donor.[57,58] Some of the genes in this cluster, such as *hybS* and *hybP*, showed a slightly higher expression (~1.5-fold higher number of counts) at −0.15 V, which could be related to higher nitrogenase activity. The majority of the genes on this cluster did not show different expression levels between E_{AN}, which is consistent with the almost identical harvesting current density displayed by these reactors. Current density is directly proportional to H_2 generation in an MEC, so the availability of cathodically-generated H_2 as an electron donor to the anode biofilms was likely similar at both E_{AN}. Interestingly, the cluster *mvh*, which encodes a cytoplasmic hydrogenase related to the hydrogenases found in methanogens[58] was downregulated at −0.15 V (**Fig. 5.6B**). Although the expression of these genes was lower than the *hyb* cluster, this hydrogenase is also involved in H_2 uptake, and it may be involved in other functions such as converting forms of reducing power to or from hydrogen.[58] As the expression of *mvh* genes behaves in direct opposition with HgtR and N_2 fixation, an antagonistic relationship may be occurring, although the exact role and regulation of Mvh remains unclear. Regarding the remaining hydrogenases, the gene clusters *hox*, which may be involved in H_2 production,[58,59] and *hya*, likely involved in oxidative stress defense rather than hydrogen uptake,[60] did not display high counts nor differential expression between treatments (data not shown), most likely due to the experimental

conditions analyzed (i.e., biofilm anode instead of biofilm cathode, and anaerobic conditions when comparing E_{AN}). Additional experiments where cathodically produced H_2 is not influencing gene expression may offer a deeper insight into the relationship between the aforementioned H_2 uptake systems and H_2 production due to nitrogenase activity.

5.3.4 Effect of NH_4^+ on gene expression profiles

The addition of NH_4^+ resulted in differential expression of a wide array of genes related to biosynthesis and reduction in the expression of N_2 fixation genes. While addition of a high concentration of NH_4^+ (11.6 mM) resulted in a higher number of differentially expressed genes, change in expression was almost identical, which resulted in no genes that were differentially expressed between the low and high NH_4^+ treatments (**Figs. 5.7** and **5.8**). Classes of up-regulated biosynthesis-related genes included those categorized under translation (e.g., ribosomal proteins), protein folding and stabilization (e.g., chaperones), as well as genes encoding NADH dehydrogenases. This result was expected because sufficient NH_4^+ availability usually suppresses N_2 fixation and makes available electrons and ATP that would otherwise be used for this metabolically demanding process.[61] The up-regulation of genes associated with the tricarboxylic (TCA) cycle and genes involved in amino acid production when NH_4^+ was present (**Figs. 5.7** and **5.8**) support this hypothesis. At the physiological level, the lower maximum I_A (which is a direct measure of respiration) when NH_4^+ was present in the medium (**Table 5.2**, and **Figs. 5.3C&D**) also supports this hypothesis.

The addition of NH_4^+ (at both concentrations) was associated with down-regulation of the majority of genes corresponding to N_2 fixation (**Fig. 5.9**), which is consistent with prior reports of free-living diazotrophs suppressing N_2 fixation if sufficient NH_4^+ is available. The gene encoding

the ammonium transporter *amtB* was also down-regulated, which was expected, as NH_4^+ at sufficiently high concentrations (more than 1 mM) diffuses through the membrane, and energy is not directed towards synthesizing the transporter.[36] In contrast, the gene *gdhA* was upregulated and highly expressed, which supports our findings, as this gene encodes glutamate dehydrogenase, the enzyme responsible for NH_4^+ uptake when sufficient amounts are present, and is known to be repressed under N_2-fixing conditions.[11] Interestingly, many of the electron transfer activity genes known to be highly expressed under anode respiration, such as *omcS*, *omcE*, *omcB* and *pilA*, were up-regulated with NH_4^+ addition (**Fig. 5.10A**), most likely in response to the reduced energy expenditure resulting from decreased N_2 fixation or NH_4^+ transporter synthesis.[17] Related to that are the higher expression levels of *hgtR* and the *hyb* genes (**Fig. 5.10B**), which again suggest that H_2 is utilized as an electron donor. Based on our current density observations and the repression of nitrogenase activity, the addition of NH_4^+ should result in lower H_2 availability to the anode biofilms. Although counterintuitive, the *hyb* cluster may be expressed to maximize H_2 uptake and recycle electrons towards biomass production when high concentrations of nutrients (i.e., NH_4^+) are available, which is understandable given *Geobacter* spp. frequently faces oligotrophic conditions.[62] Since *mvh* genes were also downregulated with the presence of NH_4^+, *G. sulfurreducens* should be able to express different mechanisms of H_2 uptake (and possible H_2 production) depending on the environmental conditions as it occurs in other microorganisms with several hydrogenase systems,[63] although the exact regulation and H_2 affinity of these systems requires further studies.

5.3.5 Possible association between N_2 fixation with extracellular electron transfer

Based on the transcriptome profiles described above, here we discuss a hypothetical model of N_2 fixation pathways and their regulation in *G. sulfurreducens* as a function of anode potential and availability of NH_4^+. N_2 fixation requires considerable metabolic energy and electrons to reduce N_2 to NH_4^+. When NH_4^+ is available, it is readily converted by glutamate dehydrogenase into amino acids, bypassing energy expenditures associated with fixing N_2 (**Fig. 5.11A)**. It is not surprising that electrons used for N_2 fixation can instead be directed toward biomass production pathways and NH_4^+ uptake when NH_4^+ is present (**Fig. 5.12A**). This observation is supported by the lower respiration rates (current densities) recorded when NH_4^+ was present.[64]

From this same energy conservation perspective, we hypothesized that thermodynamic conditions that allowed faster electron transfer rates and higher metabolic activity (i.e., more positive E_{AN}) would translate into higher expression of genes related to N_2 fixation. However, our results suggest the opposite. Many key N_2 fixation genes were highly expressed during growth at $E_{AN} = -0.15$ V relative to +0.15 V (**Fig. 4**), including genes that code for the nitrogenase subunits such as *nifD*. One explanation for this result may be related to the required metabolic optimization occurring at low E_{AN}, as it has been suggested that some metabolic routes in *Geobacter* sp. are only expressed during growth at certain anode potentials.[15,53] At negative E_{AN} values, the energy available for harvesting by the cell is limited due to the difference between electron donor and acceptor. Under these conditions, many respiratory cytochromes will be in a reduced state, and the ratio between electron carriers such as NAD^+/NADH will be low due to slow electron transfer kinetics, leading to suboptimal growth conditions.[17] We observed no change in expression of NADH dehydrogenase genes, lending support to the idea that reduced electron carriers at $E_{AN} = -0.15$ V may need to be regenerated through other means. To alleviate electron imbalance, other

microorganisms, such as the fungi *Aspergillus nidulans* and the bacterium *Clostridium thermocellum,* produce amino acids as electron sinks when grown under conditions that limit electron acceptor pools (e.g., hypoxia, fermentation), as several enzymes involved in their synthesis utilize NADH or NADPH, effectively regenerating the oxidized forms (i.e., NAD^+, $NADP^+$).[44–46] *Geobacter* species can resort to similar mechanisms, utilizing OMCs as temporal electron sinks when no other electron acceptors are available.[65] Since the nitrogenase utilizes at least eight electrons to produce NH_4^+ (and the by-product H_2), N_2 fixation may be an option to mitigate electron imbalances caused at $E_{AN} = -0.15$ V, which in addition provides an essential nutrient in the form of NH_4^+. Additionally, our results indicated that the genes *glnA*, *nfnA*, and *gltS* were highly expressed and up-regulated at $E_{AN} = -0.15$ V, suggesting that glutamine and glutamate may have also functioned as an electron sink because the *nfnA*/*gltS* system utilizes one reduced equivalent of NADPH per mole of glutamine (**Fig. 5.11B**).[66] Measuring metabolite profiles of these amino acids should provide better insight into their role during simultaneous N_2 fixation and anode respiration.

Other observed up-regulated genes related to electron transfer activity, such as *omcE* and *pilA* (the latter is dependent on the nitrogen regulon $RpoN^7$), are likely involved as response mechanisms to maximize electron transfer to the electrode and obtain the required energy for N_2 reduction, although more study of both proteins is needed to properly characterize their function under N_2 fixation conditions. Overall, N_2 fixation may provide the opportunity to generate electron sinks that may be needed when growth conditions result in the low availability of electron accepting pools required for continued cell viability (**Fig. 5.12B**). Additional experiments, such as studying the effect of NH_4^+ on low E_{AN} gene expression profiles, will help elucidate metabolic

controls of N_2 fixation genes during anode respiration to better understand and optimize conditions that lead to higher N_2 fixation rates.

5.4 Conclusions

N_2 fixation in free-living diazotrophs such as *G. sulfurreducens* is tightly controlled by several regulatory genes. The use of a microbial electrolysis cell (MEC) to adjust electron acceptor (anode) potentials led to differential gene expression profiles for this organism depending on the applied potential or the addition of fixed nitrogen (i.e., NH_4^+). At a low potential (E_{AN} = -0.15 V vs. SHE), nitrogen fixation–related genes showed the highest expression, implying a connection between both processes that remains to be elucidated. Using the anode as artificial electron acceptor may provide a tool to understand the regulation and connections between N_2 fixation and anode respiration, while providing new alternatives to optimize the use of these pathways for eventual NH_4^+ production.

Chapter 5 References

(1) Bazylinski, D. A.; Dean, A. J.; Schuler, D.; Phillips, E. J. P.; Lovley, D. R. N_2-Dependent Growth and Nitrogenase Activity in the Metal-Metabolizing Bacteria, *Geobacter* and *Magnetospirillum* Species. *Environ. Microbiol.* **2000**, *2* (3), 266–273. https://doi.org/10.1046/j.1462-2920.2000.00096.x.

(2) Coppi, M. V.; Leang, C.; Sandler, S. J.; Lovley, D. R. Development of a Genetic System for *Geobacter sulfurreducens*. *Appl. Environ. Microbiol.* **2001**, *67* (7), 3180–3187. https://doi.org/10.1128/AEM.67.7.3180-3187.2001.

(3) Bali, A.; Blanco, G.; Hill, S.; Kennedy, C. Excretion of Ammonium by a *nifL* Mutant of *Azotobacter vinelandii* Fixing Nitrogen. *Appl. Environ. Microbiol.* **1992**, *58* (5), 1711–1718.

(4) Bageshwar, U. K.; Srivastava, M.; Pardha-Saradhi, P.; Paul, S.; Gothandapani, S.; Jaat, R. S.; Shankar, P.; Yadav, R.; Biswas, D. R.; Kumar, P. A.; Padaria, J. C.; Mandal, P. K.; Annapurna, K.; Das, H. K. An Environmentally Friendly Engineered *Azotobacter* Strain That Replaces a Substantial Amount of Urea Fertilizer While Sustaining the Same Wheat Yield. *Appl. Environ. Microbiol.* **2017**, *83* (15), 1–14. https://doi.org/10.1128/AEM.00590-17.

(5) Barney, B. M.; Plunkett, M. H.; Natarajan, V.; Mus, F.; Knutson, C. M.; Peters, J. W. Transcriptional Analysis of an Ammonium-Excreting Strain of *Azotobacter vinelandii* Deregulated for Nitrogen Fixation. *Appl. Environ. Microbiol.* **2017**, *83* (20), e01534-17. https://doi.org/10.1128/AEM.01534-17.

(6) Dixon, R.; Kahn, D. Genetic Regulation of Biological Nitrogen Fixation. *Nat. Rev. Microbiol.* **2004**, *2* (8), 621–631. https://doi.org/10.1038/nrmicro954.

(7) Leang, C.; Krushkal, J.; Ueki, T.; Puljic, M.; Sun, J.; Juárez, K.; Núñez, C.; Reguera, G.; DiDonato, R.; Postier, B.; Adkins, R. M.; Lovley, D. R. Genome-Wide Analysis of the RpoN Regulon in *Geobacter sulfurreducens*. *BMC Genomics* **2009**, *10* (1), 331. https://doi.org/10.1186/1471-2164-10-331.

(8) Dombrecht, B.; Marchal, K.; Vanderleyden, J.; Michiels, J. Prediction and Overview of the RpoN-Regulon in Closely Related Species of the Rhizobiales. *Genome Biol.* **2002**, *3* (12), research0076. https://doi.org/10.1186/gb-2002-3-12-research0076.

(9) Merrick, M. J. Regulation of Nitrogen Fixation in Free-Living Diazotrophs. In *Genetics and Regulation of Nitrogen Fixation in Free-Living Bacteria*; Kluwer Academic Publishers: Dordrecht, 2004; pp 197–223. https://doi.org/10.1007/1-4020-2179-8_9.

(10) Holmes, D. E. Comparison of 16S rRNA, *nifD*, *recA*, *gyrB*, *rpoB* and *fusA* Genes within the Family Geobacteraceae Fam. Nov. *Int. J. Syst. Evol. Microbiol.* **2004**, *54* (5), 1591–1599. https://doi.org/10.1099/ijs.0.02958-0.

(11) Ueki, T.; Lovley, D. R. Novel Regulatory Cascades Controlling Expression of Nitrogen-Fixation Genes in *Geobacter sulfurreducens*. *Nucleic Acids Res.* **2010**, *38* (21), 7485–7499. https://doi.org/10.1093/nar/gkq652.

(12) Aelterman, P.; Freguia, S.; Keller, J.; Verstraete, W.; Rabaey, K. The Anode Potential Regulates Bacterial Activity in Microbial Fuel Cells. *Appl. Microbiol. Biotechnol.* **2008**, *78* (3), 409–418. https://doi.org/10.1007/s00253-007-1327-8.

(13) Torres, C. I.; Krajmalnik-Brown, R.; Parameswaran, P.; Marcus, A. K.; Wanger, G.; Gorby, Y. A.; Rittmann, B. E. Selecting Anode-Respiring Bacteria Based on Anode Potential: Phylogenetic, Electrochemical, and Microscopic Characterization. *Environ. Sci. Technol.* **2009**, *43* (24), 9519–9524. https://doi.org/10.1021/es902165y.

(14) Zacharoff, L.; Chan, C. H.; Bond, D. R. Reduction of Low Potential Electron Acceptors Requires the CbcL Inner Membrane Cytochrome of *Geobacter sulfurreducens*. *Bioelectrochemistry* **2016**, *107*, 7–13. https://doi.org/10.1016/j.bioelechem.2015.08.003.

(15) Levar, C. E.; Hoffman, C. L.; Dunshee, A. J.; Toner, B. M.; Bond, D. R. Redox Potential as a Master Variable Controlling Pathways of Metal Reduction by *Geobacter sulfurreducens*. *ISME J.* **2017**, *11* (3), 741–752. https://doi.org/10.1038/ismej.2016.146.

(16) Wei, J.; Liang, P.; Cao, X.; Huang, X. A New Insight into Potential Regulation on Growth and Power Generation of *Geobacter sulfurreducens* in Microbial Fuel Cells Based on Energy Viewpoint. *Environ. Sci. Technol.* **2010**, *44* (8), 3187–3191. https://doi.org/10.1021/es903758m.

(17) Korth, B.; Harnisch, F. Spotlight on the Energy Harvest of Electroactive Microorganisms: The Impact of the Applied Anode Potential. *Front. Microbiol.* **2019**, *10* (June), 1–9. https://doi.org/10.3389/fmicb.2019.01352.

(18) Methe, B. A.; Nelson, K. E.; Eisen, J. A.; Paulsen, I. T.; Nelson, W.; Heidelberg, J. F.; Wu, D.; Wu, M.; Ward, N.; Beanan, M. J.; Dodson, R. J.; Madupu, R.; Brinkac, L. M.; Daughterty, S. C.; DeBoy, R. T.; Durkin, A. S.; Gwinn, M.; Kolonay, J. F. Genome of Geobacter Sulfurreducens: Metal Reduction in Subsurface Environments. *Science.* **2003**, *302* (5652), 1967–1969. https://doi.org/10.1126/science.1088727.

(19) Lin, W. C.; Coppi, M. V.; Lovley, D. R. *Geobacter sulfurreducens* Can Grow with Oxygen as a Terminal Electron Acceptor. *Appl. Environ. Microbiol.* **2004**, *70* (4), 2525–2528. https://doi.org/10.1128/AEM.70.4.2525-2528.2004.

(20) Zamora, P.; Georgieva, T.; Ter Heijne, A.; Sleutels, T. H. J. A.; Jeremiasse, A. W.; Saakes, M.; Buisman, C. J. N.; Kuntke, P. Ammonia Recovery from Urine in a Scaled-up Microbial Electrolysis Cell. *J. Power Sources* **2017**, *356*, 491–499. https://doi.org/10.1016/j.jpowsour.2017.02.089.

(21) Methe, B. A.; Webster, J.; Nevin, K.; Butler, J.; Lovley, D. R. DNA Microarray Analysis of Nitrogen Fixation and Fe(III) Reduction in *Geobacter sulfurreducens*. *Appl. Environ. Microbiol.* **2005**, *71* (5), 2530–2538. https://doi.org/10.1128/AEM.71.5.2530-2538.2005.

(22) Fay, P. Oxygen Relations of Nitrogen Fixation in Cyanobacteria. *Microbiol. Rev.* **1992**, *56* (2), 340–373.

(23) Qiu, Y.; Nagarajan, H.; Embree, M.; Shieu, W.; Abate, E.; Juárez, K.; Cho, B.-K.; Elkins, J. G.; Nevin, K. P.; Barrett, C. L.; Lovley, D. R.; Palsson, B. O.; Zengler, K. Characterizing the Interplay between Multiple Levels of Organization within Bacterial Sigma Factor Regulatory Networks. *Nat. Commun.* **2013**, *4* (1), 1755. https://doi.org/10.1038/ncomms2743.

(24) Nevin, K. P.; Kim, B.-C.; Glaven, R. H.; Johnson, J. P.; Woodard, T. L.; Methé, B. A.; DiDonato, R. J.; Covalla, S. F.; Franks, A. E.; Liu, A.; Lovley, D. R. Anode Biofilm Transcriptomics Reveals Outer Surface Components Essential for High Density Current Production in *Geobacter sulfurreducens* Fuel Cells. *PLoS One* **2009**, *4* (5), e5628. https://doi.org/10.1371/journal.pone.0005628.

(25) Ishii, S.; Suzuki, S.; Norden-Krichmar, T. M.; Tenney, A.; Chain, P. S. G.; Scholz, M. B.; Nealson, K. H.; Bretschger, O. A Novel Metatranscriptomic Approach to Identify Gene Expression Dynamics during Extracellular Electron Transfer. *Nat. Commun.* **2013**, *4*, 1–10. https://doi.org/10.1038/ncomms2615.

(26) Call, D. F.; Logan, B. E. A Method for High Throughput Bioelectrochemical Research Based on Small Scale Microbial Electrolysis Cells. *Biosens. Bioelectron.* **2011**, *26* (11), 4526–4531. https://doi.org/10.1016/j.bios.2011.05.014.

(27) Bolger, A. M.; Lohse, M.; Usadel, B. Trimmomatic: A Flexible Trimmer for Illumina Sequence Data. *Bioinformatics* **2014**, *30* (15), 2114–2120. https://doi.org/10.1093/bioinformatics/btu170.

(28) Langmead, B.; Salzberg, S. L. Fast Gapped-Read Alignment with Bowtie 2. *Nat. Methods* **2012**, *9* (4), 357–359. https://doi.org/10.1038/nmeth.1923.

(29) Anders, S.; Pyl, P. T.; Huber, W. HTSeq--a Python Framework to Work with High-Throughput Sequencing Data. *Bioinformatics* **2015**, *31* (2), 166–169. https://doi.org/10.1093/bioinformatics/btu638.

(30) Love, M. I.; Huber, W.; Anders, S. Moderated Estimation of Fold Change and Dispersion for RNA-Seq Data with DESeq2. *Genome Biol.* **2014**, *15* (12), 550. https://doi.org/10.1186/s13059-014-0550-8.

(31) Call, D.; Logan, B. E. Hydrogen Production in a Single Chamber Microbial Electrolysis Cell Lacking a Membrane. *Environ. Sci. Technol.* **2008**, *42* (9), 3401–3406. https://doi.org/10.1021/es8001822.

(32) Mahmoud, M.; Parameswaran, P.; Torres, C. I.; Rittmann, B. E. Electrochemical Techniques Reveal That Total Ammonium Stress Increases Electron Flow to Anode Respiration in Mixed-Species Bacterial Anode Biofilms. *Biotechnol. Bioeng.* **2017**, *114* (6), 1151–1159. https://doi.org/10.1002/bit.26246.

(33) Belleville, P.; Strong, P. J.; Dare, P. H.; Gapes, D. J. Influence of Nitrogen Limitation on Performance of a Microbial Fuel Cell. *Water Sci. Technol.* **2011**, *63* (8), 1752. https://doi.org/10.2166/wst.2011.111.

(34) Carbon, S.; Ireland, A.; Mungall, C. J.; Shu, S.; Marshall, B.; Lewis, S. AmiGO: Online Access to Ontology and Annotation Data. *Bioinformatics* **2009**, *25* (2), 288–289. https://doi.org/10.1093/bioinformatics/btn615.

(35) Kersey, P. J.; Allen, J. E.; Allot, A.; Barba, M.; Boddu, S.; Bolt, B. J.; Carvalho-Silva, D.; Christensen, M.; Davis, P.; Grabmueller, C.; Kumar, N.; Liu, Z.; Maurel, T.; Moore, B.; McDowall, M. D.; Maheswari, U.; Naamati, G.; Newman, V.; Ong, C. K.; Paulini, M.; Pedro, H.; Perry, E.; Russell, M.; Sparrow, H.; Tapanari, E.; Taylor, K.; Vullo, A.; Williams, G.; Zadissia, A.; Olson, A.; Stein, J.; Wei, S.; Tello-Ruiz, M.; Ware, D.; Luciani, A.; Potter, S.; Finn, R. D.; Urban, M.; Hammond-Kosack, K. E.; Bolser, D. M.; De Silva, N.; Howe, K. L.; Langridge, N.; Maslen, G.; Staines, D. M.; Yates, A. Ensembl Genomes 2018: An Integrated Omics Infrastructure for Non-Vertebrate Species. *Nucleic Acids Res.* **2018**, *46* (D1), D802–D808. https://doi.org/10.1093/nar/gkx1011.

(36) Mouser, P. J.; N'Guessan, A. L.; Elifantz, H.; Holmes, D. E.; Williams, K. H.; Wilkins, M. J.; Long, P. E.; Lovley, D. R. Influence of Heterogeneous Ammonium Availability on Bacterial Community Structure and the Expression of Nitrogen Fixation and Ammonium Transporter Genes during in Situ Bioremediation of Uranium-Contaminated Groundwater. *Environ. Sci. Technol.* **2009**, *43* (12), 4386–4392. https://doi.org/10.1021/es8031055.

(37) Holmes, D. E.; O'Neil, R. A.; Chavan, M. A.; N'Guessan, L. A.; Vrionis, H. A.; Perpetua, L. A.; Larrahondo, M. J.; DiDonato, R.; Liu, A.; Lovley, D. R. Transcriptome of *Geobacter uraniireducens* Growing in Uranium-Contaminated Subsurface Sediments. *ISME J.* **2009**, *3* (2), 216–230. https://doi.org/10.1038/ismej.2008.89.

(38) Oetjen, J.; Reinhold-Hurek, B. Characterization of the DraT/DraG System for Posttranslational Regulation of Nitrogenase in the Endophytic Betaproteobacterium *Azoarcus* sp. Strain BH72. *J. Bacteriol.* **2009**, *191* (11), 3726–3735. https://doi.org/10.1128/JB.01720-08.

(39) Schulz, A. A.; Collett, H. J.; Reid, S. J. Nitrogen and Carbon Regulation of Glutamine Synthetase and Glutamate Synthase in *Corynebacterium glutamicum* ATCC 13032. *FEMS Microbiol. Lett.* **2001**, *205* (2), 361–367. https://doi.org/10.1111/j.1574-6968.2001.tb10973.x.

(40) Hagen, W. R.; Vanoni, M. A.; Rosenbaum, K.; Schnackerz, K. D. On the Iron-Sulfur Clusters in the Complex Redox Enzyme Dihydropyrimidine Dehydrogenase. *Eur. J. Biochem.* **2000**, *267* (12), 3640–3646. https://doi.org/10.1046/j.1432-1327.2000.01393.x.

(41) Makemson, J. C.; Hastings, J. W. Glutamate Functions in Osmoregulation in a Marine Bacterium. *Appl. Environ. Microbiol.* **1979**, *38* (1), 178–180. https://doi.org/10.1128/AEM.38.1.178-180.1979.

(42) Feehily, C.; Karatzas, K. A. G. Role of Glutamate Metabolism in Bacterial Responses towards Acid and Other Stresses. *J. Appl. Microbiol.* **2013**, *114* (1), 11–24. https://doi.org/10.1111/j.1365-2672.2012.05434.x.

(43) Goude, R.; Renaud, S.; Bonnassie, S.; Bernard, T.; Blanco, C. Glutamine, Glutamate, and α-Glucosylglycerate Are the Major Osmotic Solutes Accumulated by *Erwinia chrysanthemi* Strain 3937. *Appl. Environ. Microbiol.* **2004**, *70* (11), 6535–6541. https://doi.org/10.1128/AEM.70.11.6535-6541.2004.

(44) Shimizu, M.; Fujii, T.; Masuo, S.; Takaya, N. Mechanism of de Novo Branched-Chain Amino Acid Synthesis as an Alternative Electron Sink in Hypoxic *Aspergillus nidulans* Cells. *Appl. Environ. Microbiol.* **2010**, *76* (5), 1507–1515. https://doi.org/10.1128/AEM.02135-09.

(45) Van Der Veen, D.; Lo, J.; Brown, S. D.; Johnson, C. M.; Tschaplinski, T. J.; Martin, M.; Engle, N. L.; Van Den Berg, R. A.; Argyros, A. D.; Caiazza, N. C.; Guss, A. M.; Lynd, L. R. Characterization of *Clostridium thermocellum* Strains with Disrupted Fermentation End-Product Pathways. *J. Ind. Microbiol. Biotechnol.* **2013**, *40* (7), 725–734. https://doi.org/10.1007/s10295-013-1275-5.

(46) Rydzak, T.; Garcia, D.; Stevenson, D. M.; Sladek, M.; Klingeman, D. M.; Holwerda, E. K.; Amador-Noguez, D.; Brown, S. D.; Guss, A. M. Deletion of Type I Glutamine Synthetase Deregulates Nitrogen Metabolism and Increases Ethanol Production in *Clostridium thermocellum*. *Metab. Eng.* **2017**, *41* (September 2016), 182–191. https://doi.org/10.1016/j.ymben.2017.04.002.

(47) Holmes, D. E.; Chaudhuri, S. K.; Nevin, K. P.; Mehta, T.; Methé, B. A.; Liu, A.; Ward, J. E.; Woodard, T. L.; Webster, J.; Lovley, D. R. Microarray and Genetic Analysis of Electron Transfer to Electrodes in *Geobacter sulfurreducens*. *Environ. Microbiol.* **2006**, *8* (10), 1805–1815. https://doi.org/10.1111/j.1462-2920.2006.01065.x.

(48) Stephen, C. S.; LaBelle, E. V.; Brantley, S. L.; Bond, D. R. Abundance of the Multiheme C-Type Cytochrome OmcB Increases in Outer Biofilm Layers of Electrode-Grown *Geobacter sulfurreducens*. *PLoS One* **2014**, *9* (8), e104336. https://doi.org/10.1371/journal.pone.0104336.

(49) Mehta, T.; Coppi, M. V.; Childers, S. E.; Lovley, D. R. Outer Membrane *c*-Type Cytochromes Required for Fe(III) and Mn(IV) Oxide Reduction in *Geobacter sulfurreducens*. *Appl. Environ. Microbiol.* **2005**, *71* (12), 8634–8641. https://doi.org/10.1128/AEM.71.12.8634-8641.2005.

(50) Shi, L.; Richardson, D. J.; Wang, Z.; Kerisit, S. N.; Rosso, K. M.; Zachara, J. M.; Fredrickson, J. K. The Roles of Outer Membrane Cytochromes of Shewanella and Geobacter in Extracellular Electron Transfer. *Environ. Microbiol. Rep.* **2009**, *1* (4), 220–227. https://doi.org/10.1111/j.1758-2229.2009.00035.x.

(51) Santos, T. C.; Silva, M. A.; Morgado, L.; Dantas, J. M.; Salgueiro, C. A. Diving into the Redox Properties of *Geobacter sulfurreducens* Cytochromes: A Model for Extracellular Electron Transfer. *Dalt. Trans.* **2015**, *44* (20), 9335–9344. https://doi.org/10.1039/C5DT00556F.

(52) Ishii, S.; Suzuki, S.; Tenney, A.; Nealson, K. H.; Bretschger, O. Comparative Metatranscriptomics Reveals Extracellular Electron Transfer Pathways Conferring Microbial Adaptivity to Surface Redox Potential Changes. *ISME J.* **2018**, *12* (12), 2844–2863. https://doi.org/10.1038/s41396-018-0238-2.

(53) Zacharoff, L.; Chan, C. H.; Bond, D. R. Reduction of Low Potential Electron Acceptors Requires the CbcL Inner Membrane Cytochrome of *Geobacter sulfurreducens*. *Bioelectrochemistry* **2016**, *107*, 7–13. https://doi.org/10.1016/j.bioelechem.2015.08.003.

(54) Richter, L. V.; Sandler, S. J.; Weis, R. M. Two Isoforms of *Geobacter sulfurreducens* PilA Have Distinct Roles in Pilus Biogenesis, Cytochrome Localization, Extracellular Electron Transfer, and Biofilm Formation. *J. Bacteriol.* **2012**, *194* (10), 2551–2563. https://doi.org/10.1128/JB.06366-11.

(55) Ueki, T.; Lovley, D. R. Genome-Wide Gene Regulation of Biosynthesis and Energy Generation by a Novel Transcriptional Repressor in *Geobacter* Species. *Nucleic Acids Res.* **2010**, *38* (3), 810–821. https://doi.org/10.1093/nar/gkp1085.

(56) Bičáková, O.; Straka, P. Production of Hydrogen from Renewable Resources and Its Effectiveness. *Int. J. Hydrogen Energy* **2012**, *37* (16), 11563–11578. https://doi.org/10.1016/j.ijhydene.2012.05.047.

(57) Coppi, M. V.; O'Neil, R. A.; Lovley, D. R. Identification of an Uptake Hydrogenase Required for Hydrogen-Dependent Reduction of Fe(III) and Other Electron Acceptors by *Geobacter sulfurreducens*. *J. Bacteriol.* **2004**, *186* (10), 3022–3028. https://doi.org/10.1128/JB.186.10.3022-3028.2004.

(58) Coppi, M. V. The Hydrogenases of *Geobacter sulfurreducens*: A Comparative Genomic Perspective. *Microbiology* **2005**, *151* (4), 1239–1254. https://doi.org/10.1099/mic.0.27535-0.

(59) Croese, E.; Jeremiasse, A. W.; Marshall, I. P. G.; Spormann, A. M.; Euverink, G.-J. W.; Geelhoed, J. S.; Stams, A. J. M.; Plugge, C. M. Influence of Setup and Carbon Source on the Bacterial Community of Biocathodes in Microbial Electrolysis Cells. *Enzyme Microb. Technol.* **2014**, *61–62*, 67–75. https://doi.org/10.1016/j.enzmictec.2014.04.019.

(60) Tremblay, P.-L.; Lovley, D. R. Role of the NiFe Hydrogenase Hya in Oxidative Stress Defense in *Geobacter sulfurreducens*. *J. Bacteriol.* **2012**, *194* (9), 2248–2253. https://doi.org/10.1128/JB.00044-12.

(61) Saikia, S. P.; Jain, V. Biological Nitrogen Fixation with Non-Legumes: An Achievable Target or a Dogma? *Curr. Sci.* **2007**, *92* (3), 317–322.

(62) Marozava, S.; Röling, W. F. M.; Seifert, J.; Küffner, R.; von Bergen, M.; Meckenstock, R. U. Physiology of *Geobacter metallireducens* under Excess and Limitation of Electron Donors. Part II. Mimicking Environmental Conditions during Cultivation in Retentostats. *Syst. Appl. Microbiol.* **2014**, *37* (4), 287–295. https://doi.org/10.1016/j.syapm.2014.02.005.

(63) Greening, C.; Cook, G. M. Integration of Hydrogenase Expression and Hydrogen Sensing in Bacterial Cell Physiology. *Curr. Opin. Microbiol.* **2014**, *18*, 30–38. https://doi.org/10.1016/j.mib.2014.02.001.

(64) Meng, J.; Xu, Z.; Guo, J.; Yue, Y.; Sun, X. Analysis of Enhanced Current-Generating Mechanism of *Geobacter sulfurreducens* Strain via Model-Driven Metabolism Simulation. *PLoS One* **2013**, *8* (9), e73907. https://doi.org/10.1371/journal.pone.0073907.

(65) Esteve-Núñez, A.; Sosnik, J.; Visconti, P.; Lovley, D. R. Fluorescent Properties of *c*-Type Cytochromes Reveal Their Potential Role as an Extracytoplasmic Electron Sink in *Geobacter sulfurreducens*. *Environ. Microbiol.* **2008**, *10* (2), 497–505. https://doi.org/10.1111/j.1462-2920.2007.01470.x.

(66) Vanoni, M. A.; Edmondson, D. E.; Rescigno, M.; Zanetti, G.; Curti, B. Mechanistic Studies on *Azospirillum brasilense* Glutamate Synthase. *Biochemistry* **1991**, *30* (48), 11478–11484. https://doi.org/10.1021/bi00112a016.

Tables

Table 5.1. The treatments used in this study to compare differences in gene expression in the microbial electrolysis cells. The codenames are structured as follows: first N – no NH_4^+; second N – negative anode potential; P – positive anode potential; L – low NH_4^+ concentration; H – high NH_4^+ concentration; O – 5% O_2; A – air (21% O_2).

Codename	E_{AN} (V vs. SHE)	Gas in headspace	NH_4^+ added (mM)	Purpose of treatment
NP	+0.15	100 % N_2	-	Reference operational condition
NN	-0.15	100 % N_2	-	Effect of low E_{AN}
LP	+0.15	100 % N_2	5.8	Effect of NH_4^+
HP	+0.15	100 % N_2	11.6	Effect of high NH_4^+ concentration
OP	+0.15	95% N_2, 5% O_2	-	Effect of microaerobic conditions
AP	+0.15	Air	-	Effect of aerobic conditions

Table 5.2. Current density (I_A; normalized to anode surface area) values obtained during chronoamperometry tests. Treatments are identified using the codenames employed in Table 5.1. Max I_A is the maximum current obtained during the entire time the MEC was operated. Startup time is defined as the time needed for I_A to reach a value of 0.1 A/m^2. Harvesting I_A represents the value measured prior to RNA extraction.

Treatment	NP	NN	LP	HP	OP
Max I_A (A/m^2)	5.93 ± 1.45	4.72 ± 0.35	3.34 ± 0.18	3.35 ± 0.44	5.56 ± 1.13
Startup time (d)	3.35 ± 0.41	3.39 ± 0.02	3.79 ± 1.65	3.55 ± 0.68	6.35 ± 3.11
Harvesting I_A (A/m^2)	3.29 ± 0.38	3.58 ± 0.10	1.59 ± 0.16	1.59 ± 0.10	2.57 ± 0.01

Table 5.3. Comparison of gene expression profiles of *G. sulfurreducens* in the MECs. Reactors operating at +0.15 V vs. SHE and no NH_4^+ added ("NP") were used as a reference for comparison across treatments. Differentially expressed genes displayed a log2-fold change higher than 2.0 ("up-regulated") or lower than -2.0 ("down-regulated"), as well as an adjusted *p*-value < 0.05.

Treatment comparison	Total observed genes	Differentially expressed genes	Up-regulated	Down-regulated
NN/NP	3432	290	110	180
LP/NP	3430	193	153	40
HP/NP	3435	304	189	115

Figures

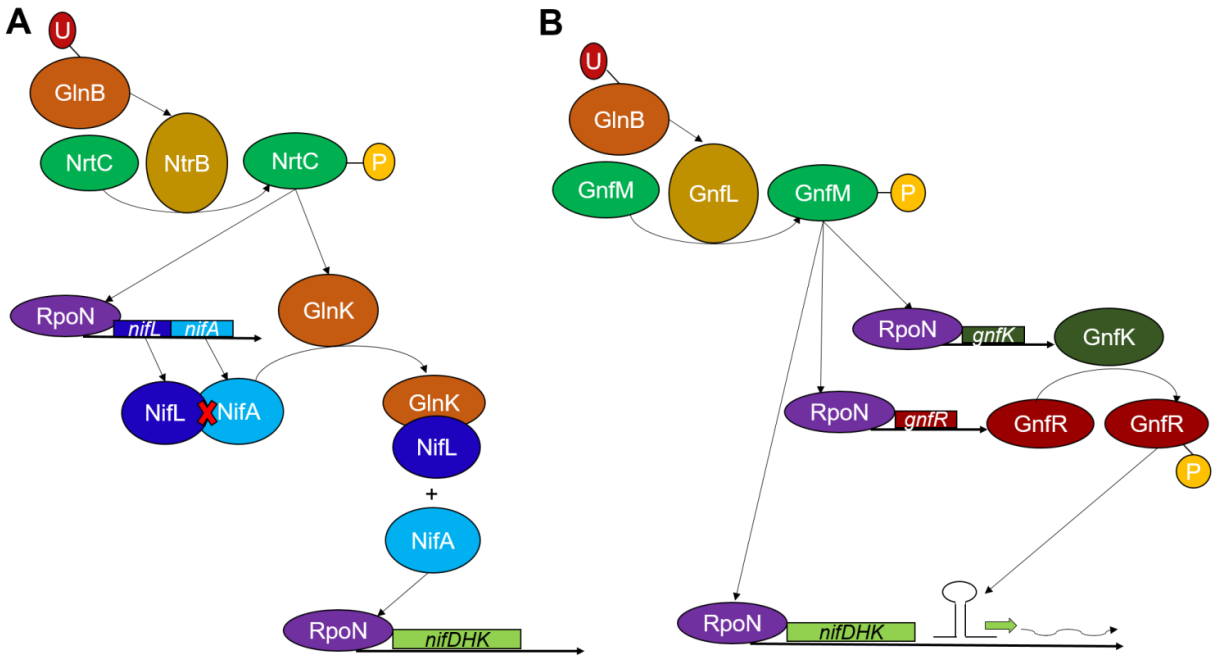

Fig. 5.1. Regulatory controls for nitrogen (N_2) fixation in A) *Klebsiella pneumoniae* (a well-studied free-living diazotroph) and B) *Geobacter sulfurreducens*. In the absence of fixed nitrogen, the uridylylated form of the protein GlnB facilitates the phosphorylation of either NtrC or GnfM, which assist the transcription of genes alongside RpoN, the sigma factor responsible for transcription under nitrogen-limiting conditions. In the case of *K. pneumoniae*, the second regulatory control is the system NifL/NifA, which is separated by non-uridylylated GlnK so NifA can assist RpoN in the transcription of N_2 fixation specific genes such as nitrogenase. For *G. sulfurreducens*, GnfM assists in the transcription of the system GnfK/GnfR alongside the direct transcription of N_2 fixation genes. The latter system works as an anti-termination mechanism, where phosphorylated GnfR (due to GnfK) dissociates the typical hairpin termination factor in order to continue transcription of the pertinent genes. Adapted from Dixon and Kahn,[6] and Ueki and Lovley.[11]

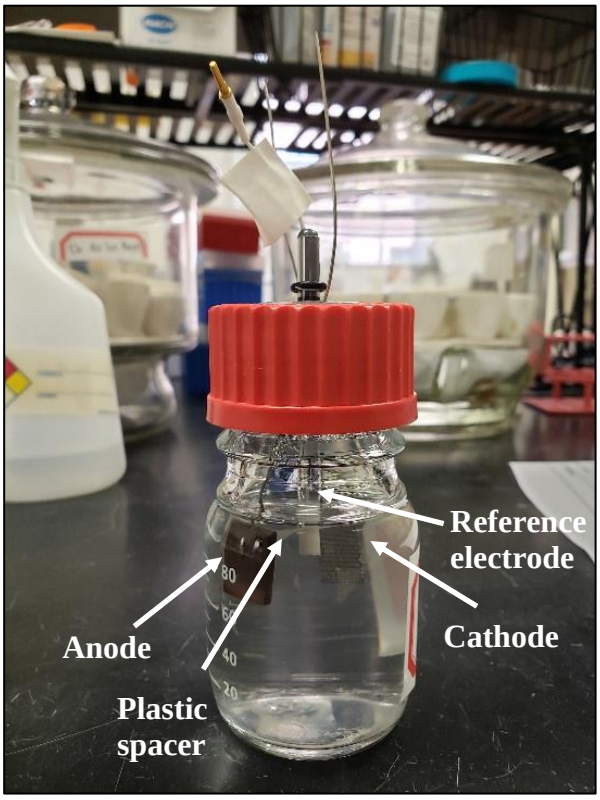

Fig. 5.2. Example of a gas-tight microbial electrolysis cell (MEC) utilized to culture *Geobacter sulfurreducens* and obtain the required amount of RNA for gene expression analysis. *G. sulfurreducens* respires on the anode (graphite plate) as the terminal electron acceptor. A cathode (stainless steel mesh) and a reference electrode (silver-silver chloride) are placed alongside the anode in growth medium.

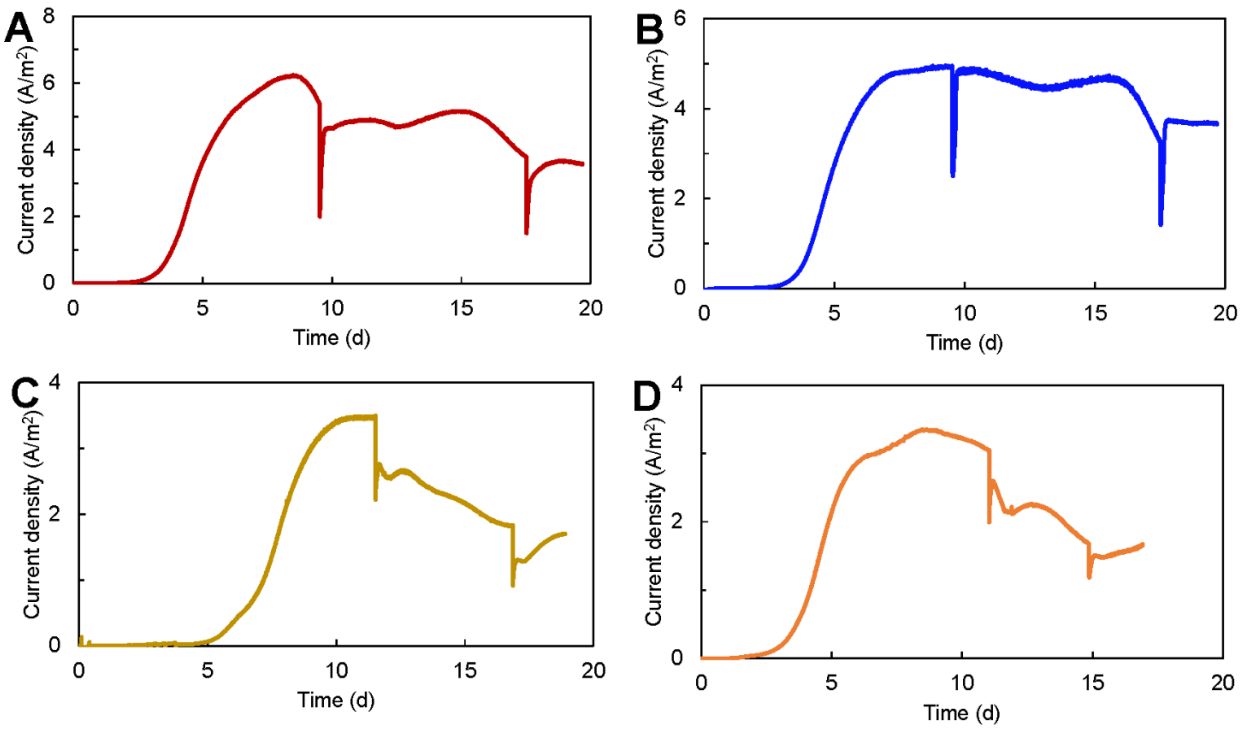

Fig. 5.3. Current density (I_A) profiles of MECs inoculated with *G. sulfurreducens* for gene expression analysis at A) fixed anode potential (E_{AN}) = +0.15 V vs. standard hydrogen electrode (SHE) and no NH_4^+ added ("NP"), B) E_{AN} = −0.15 V vs. SHE and no NH_4^+ added ("NN"), C) E_{AN} = +0.15 V vs. SHE and 5.8 mM NH_4^+ added ("LP"), and D) E_{AN} = +0.15 V vs. SHE and 11.6 mM NH_4^+ added ("HP"). All reactors were operated for three batch cycles, characterized by sudden a sharp drop of I_A at the beginning of each cycle. RNA was extracted immediately after the beginning of the third cycle. Curves represent the average of triplicates operated for each treatment. Error bars are omitted for clarity.

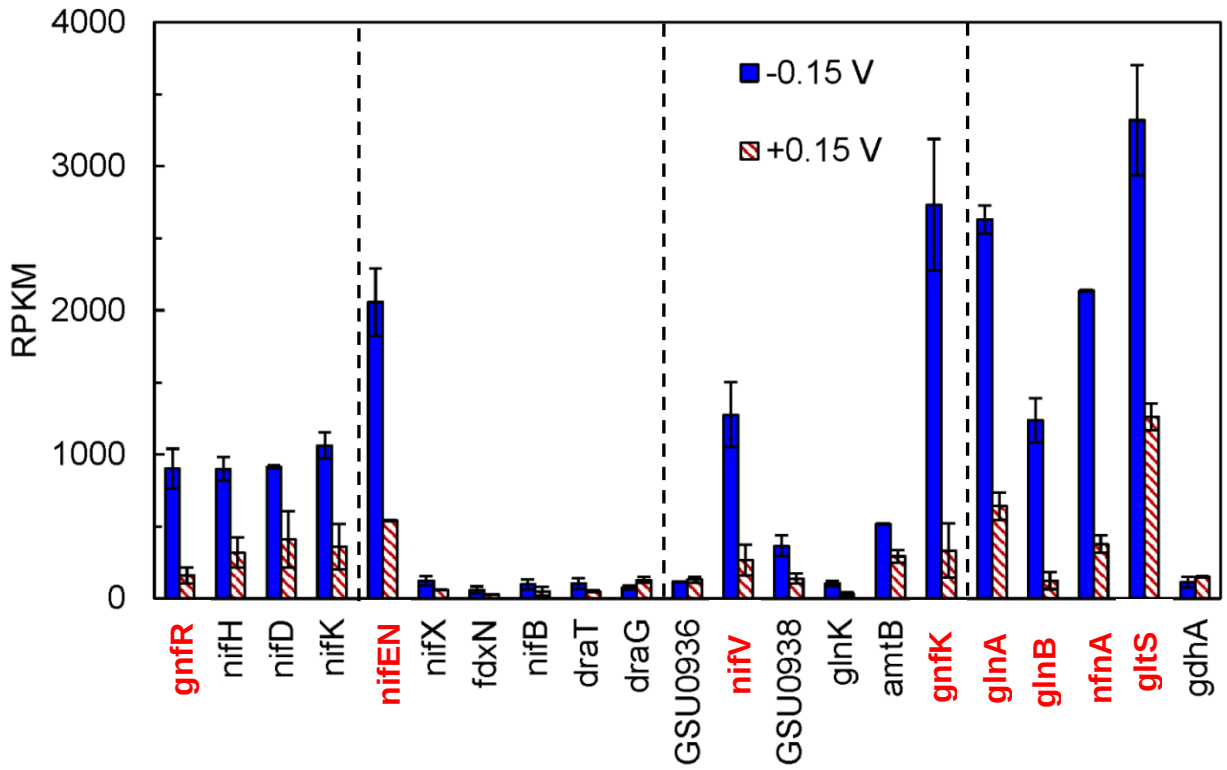

Fig. 5.4. Normalized gene counts of genes involved in N_2 fixation in MECs operating at E_{AN} = −0.15 V vs. SHE compared to E_{AN} = +0.15 V. No NH_4^+ was added for both conditions. Genes indicated in red text are considered "upregulated" at −0.15 V (log2-fold difference > 2.00 and p < 0.05 when compared to +0.15 V). Adjacent genes are grouped based on their location within the genome of *G. sulfurreducens*, and separated by dashed lines. Genes from *glnA* to *gdhA* are included because they are involved in NH_4^+ assimilation after N_2 fixation. Gene counts are expressed in reads per kilobase per million (RPKM).

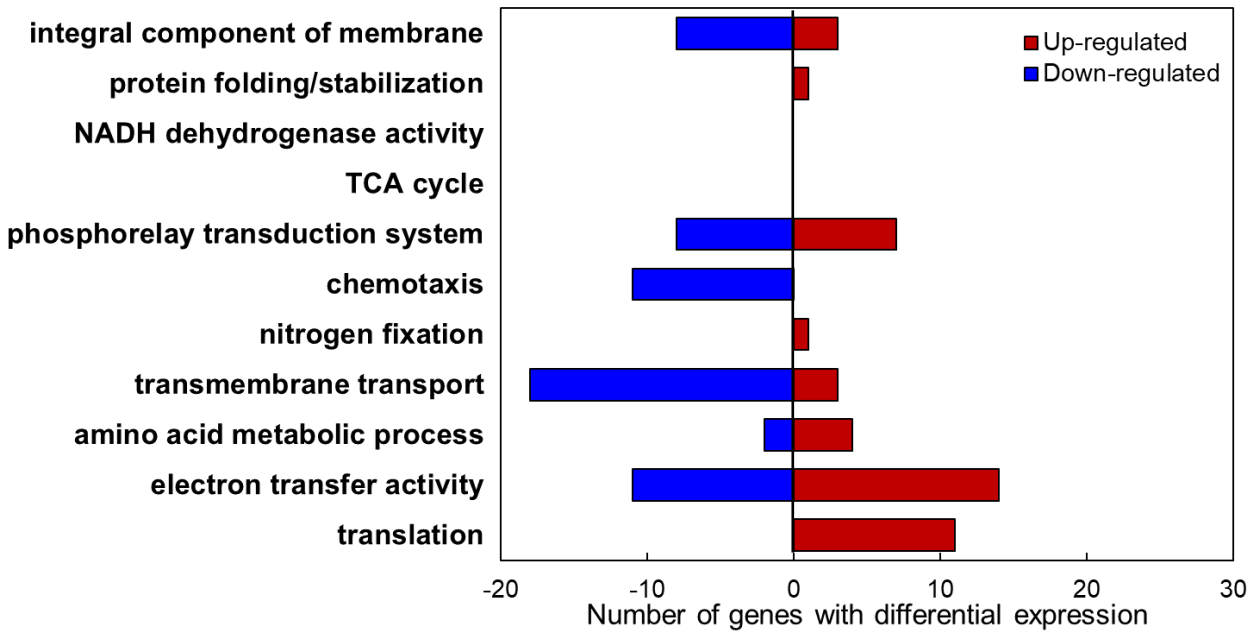

Fig. 5.5. Functional class distribution of differentially expressed genes (log2-fold difference > 2.00 and $p < 0.05$) of *G. sulfurreducens* in MECs operating at $E_{AN} = -0.15$ V vs. SHE ("NN") compared to $E_{AN} = +0.15$ V ("NP"). No NH_4^+ was added for both conditions. Genes were grouped in classes based on annotations found in the Gene Ontology (OG) and Ensembl Genome databases.

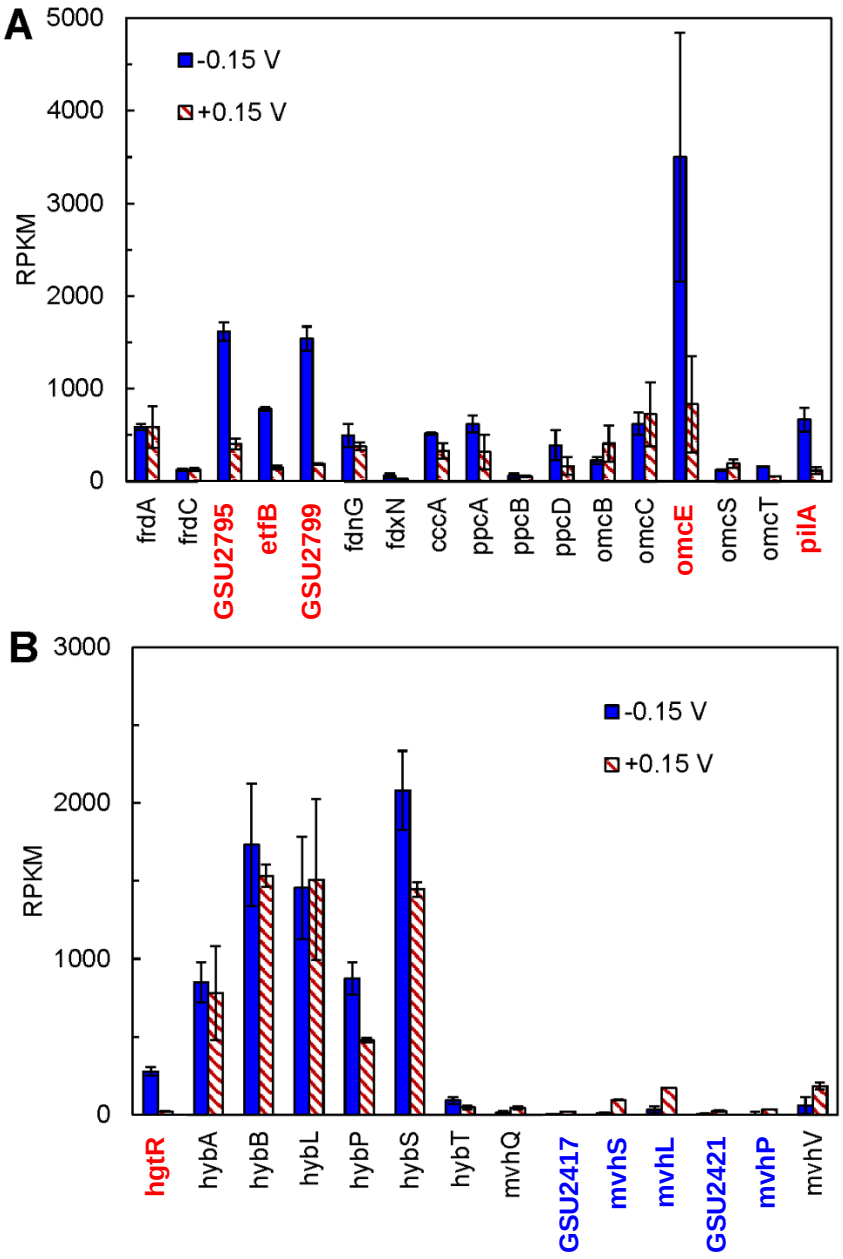

Fig. 5.6. Normalized gene counts of selected genes associated with A) electron transfer activity and B) hydrogenase activity in *G. sulfurreducens*. Treatments are MECs operating at $E_{AN} = -0.15$ V vs. SHE compared to $E_{AN} = +0.15$ V. No NH_4^+ was added in both conditions. Genes shown in bold are considered to be differentially expressed (log2-fold difference > 2.00 and $p < 0.05$; red: up-regulated, blue: down-regulated) with respect to +0.15 V. Gene counts are expressed in reads per kilobase per million (RPKM).

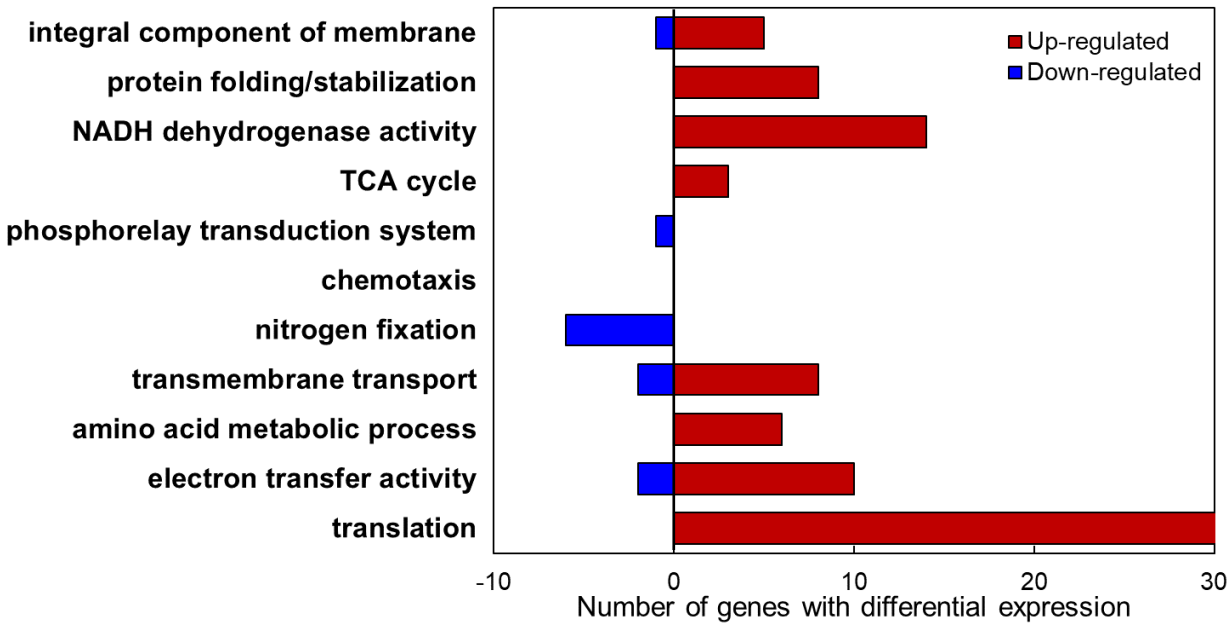

Fig. 5.7. Functional class distribution of differentially expressed genes of *G. sulfurreducens* in MECs operating with 5.8 mM NH_4^+ added ("LP") compared to no NH_4^+ added ("NP"). Both treatments were operated at E_{AN} = +0.15 V vs. SHE. Genes were grouped based on annotations found in the Gene Ontology (OG) and Ensembl Genome databases.

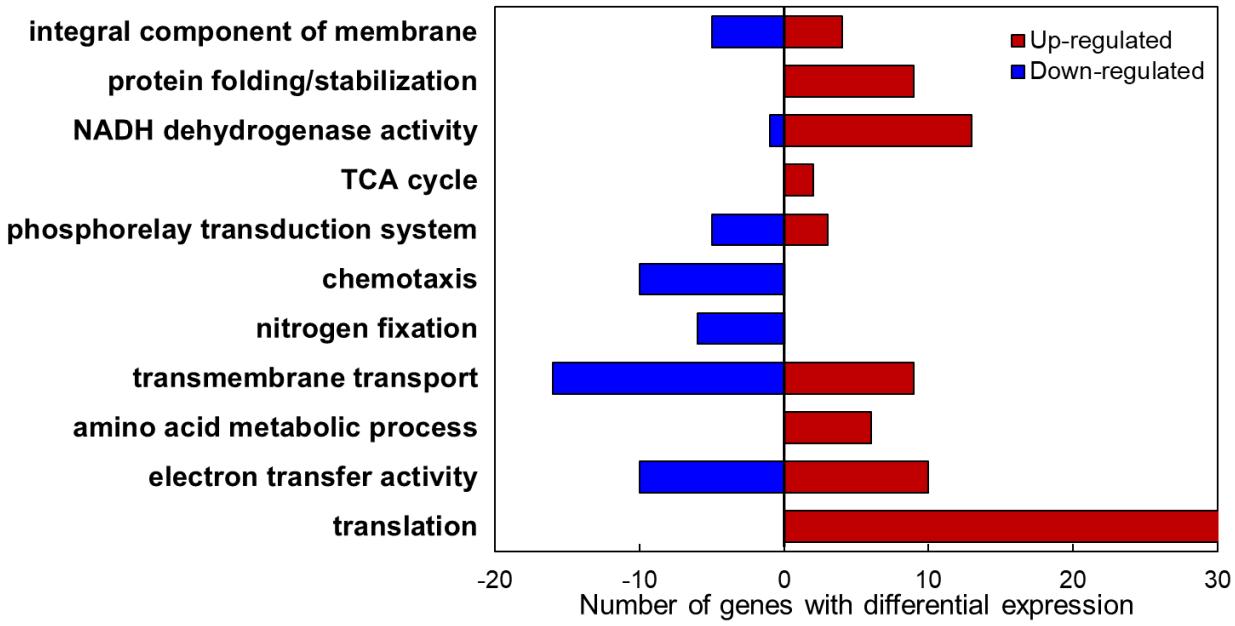

Fig. 5.8. Functional class distribution of differentially expressed genes of *G. sulfurreducens* in MECs operating with 11.6 mM NH_4^+ added ("HP"), compared to no NH_4^+ added ("NP"). Both treatments were operated at E_{AN} = +0.15 V vs. SHE. Genes were grouped based on annotations found in the Gene Ontology (OG) and Ensembl Genome databases.

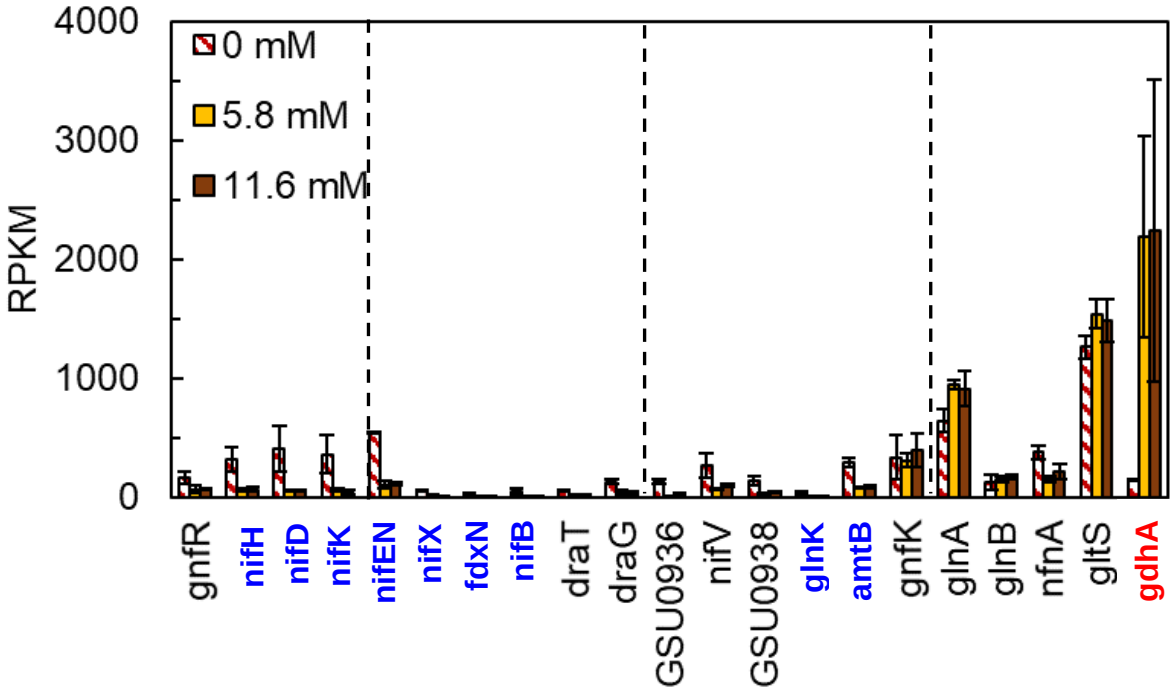

Fig. 5.9. Normalized gene counts of genes involved in N_2 fixation in MECs with 5.8 and 11.6 mM NH_4^+ compared to 0 mM NH_4^+. All MECs were operated at E_{AN} = +0.15 V vs. SHE. Genes in blue text have significantly decreased differential expression (log2-fold difference > 2.00 and $p < 0.05$) with respect to 0 mM NH_4^+ and the gene shown in red text has significantly increased expression. Adjacent genes are grouped based on their location within the genome of *G. sulfurreducens* and separated by dashed lines. Genes from *glnA* to *gdhA* are included because they are involved in NH_4^+ assimilation after N_2 fixation. Gene counts are expressed in reads per kilobase per million (RPKM).

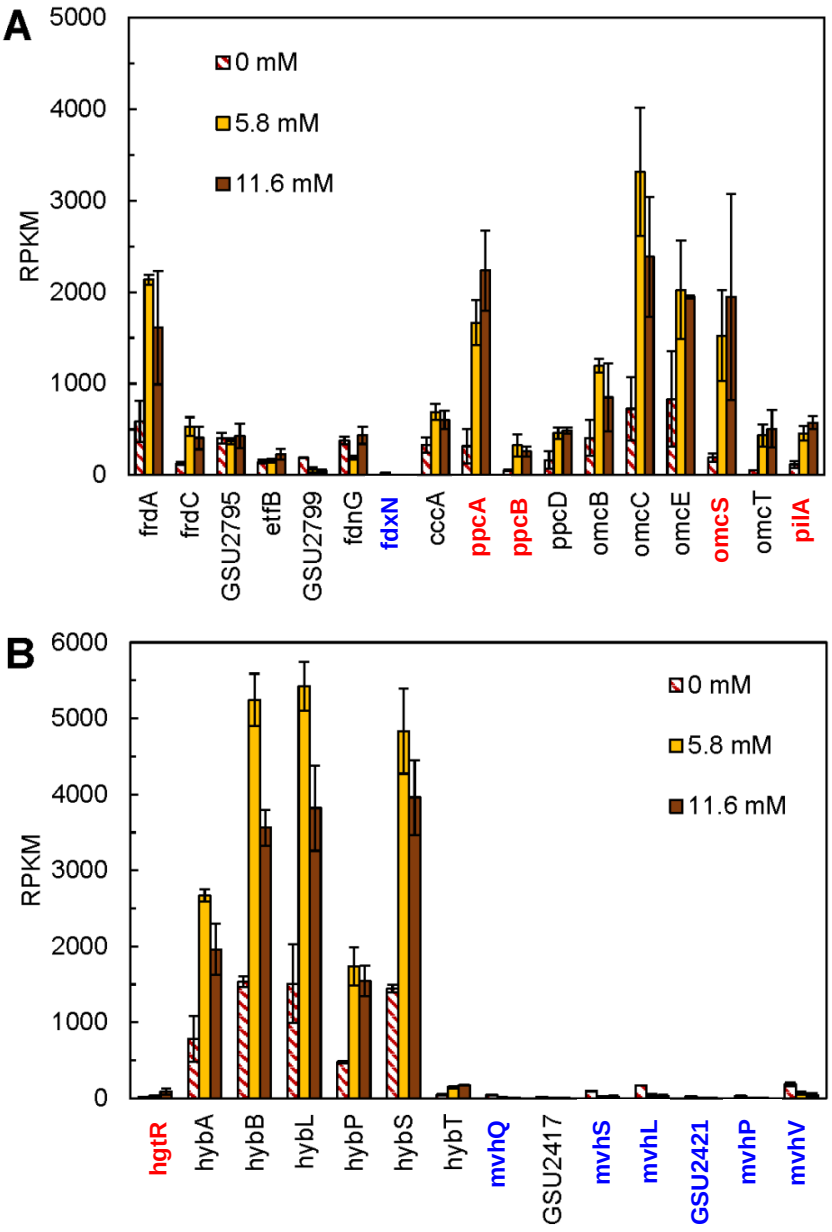

Fig. 5.10. Normalized gene counts of selected genes that are associated with A) electron transfer activity and B) hydrogenase activity in *G. sulfurreducens* with 5.8 and 11.6 mM NH_4^+ compared to 0 mM NH_4^+. Genes in bold are considered to be differentially expressed (log2-fold difference > 2.00 and $p < 0.05$; red: up-regulated, blue: down-regulated) with respect to 0 mM NH_4^+. All MECs were operated at E_{AN} = +0.15 V vs. SHE. Gene counts are expressed in reads per kilobase per million (RPKM).

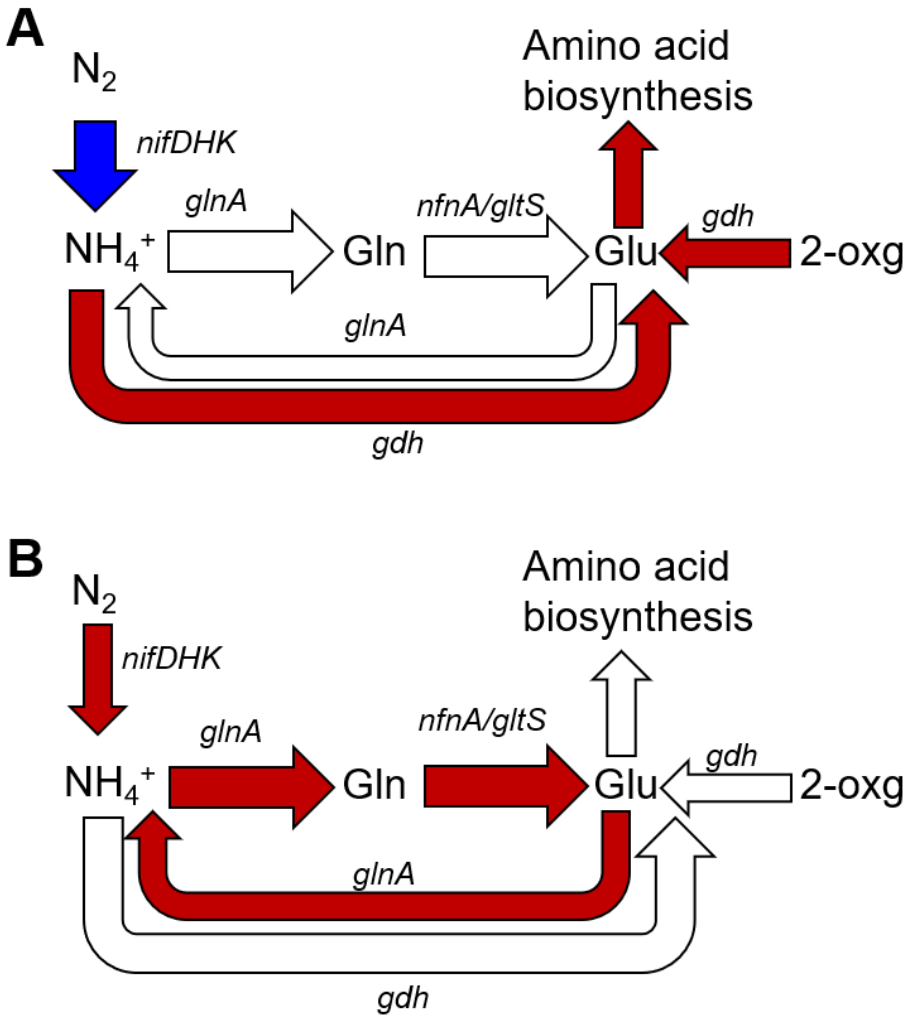

Figure 5.11. Gene expression changes in N_2 fixation and NH_4^+ assimilation pathways: A) when NH_4^+ was added compared to no NH_4^+ added at E_{AN} = +0.15 V, B) when E_{AN} changed from +0.15 V to −0.15 V, both with no NH_4^+ added. Annotations in italics denote the genes that encode enzymes involved in the corresponding conversion reactions. Red arrows correspond to genes with higher expression levels than the reference ("NP"), while blue arrows are for genes having lower expression levels. White arrows indicate genes that did not show significant change in expression when compared to the reference treatment. Abbreviations: Gln:glutamine, Glu, glutamate, 2-oxg: 2-oxoglutarate.

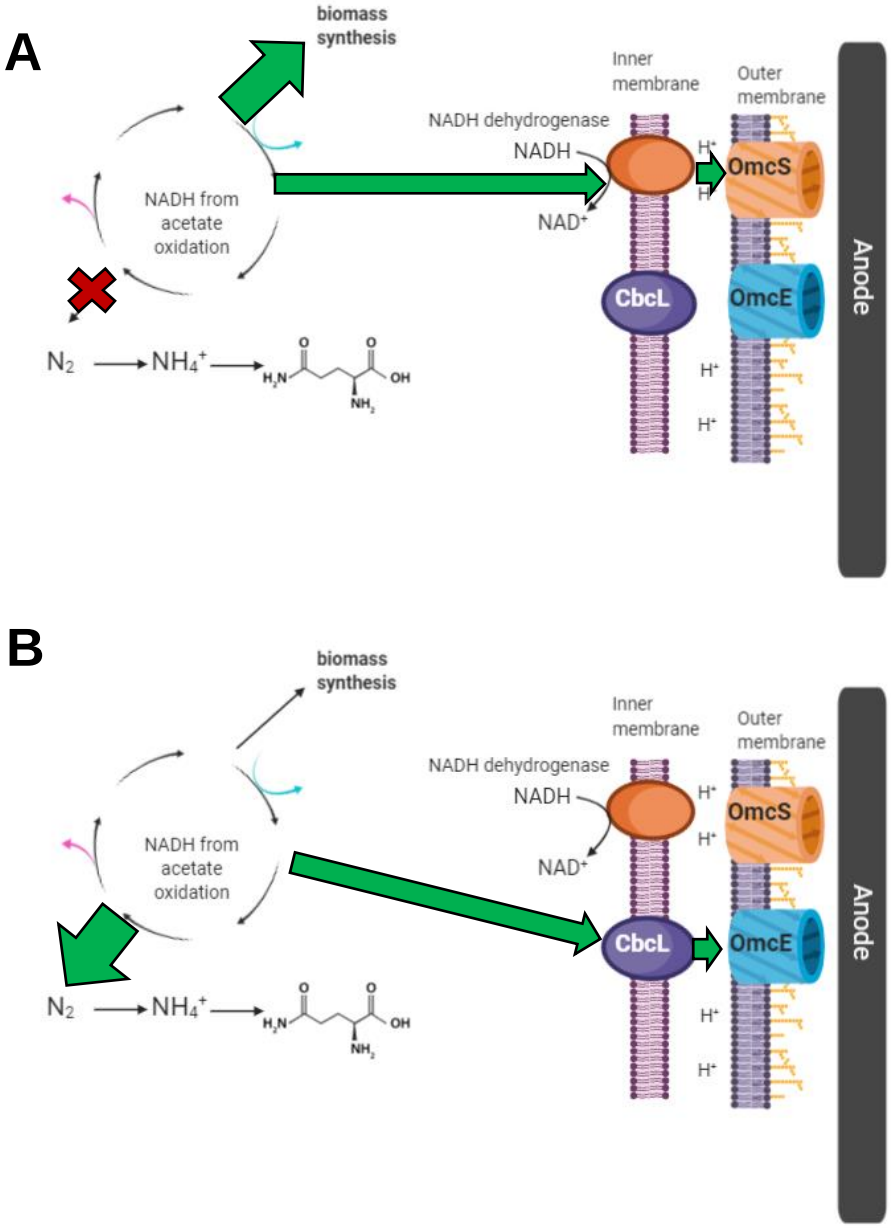

Figure 5.12. Proposed distribution of electrons within anode-respiring *G. sulfurreducens* under A) E_{AN} = +0.15 V with NH_4^+ added to the medium and B) at E_{AN} = −0.15 V under N_2 fixing conditions (no NH_4^+ added). Green, bold arrows indicate electron sinks that may be favored for each treatment, while the red X identifies pathways that may be suppressed. Figures were created using BioRender.com.

APPENDICES

Appendix A

Supplementary Information for Chapter 3: Electrochemical and Microbiological Characterization of Bioanode Communities Exhibiting Variable Levels of Startup Activity

Supporting figures

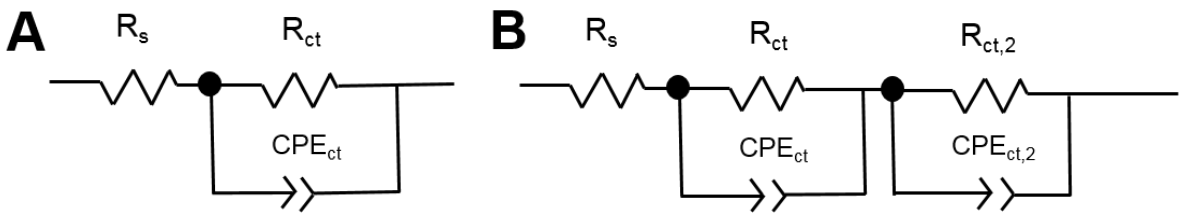

Fig. S1. Equivalent circuits used for electrochemical impedance spectroscopy (EIS) analysis A) for the majority of the bioanodes and B) for high activity bioanodes enriched at E_{AN} = −0.15 V [vs. standard hydrogen electrode (SHE)]. The first equivalent circuit (A) consists of solution resistance (R_s) and one time-constant circuit. The first time-constant circuit represents the anodic charge transfer impedance, composed of a charge transfer resistance (R_{ct}) and a constant phase element (CPE_{ct}). The second equivalent circuit (B), utilized for high activity bioanodes at −0.15 V, incorporates a second time-constant circuit to account for the second charge transfer resistance ($R_{ct,2}$) found in those systems. Circuit schematics are based on Srikanth et al.[1] and Martin et al.[2]

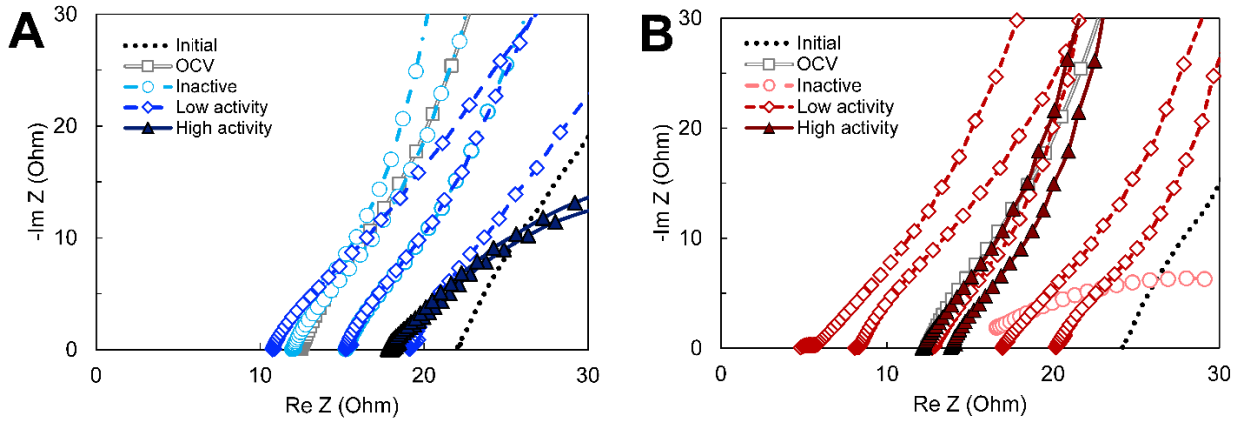

Fig. S2. Nyquist plots of bioanodes fixed at A) E_{AN} = –0.15 V and B) E_{AN} = +0.15 V taken at the end of the startup cycle. These plots show a magnification at the high frequency region of **Fig. 3**. Small semicircles and distortions in the curves can be attributed to phenomena such as small resistances or capacitances hidden under the larger impedance behaviors. All curves in the same plot are replicates. High-, low-activity, and inactive bioanode levels are defined based on the time required to reach the startup current threshold (**Fig. 1**). OCV – open circuit voltage (gray double line with squares); Initial – prior to inoculation (dotted line).

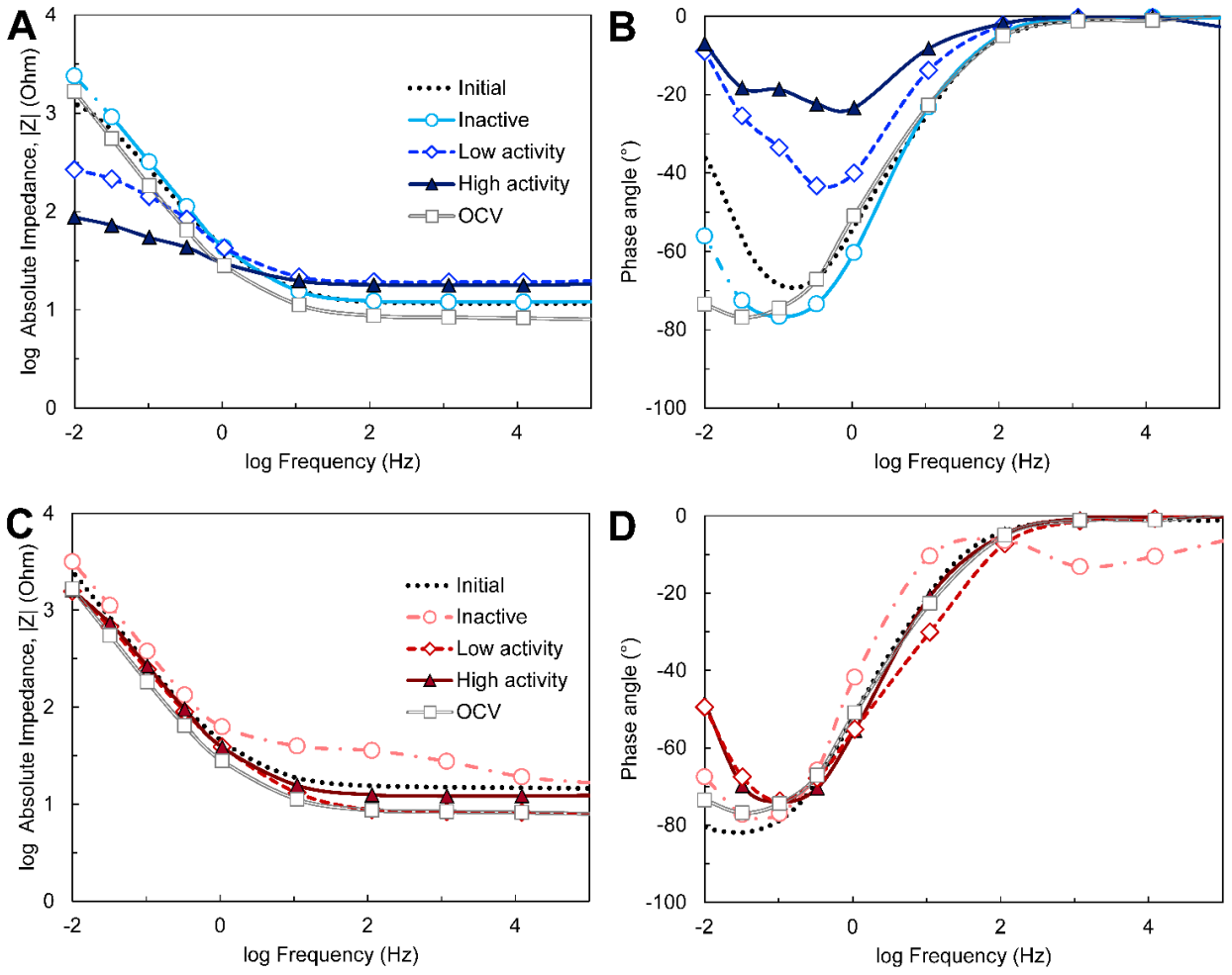

Fig. S3. Bode plots of the two high-activity bioanodes at E_{AP} = −0.15 V (A and B) and E_{AP} = +0.15 V (C and D). The plots were obtained through EIS at the end of the startup cycle. High-, low-activity, and inactive bioanode levels are defined based on the time required to reach the startup current threshold. The numbers next to each curve are the current density recorded at the end of the startup period. OCV - open circuit voltage (gray double line with squares) Initial -prior to inoculation (dotted line). Representative curves for each level of activity are shown.

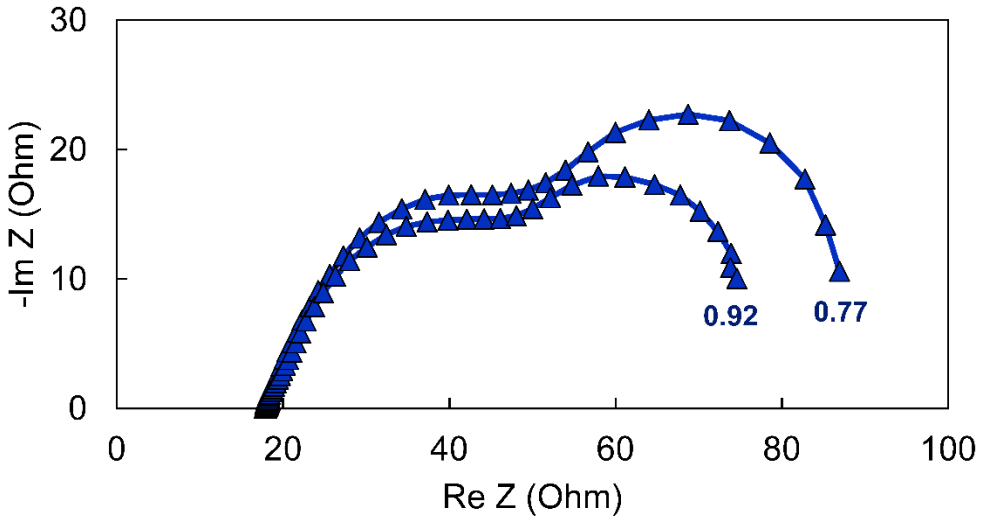

Fig. S4. Nyquist plot of the two high-activity bioanodes at $E_{AN} = -0.15$ V. The plots were obtained through EIS at the end of the startup cycle (maximum current density reached at the end of the cycle shown next to the curves). The two semi-circles in both curves are indicative of two charge transfer components.[3]

A)

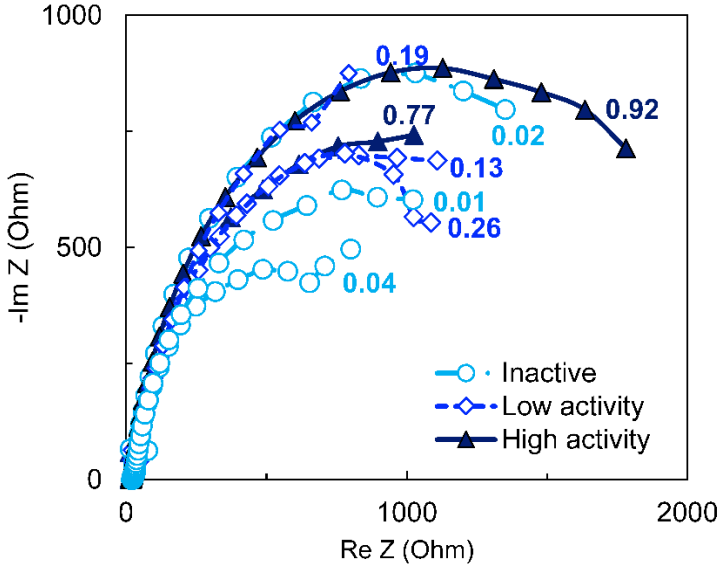

B)

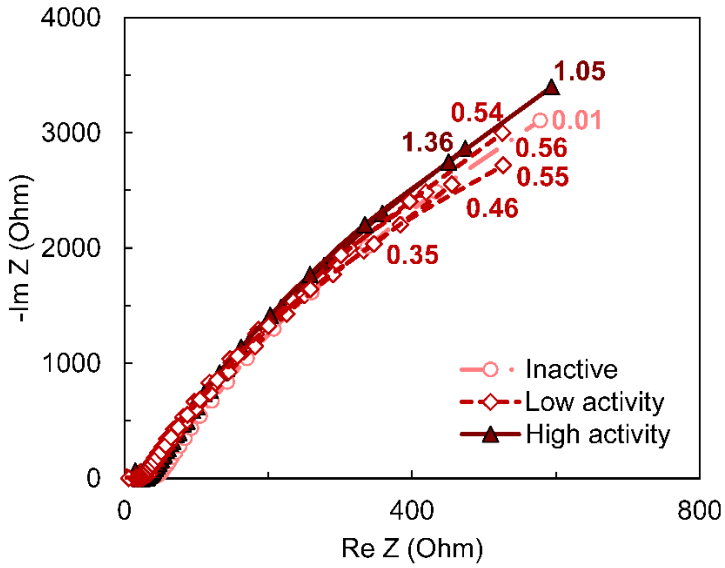

Fig. S5. Initial Nyquist plots of bioanodes (before inoculation) at a) $E_{AN} = -0.15$ V and b) $E_{AN} = +0.15$ V. The magnitude of impedance is lower when the ratio of the curve is lower, which translates into lower total resistance. All curves in the same plot are replicates. The points and curves are shaded to reflect bioanode activity level (dark – high-activity; medium – low-activity; light – inactive). The numbers next to each curve are the current density recorded at the end of the startup period.

A)

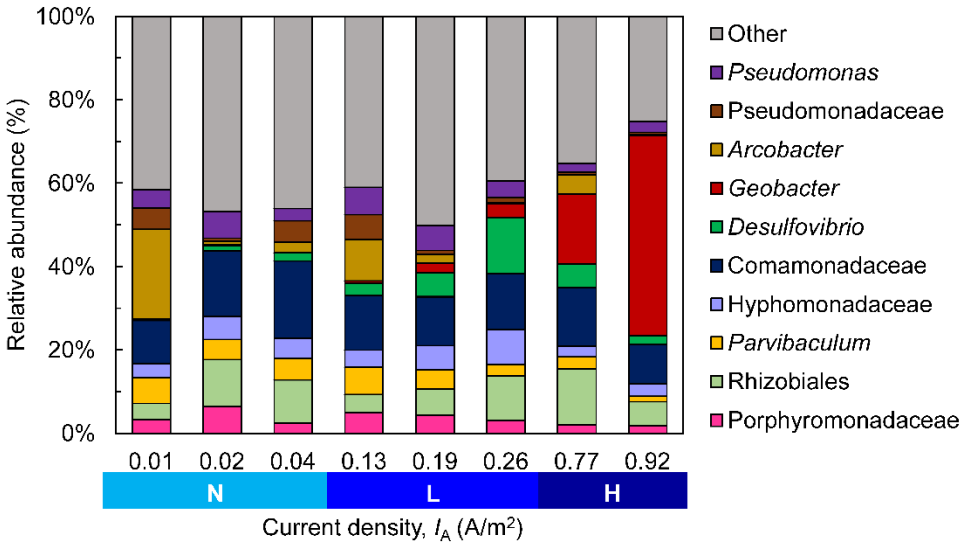

B)

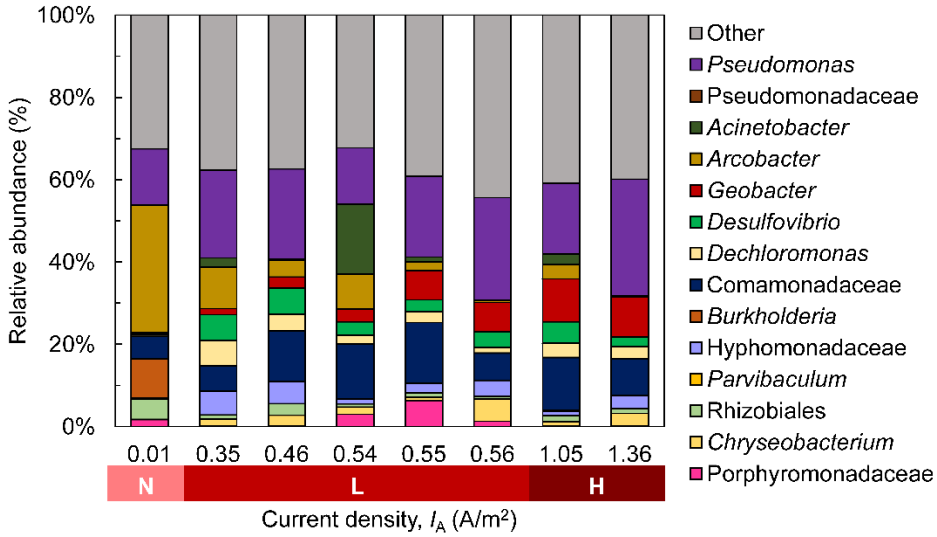

Fig. S6. Microbial community composition of the suspended fraction of the bioreactors at A) −0.15 V and B) +0.15 V. The replicates for each anode potential are ordered from lowest to highest current density (I_A) recorded at the end of the startup cycle and are categorized according to their activity level during the startup cycle [Inactive (N), low-activity (L), high-activity (H)]. Genera with a relative abundance less than 5% are grouped into "Other".

A)

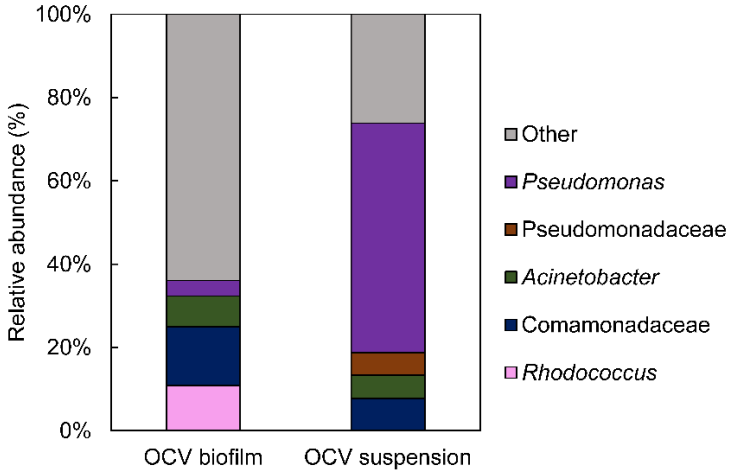

B)

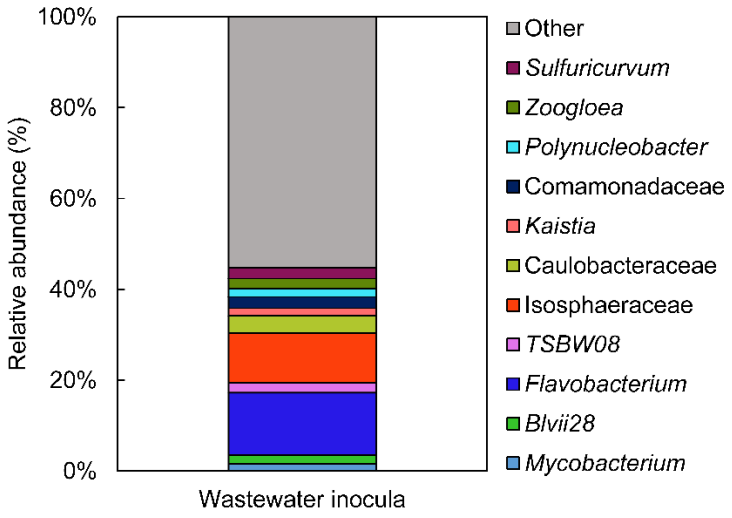

Fig. S7. Microbial community composition from A) biofilm and suspension of bioanodes at open circuit voltage (OCV) and B) wastewater innoculum. For OCV, genus with a relative abundance smaller than 5% in all reactors are grouped into "Other". For wastewater inocula, due to the high microbial diversity of the source, genus with a relative abundance smaller than 2% in all reactors (instead of 5% as other figures) are grouped into "Other" to improve clarity.

Appendix A References

(1) Srikanth, S.; Marsili, E.; Flickinger, M. C.; Bond, D. R. Electrochemical Characterization of *Geobacter sulfurreducens* Cells Immobilized on Graphite Paper Electrodes. *Biotechnol. Bioeng.* **2008**, *99* (5), 1065–1073. https://doi.org/10.1002/bit.21671.

(2) Martin, E.; Savadogo, O.; Guiot, S. R.; Tartakovsky, B. Electrochemical Characterization of Anodic Biofilm Development in a Microbial Fuel Cell. *J. Appl. Electrochem.* **2013**, *43* (5), 533–540. https://doi.org/10.1007/s10800-013-0537-2.

(3) Ramasamy, R. P.; Gadhamshetty, V.; Nadeau, L. J.; Johnson, G. R. Impedance Spectroscopy as a Tool for Non-Intrusive Detection of Extracellular Mediators in Microbial Fuel Cells. *Biotechnol. Bioeng.* **2009**, *104* (5), 882–891. https://doi.org/10.1002/bit.22469.

Appendix B

Supplementary Information for Chapter 4: Nitrogen Gas Fixation and Conversion to Ammonium Using Microbial Electrolysis Cells.

Supporting figures

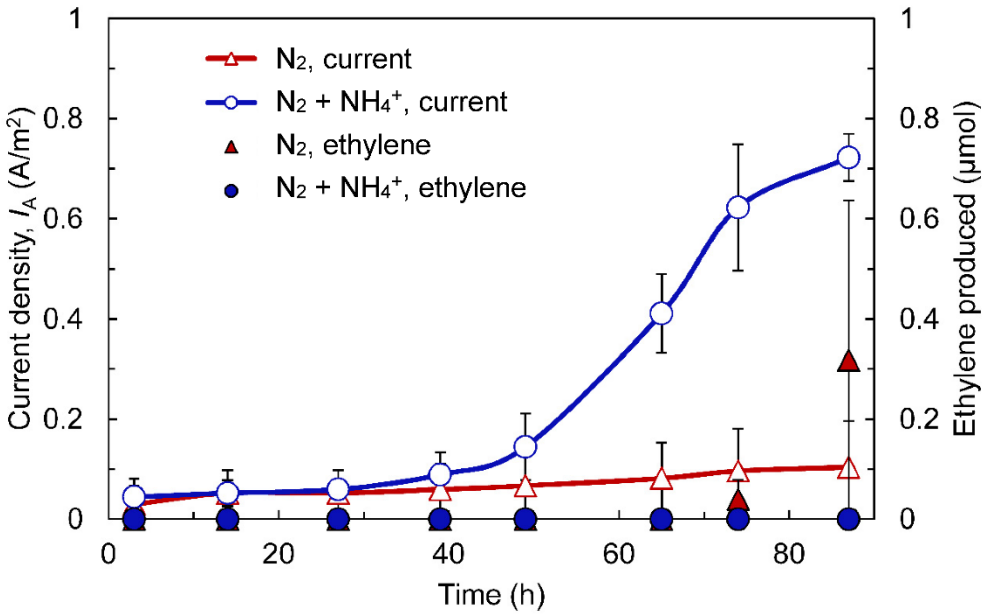

Figure S1. Current density (primary y-axis) and ethylene (C_2H_4) generation (secondary y-axis) at an applied voltage (E_{AP}) of 0.7 V with H_2 provided as the sole electron donor. Acetate was not provided in these tests. A H_2 headspace concentration of 45% was used. To estimate N_2 fixation rates, the acetylene gas (C_2H_2) assay was performed, wherein the nitrogenase enzyme within the microorganisms reduces acetylene to C_2H_4. Error bars show the standard deviation of triplicate MECs.

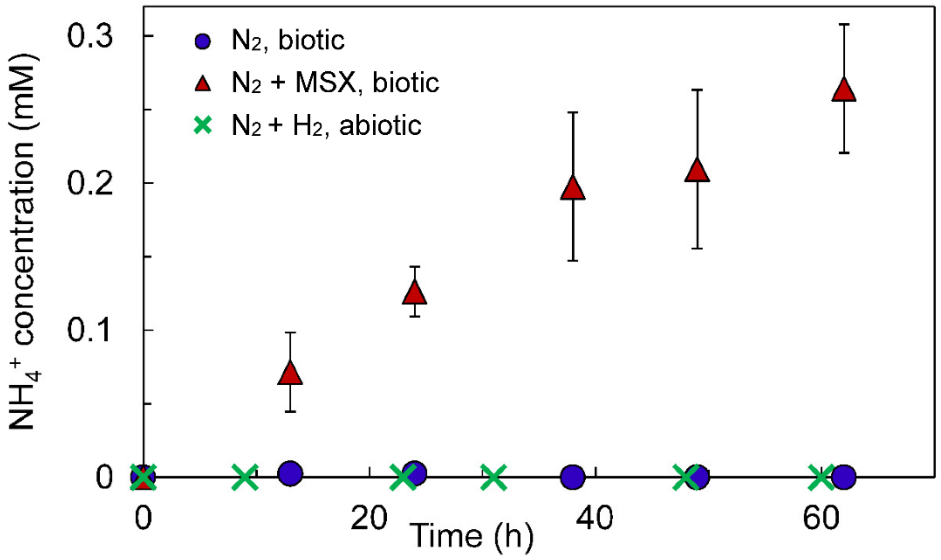

Figure S2. Ammonium (NH_4^+) concentrations in abiotic microbial electrolysis cells (MECs) with a H_2/N_2 [50/50 (v/v)] headspace composition. For reference, the NH_4^+ concentrations measured in the biological MECs with and without the inhibitor MSX are included. All reactors were operated at E_{AP} = 1.0 V. One complete MEC cycle is shown (~60 hours). Error bars show standard deviation of triplicate MECs.

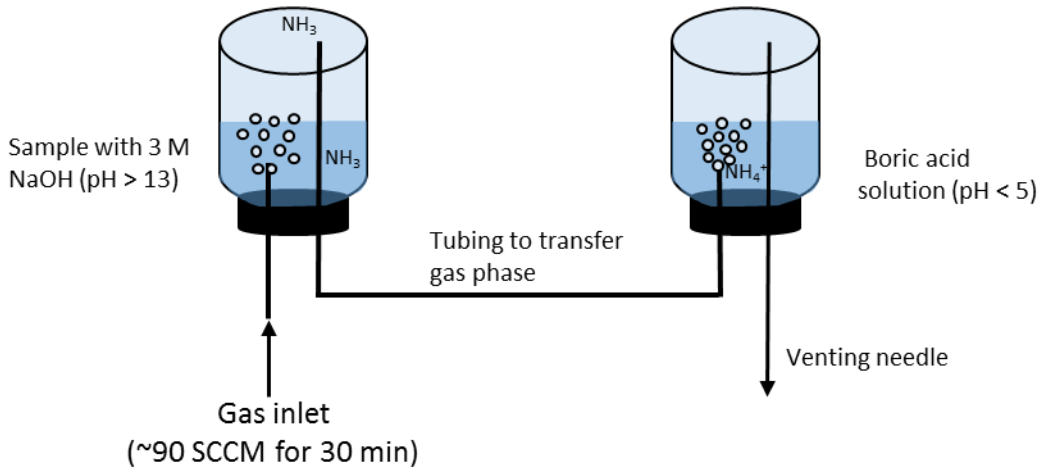

Figure S3. Schematic of the acid trap used to recover NH_4^+ from medium containing the inhibitor MSX. Microbial electrolysis cell (MEC) samples were added to vials containing 3 M NaOH (pH > 13) and N_2 was purged to promote the conversion and transfer of NH_4^+ as NH_3 to a second vial containing boric acid (pH < 5). The NH_3 dissolved as NH_4^+ and NH_4^+ concentrations were then measured. SCCM – standard cubic centimeters per minute.

Supporting methods

Ammonium trap and quantification

An ammonium (NH_4^+) trap was used to separate NH_4^+ from the medium containing the methionine sulfoximine (MSX) inhibitor (**Figure S2**). Initial tests showed that MSX interfered with the NH_4^+ measurement method (Low Range AmVer™ Salicylate Test N'Tube™ method, Hach Company, Loveland, CO). For example, a solution of MSX (5 mM, no NH_4^+ added) resulted in a reading of 7 mg/L NH_4^+-N (0.5 mM NH_4^+). To separate NH_4^+ from MSX, samples (0.5 mL) were extracted from the MECs, filtered (0.22 μm syringe filter), injected into screw thread autosampler vials (2.0 mL) containing 3 M (0.1 mL) sodium hydroxide to maintain pH > 13 and closed tightly. After mixing, the vials were connected to another vial that contained 0.5 mL of a boric acid solution (20 g/L) using gas-tight tubing and syringe needles inserted through the tops. A N_2 flow of (90-100 mL/min) was purged for 30 minutes through both vials to transport the NH_3 gas to the vial containing boric acid. After purging, the vials were disconnected and the acidic vial was mixed to ensure proper dissolution of NH_3 to NH_4^+. The pH was adjusted again to pH 7 and the NH_4^+ concentration measured. Controls using ammonium chloride (NH_4Cl) yielded NH_4^+ recoveries > 90%, and solutions with only MSX (5 mM; no NH_4^+) did not yield detectable NH_4^+. This procedure is based on the method developed by Kuntke et al.[1]

Protein determination

Protein measurements were done on anode biofilms that were not previously exposed to MSX and were only operated at E_{AP} = 1.0 V. After reproducible current was obtained, the anodes were removed and rinsed with fresh PBM to remove loosely attached cells. The biofilm was scraped using a sterile razor blade and deposited into microcentrifuge tubes with 1 ml of PBM[2].

The samples were centrifuged at 14,000 x ***g*** for 5 min, the pellet resuspended in 0.2 M NaOH, and the resulting suspension was incubated at 95°C for 10 minutes to solubilize all protein[3]. Protein was quantified using the Pierce™ bicinchoninic acid (BCA) protein assay kit (Thermo Scientific, Waltham, MA) following the instructions provided by the manufacturer. Absorbance was converted to mg protein by creating a standard curve with bovine serum albumin (BSA) standard solutions provided with the kit.

Gas analysis of headspace

To determine the headspace gas composition at the end of a batch cycle, a sample (100 µL) was taken from the headspace of each MEC. The gas was analyzed using a GC (310C, SRI Instruments, Torrance, CA) equipped with thermal conductivity detector (TCD) and a molecular sieve column (MoleSieve 5A (80/100 mesh); 6 ft x 2.1 mm). Argon was used as a carrier gas (20 mL/min). The temperature of the column oven was 40°C, and the temperature of the detector and the TCD cell was 150 °C. Peak areas were determined using the PeakSimple software and converted into percentages using standard curves. CH_4 was the only gas detected besides N_2. The total moles of CH_4 were determined from the headspace and dissolved aqueous compositions. Headspace pressure was measured using a pressure gauge and then converted to moles of CH_4 using the ideal gas law. A Henry's law constant of 1.4×10^{-5} mol/ (Pa-m^3) was used to calculate the moles of CH_4 dissolved in the aqueous phase.[4]

Supporting analysis

Calculation of normalized nitrogen fixation rates from Wong et al.[5]

To compare our nitrogen fixation rates with a prior study by Wong et al.[5], the following assumptions and calculations were made. They reported ethylene (C_2H_4) production rates in µmol of C_2H_4/($L_{headspace}$-h) in a microbial electrochemical technology (MET) that used graphite granules as the anode. The anode surface area was not specified, so we estimated it based on the information available in the paper from Cheng et al.[6]

Cheng et al.[6] used an anolyte chamber with a volume of 336 mL. When filled with graphite granules (size 3-5 mm in diameter), the liquid volume was 220 mL. The graphite granules occupied 116 mL or about 35% of the chamber. We assumed that the granules occupied the same space in the chamber used by Wong et al.[5] (400 mL), which yields an electrode volume close to 138 cm^2. Assuming each granule was a sphere of 4 mm diameter (area = 0.50 cm^2), we estimated a total of 4,120 granules, and a total anode surface area of 2,070 cm^2.

The total moles of C_2H_4 present both in the headspace and dissolved in solution were estimated as well. Given the information provided by Wong et al.[5] on the acetylene volume injected (35 mL to obtain a final concentration of 20% v/v), the headspace volume was estimated to be 175 mL. Their average rate of 237 µmol C_2H_4 ($L_{headspace}$-h) therefore translated into a rate of 0.69 µmol C_2H_4 /min. Regarding the dissolved C_2H_4, the partial pressure per hour was obtained with the ideal gas law (T = 43°C = 316.15 K), converted to dissolved concentration per hour using Henry's law (H = 0.0048 M atm^{-1})[7] and multiplied by the liquid volume in the anolyte (262 mL). Under these assumptions, we calculated a rate of 0.13 µmol of dissolved C_2H_4/min. Adding the aforementioned rates, we estimated a total rate of 0.82 µmol C_2H_4/min, or 0.40 nmol C_2H_4/(min-cm^2) when normalized to the previously obtained area.

Appendix B References

(1) Kuntke, P.; Śmiech, K. M.; Bruning, H.; Zeeman, G.; Saakes, M.; Sleutels, T. H. J. A.; Hamelers, H. V. M.; Buisman, C. J. N. Ammonium Recovery and Energy Production from Urine by a Microbial Fuel Cell. *Water Res.* **2012**, *46* (8), 2627–2636. https://doi.org/10.1016/j.watres.2012.02.025.

(2) Strycharz, S. M.; Malanoski, A. P.; Snider, R. M.; Yi, H.; Lovley, D. R.; Tender, L. M. Application of Cyclic Voltammetry to Investigate Enhanced Catalytic Current Generation by Biofilm-Modified Anodes of *Geobacter sulfurreducens* Strain DL1vs. Variant Strain KN400. *Energy Environ. Sci.* **2011**, *4* (3), 896–913. https://doi.org/10.1039/C0EE00260G.

(3) Marsili, E.; Sun, J.; Bond, D. R. Voltammetry and Growth Physiology of *Geobacter sulfurreducens* Biofilms as a Function of Growth Stage and Imposed Electrode Potential. *Electroanalysis* **2010**, *22* (7–8), 865–874. https://doi.org/10.1002/elan.200800007.

(4) Sander, R. Compilation of Henry's Law Constants (Version 4.0) for Water as Solvent. *Atmos. Chem. Phys.* **2015**, *15* (8), 4399–4981. https://doi.org/10.5194/acp-15-4399-2015.

(5) Wong, P. Y.; Cheng, K. Y.; Kaksonen, A. H.; Sutton, D. C.; Ginige, M. P. Enrichment of Anodophilic Nitrogen Fixing Bacteria in a Bioelectrochemical System. *Water Res.* **2014**, *64* (1), 73–81. https://doi.org/10.1016/j.watres.2014.06.046.

(6) Cheng, K. Y.; Ginige, M. P.; Kaksonen, A. H. Ano-Cathodophilic Biofilm Catalyzes Both Anodic Carbon Oxidation and Cathodic Denitrification. *Environ. Sci. Technol.* **2012**, *46* (18), 120904133153005. https://doi.org/10.1021/es3025066.

(7) Sander, R. Compilation of Henry's Law Constants (Version 4.0) for Water as Solvent. *Atmos. Chem. Phys.* **2015**, *15* (8), 4399–4981. https://doi.org/10.5194/acp-15-4399-2015.

Appendix C

Supplementary Information for Chapter 5: Analysis of the Transcriptome of Anode-Respiring *Geobacter sulfurreducens* to Reveal Gene Expression Changes during Nitrogen Fixation.

Supporting figures.

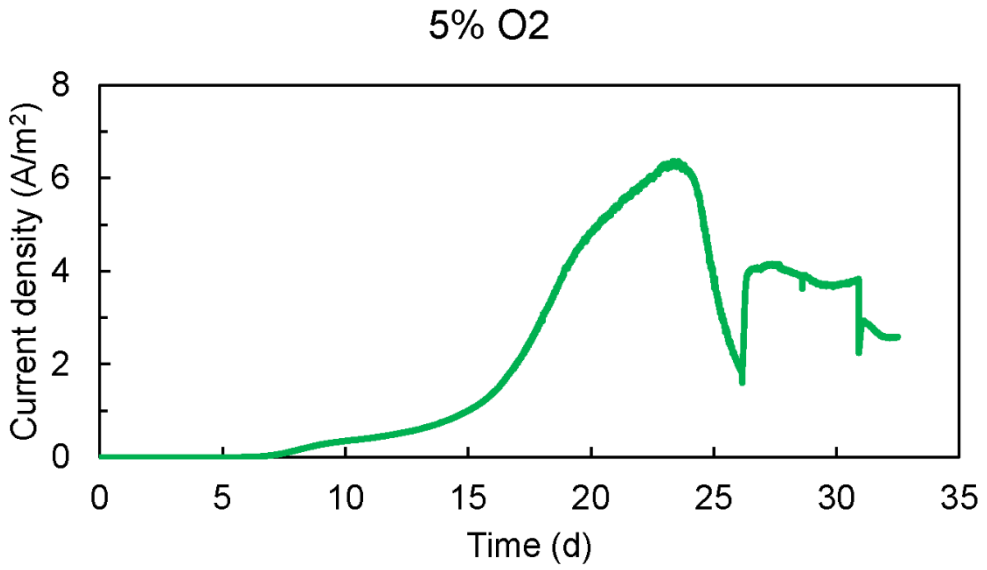

Fig. S1. Current density (I_A) profile of MECs inoculated with *Geobacter sulfurreducens* for gene expression analysis at applied potential (E_{AN}) = +0.15 V, no NH_4^+ added, under an atmosphere of 95% N_2 and 5% O_2. Reactors operated for three batch cycles, characterized by sudden sharp drops of I_A at the beginning of each. RNA was extracted a short time after the beginning of the third cycle. Curves represent averages of triplicates operated on each condition. Error bars are omitted for clarity.

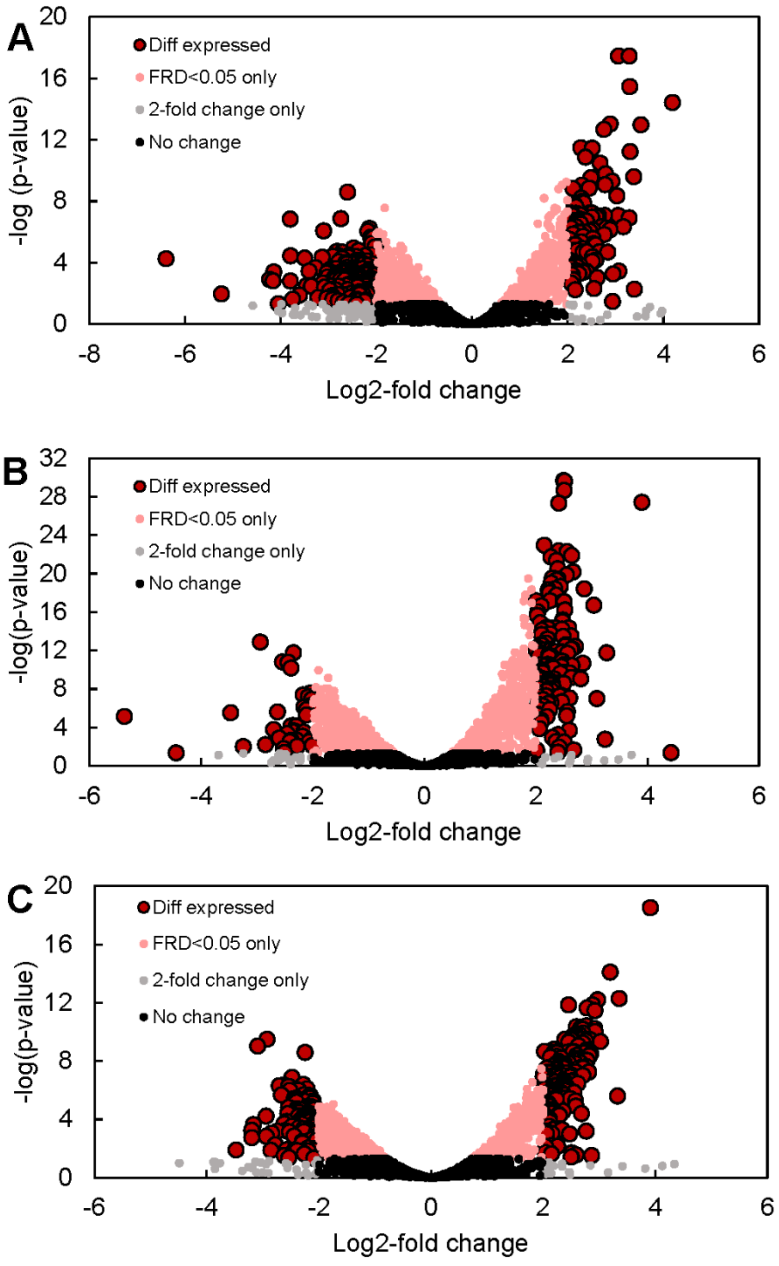

Fig. S2. Volcano plots of gene expression profiles of *G. sulfurreducens* grown in MECs, comparing A) E_{AN} = -0.15 V ("NN") vs. E_{AN} = +0.15 V ("NP"), B) 5.8 mM NH_4^+ vs. 0 mM NH_4^+, and C) 11.6 mM NH_4^+ vs. 0 mM NH_4^+. "Diff expressed" denotes genes that are differentially expressed (log2-fold change > 2.0 or <-2.0, and false discovery rate (FDR) < 0.05, while the other labels include genes that failed to meet one or both criteria.

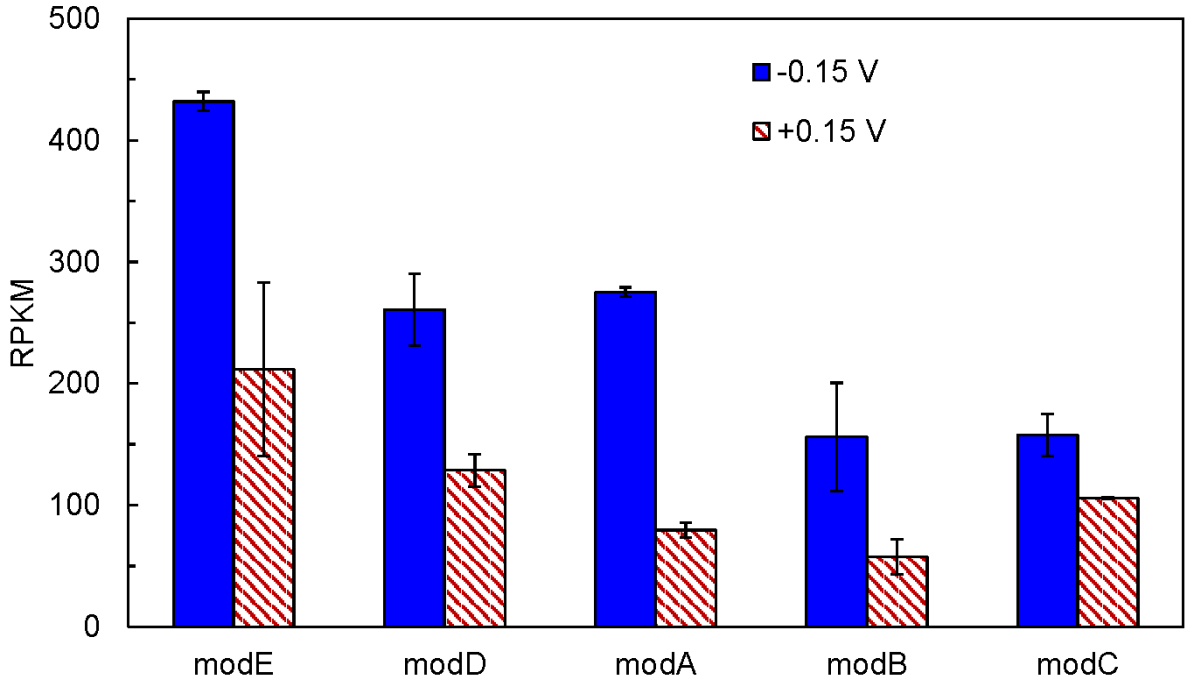

Fig. S3. Normalized gene counts genes involved in molybdenum transport in MECs operating at E_{AN} = -0.15 V vs. SHE compared to E_{AN} = +0.15 V vs. SHE. No NH_4^+ was added in both conditions. Gene counts are expressed in reads per kilobase per million (RPKM).